

EGE ÜNİVERSİTESİ



TEKSTİL VE KONFEKSİYON

DERGİSİ

ISSN : 1300-3356
E-ISSN: 2602-3075

YEAR: 34
VOLUME: 34 ISSUE: 4

EGE UNIVERSITY TEXTILE & APPAREL JOURNAL

EGE UNIVERSITY TEXTILE & APPAREL RESEARCH - APPLICATION CENTER

<http://dergipark.gov.tr/tekstilvekonfeksiyon>

PUBLISHER

On Behalf of Textile and Apparel Research
Application Center

Arif Taner ÖZGÜNEY

EDITOR IN CHIEF

Arif Taner ÖZGÜNEY
arif.taner.ozguney@ege.edu.tr

ASSOCIATE EDITORS

Mehmet KÜÇÜK
mehmet.kucuk@ege.edu.tr

Pelin SEÇİM KARAKAYA
pelinsecim@mail.ege.edu.tr

EDITORIAL BOARD

Aslı DEMİR
Gözde ERTEKİN
Hale KARAKAŞ
Hüseyin Aksef EREN
Pınar ÇELİK

ENGLISH EDITING SERVICE

Mengü Noyan ÇENGEL

SCIENTIFIC ADVISORY BOARD

Ahmet ÇAY
Andrej DEMŠAR
Arzu MARMARALI
Bojana VONČINA
Bülent ÖZİPEK
E. Perrin AKÇAKOCA KUMBASAR
Ender BULGUN
Esen ÖZDOĞAN
Hüseyin KADOĞLU
Mirela BLAGA
Nilgün ÖZDİL
Oktay PAMUK
Ozan AVİNÇ
Peter J. HAUSER
Recep EREN
Rıza ATAV
Savvas G. VASSILIADIS
Turan ATILGAN

ABSTRACTING / INDEXING

Science Citation Index Expanded (SCIE)
Scopus
WOS

TYPESETTING AND PRINTING

Printing

Bizim Büro Matbaacılık
Sanayi 1. Cad. Sedef Sok. No: 6/1 İskitler – ANKARA
Sertifika No:26649

Designed by: İ. Buhur / buhurismail@gmail.com

Printed Date: 24 December, 2024

Annual subscription rate: 40 TL (VAT included)

Annual subscription rate for textile students: 15 TL

For subscription: T. C. Ziraat Bankası Ege Tıp Şubesi,
Tekstil ve Konfeksiyon Araştırma ve Uygulama Merkezi
İBAN No: TR32 0001 0014 4607 2168 9350 32

Price: 10 TL (VAT included)

**Correlation between Different Laundry Parameters and Distressed,
Damaged and Fuzzy Clothing Inrelation
to Microfibers Detachment**

Aligina Anvitha Sudheshna, Meenu Srivastava, C. Prakash..... 387

**Investigation of Auxetic Performances of Single and Double
Layer Fabrics Woven with Braid Weft Yarns of Different
Structural Parameters**

Mine Akgun, Fatih Suvari, Recep Eren, Tuğba Yurdakul 394

**Investigation of style and design characteristics of women's
outerwear with a user-centered design approach**

Hatice Harmankaya, Meltem Özsan..... 409

**A Comperative Study on the Performance of Side-by-side
Hollow Bicomponent Yarns**

Merve Bulut, Merve Küçükali Öztürk, Cevza Candan, Banu Nergis,
Tuğba Zengin, Aysun Yenice, Rasim Boyacıoğlu, Ecenur Tor 424

**The Effect of Production Parameters of Face to Face Warp
Velvet Fabric on Abrasion Resistance and Colour Properties**

Yunus Emre Kayserili, Asım Davulcu..... 434

**The Effect of Softeners on Needle Penetration
Forces of Fabrics**

Gamze Gülşen Bakıcı, Deniz Mutlu Ala, Zeynep Nihan Kır 448

**Photocatalytic Activity of Zinc Oxide Nanoparticles and
Boric Acid for Bleaching Process on Cotton Fabric**


Zeynep Çiğeroğlu, Zeynep Omerogullari Basyigit 454

CONTACT


Ege Üniversitesi Tekstil ve Konfeksiyon Araştırma-Uygulama Merkezi
35100 Bornova – İzmir, TÜRKİYE
Tel: +90 232 311 38 89-83

www.dergipark.gov.tr/tektstilvekonfeksiyon
E-mail: tektstilkonfeksiyon@mail.ege.edu.tr

Correlation between Different Laundry Parameters and Distressed, Damaged and Fuzzy Clothing Inrelation to Microfibers Detachment

Aligina Anvitha Sudheshna¹  0000-0002-9030-9612

Meenu Srivastava¹  0000-0003-3789-2439

C. Prakash^{2,*}  0000-0003-2472-6765

¹Department of Textile and Apparel Designing, College of Community and Applied Sciences, Maharana Pratap University of Agriculture and Technology, Udaipur, Rajasthan-313 001, India

²Department of Handloom and Textile Technology, Indian Institute of Handloom Technology, Ministry of Textiles, Govt. of India, Fulia Colony, Shantipur, Nadia 741402, West Bengal, India

Corresponding Author: C. Prakash, dearcprakash@gmail.com

ABSTRACT

The influence of the clothing type, and the laundry washing parameters have a huge impact on the number of microfibers/fibers being shed during the domestic laundry trials. Distressed and damaged clothing was identified as one of the important aspects of microfiber (MFs) pollution. Although some of the factors affecting the MFs shedding are still to be explored, thus there is a need for rigorous methods of identification and quantification to understand this shedding. A novel method was adopted using different combinations of wash loads and their corresponding temperature, and wash duration on the amount of MFs being shed. Results concluded that recycled polyester fleece and distressed jeans showed heightened shedding levels (approx. 49% of total emission). When real consumer laundry was compared to laboratory laundry, consumer domestic laundry is producing 110% more MFs than the laboratory-tested fabrics. High temperature and increased wash time have a positive correlation (p-value <0.05) to the number of MFs shed.

1. INTRODUCTION

Microfibers and microplastic pollution is a widespread problem that is being faced by aquatic, marine, and terrestrial animals. Although researchers suggested that synthetic fibers are the main cause of this pollution, several reports back up the data stating that natural fibers also have an equal share in the spread of microfiber pollution [1]. Microfibers ($\leq 5\mu\text{m}$) are the fibers that are fibrillated/detached from the larger piece of fibers. In the current study, only apparel items were considered during the study thus microfibers terms were used consistently rather than microplastics (derived from larger pieces of plastics) or filaments. Diving into the diverse consumer behavior which is changing rapidly related to the purchase and care of apparel and clothing items one can deduce that these behavioral changes have a major impact on the microfiber release from domestic laundry conditions. As the fashion

cycle changes, new trends are brought into the consumer's daily life and one such change is the adoption of damaged and distressed clothing. Ripped/ distressed jeans feature frayed and a worn-out look with distinct ripped spaces usually at the knees where the skin peeps out. These rips can be caused due to over usage or can be caused by the manufacturers. The core idea is to loosen the tightly woven fabric and let the loosed fibers and frayed end protrude out. The global market for denim jeans is estimated at US\$57.3 billion in the year 2020 and is projected to reach a revised size of US\$76.1 billion by 2026, growing at a CAGR of 4.8% over the analysis period [1]

Although there are several previous researchers who are studying about the impact of different variables on the microfiber generation from the domestic laundry and stated that liquid detergent and powder detergent are causing more shedding than deionized water [2], increased shedding was

ARTICLE HISTORY

Received: 22.10.2022

Accepted: 05.05.2023

KEYWORDS

Damaged clothing, Distressed clothing, Fringe jeans, Fuzzy woolens, Microfiber pollution, Trendy clothing.

To cite this article: Sudheshna AA, Srivastava M, Prakash C. 2024. Correlation between Different Laundry Parameters and Distressed, Damaged and Fuzzy Clothing Inrelation to Microfibers Detachment. *Tekstil ve Konfeksiyon*, 34(4), 387-393.

observed while using bio-enzyme based detergents [3], lower temperature can be the cause of MFs shedding especially for polyester fibers [4], high water to fabric ratio can also be the major cause for the enhanced shedding [5], usage of fabric softener can reduce the shedding index [6], and several other studies said that new fabrics shed more MFs compared to the used once [7-9], whereas some researchers suggested that when garments were mechanically aged the aged garments were showing heightened shedding than the new apparels [10].

Apart from all these studies, the basic question remains the same, which is how consumer clothing practices are affecting domestic laundry conditions thus ultimately correlating with the increasing or decreasing number of MFs being shed. In the present study fashion trends were followed to assess the type and choice of apparel that are most favored by consumers on a large scale thus deducing the correlation between the garment type and the emission level. One of the main objectives of the study was to obtain the current apparel choice practices favored by the respondents thus estimating the cumulative amount of MFs released into the environment during washing trails from these sources. The preliminary survey on apparel choices stated that teenagers and college-going students were mostly drawn toward ripped, damaged, and distressed jeans. Thus to deduce the emission levels of these clothing items the current study was focused on the domestic laundry of the used consumer distressed clothing rather than the new apparel which were purchased from the clothing stores. The effect of wash duration, temperature, and wash loads on the amount of MFs shed was also studied to find out the inter-relating effect among the variables.

2. METHODOLOGY

2.1 Materials

Soiled clothing (which fulfills the requirements of damaged and distressed clothing, and woolens) from the consumers were procured from the households to conduct the experiments. Apart from those clothing different types of damaged, distressed, and stone-washed jeans and fringe jeans were obtained from the local markets of Rajasthan, India. Double puffer jackets, puffer jackets, fuzzy woolen t-shirts, and fuzzy acrylic shawls were obtained through online fashion websites in India, to study the release rate.

A front-load fully automated domestic washing machine was used (Samsung EcoBubble, Model number: WD70M4443JW/TL). Wool (Max. 2Kg) and Cotton (Max. 3Kg) programs were selected which were present in the washing machine were chosen. Normal tap water was used and no changes were made to the temperature settings. Surf excel liquid and powder detergent was used for the jeans, and ezee liquid detergent specially designed for woolen garments was used for woolen garments, along with surf excel powder detergent with added vinegar in the rinse

cycle, for the chemical fabric softener comfort brand was used (Ditallowoylethyl Hydroxyethylmonium Methosulfate is the fabric conditioning compound present in the softener).

2.2 Washing Procedure

Ten consecutive wash cycles were run for each garment type. Due to the difference in the shedding index, some garments were washed more, thus increasing the total number of cycles to deduce the resulting anomalies. Laundry effluent was collected using large containers. 1-liter samples were collected after stirring with a wooden ladle, and 10ml aliquots were separated and were raised to 100ml each using distilled water to dilute the dust and laundry additives. The main aim of aliquots was to save time and be able to visually count the MFs.

Before the testing, two empty wash cycles were run to thoroughly uncontaminated the washing machine from the residual MFs from the previous washes. The effluent water was passed through a filtering sieve and then small representative samples were passed through glass microfiber filters. The second wash showed no residual fibers thus rendering the process successful. Apart from this, no washout cycles were run to estimate the accurate amount of shedding, and to replicate the real domestic laundry conditions, as a minute amount of fibers from the previous wash tend to release in the consecutive wash cycles.

Microfiber Analysis

The MFs were filtered using 2.7 μm mesh filters (Axiva Glass Microfiber filter, 47mm diameter circles, GF/4F) and 0.7 μm mesh filters (Axiva Glass Microfiber filter, 47mm diameter circles, GF/5F). Subsequently, the fiber dimensions were calculated through SEM analysis for which filter papers were cut randomly and were analyzed after gold coating to enhance the image quality. Fiber identification was done through FT-IR analysis. The peak values were matched with the spectral library to the accurate fiber type, some of the fibers identified were cotton, wool, acrylic, elastane, and polyester.

2.3 Statistics

A linear mixed mode was used to determine the effect of temperature, wash load, and washing duration during the laundry process on the microfiber generation was calculated. Several other appropriate tests were conducted accordingly and the significance level was kept at $\alpha=0.05$.

3. RESULTS AND DISCUSSIONS

3.1 Effect of fabric type

As all the fabrics have protruding fibers, a high amount of emission was found in all types of fabrics irrespective of the construction type and the fiber content (Figures 1 and 2). The overall emission rates of liquid detergent tend to be 45 percent to 46 percent in jeans and woolens respectively.

Whereas for powder detergent it was 53 percent to 54 percent. Recycled polyester, knit fabrics, and cotton/polyester blends have released a significantly high number of fibers which is consistent with a study conducted by Maggipinto et al. [11], who stated that after five consequent washes cotton and polyester fabrics released up to 1.0×10^6 and 5.0×10^5 fibers per kg of fabric washed.

A paired t-test was conducted to find out that there was a significant difference between the emission rates between the liquid and powder detergents while woolen laundry with a p-value of 0.012. Whereas when damaged and distressed jeans were compared during the wash trials no significant difference was found. One of the major sheddings was observed in the recycled polyester with 36.31 percent, followed by double-sided fleece with 22.25 percent of the overall emission rates. The recycled polyester used in the present study was made out of recycled plastic pellets and other plastic debris collected from marine waste. This results in the weakened fiber structure and easy abrasion and degradation thus resulting in the heightened shedding of approximately 1,00,000 MFs in each wash cycle. These findings suggest that yarn construction and proportions and their composition plays a major role in the MFs generation during the laundry process and cannot be generalized [12].

Table 1 provides a detailed view regarding the wash cycle parameters which were used during the course of study, along with the type of garments and their corresponding

sheddability rates. In a study conducted on the denim fabrics domestic laundry and their respective microfiber waste load results showed that 100 percent cotton has the maximum loss [15].

Comparing different types of denim jeans on the sheddability index, it was evident from Figure 2 that the statistical box plot showing that ripped all-over jeans have shown the maximum emission rates contributing to 49.22 percent of the total emission, whereas the least emission (1.33%) was found in stone-washed jeans as no protruding and loose ends were observed on the surface of the jeans. It can be concluded from the results that ripped overall jeans shed more MFs due to the fact that more the number of rips and tears and more protruding/ raw ends thus resulting in more MFs released when abraded against the nearby surfaces during the laundry process.

SEM analysis was carried out to find out whether there was any difference in the fiber dimensions which were released under different laundry conditions. But the obtained images showed that irrespective of the wash cycle and the type of fiber content, similar categories of fibers were seen such as fiber which are $\leq 5 \mu\text{m}$ namely microfibers (49.16%), 50-100 μm (26.95%), 100-500 μm (15.11%) and $>500 \mu\text{m}$ (8.76%). It was also observed that apart from the microfibers nanofibers were also found on the samples suggesting the increasing level of fiber fibrillation. The only difference found was in the amount or number of the fibers being shed.

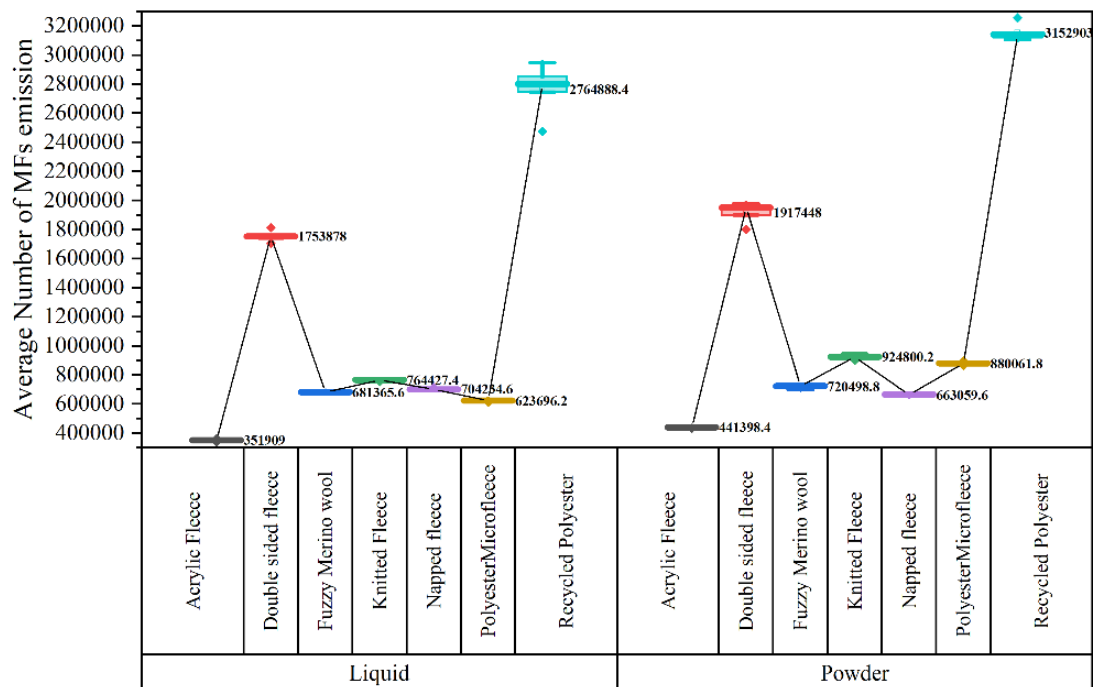


Figure 1. Distribution of the average number of MFs released during the ten wash trails of fuzzy wollen/ synthetic clothing

Table 1. Depicts the detailed view of the washing parameters along with the type of garment and the MFs detached in each wash cycle

Clothing Type	Detergent Type	Wash cycle	Temperature	Wash Time	RP M	Replicates										Mean	SD
						1	2	3	4	5	6	7	8	9	10		
Knitted Fleece	Liquid	Wool	40°C	53 min	800	754416	770406	736680	795506	764406	785601	754213	741264	763878	765214	763158.4	18091.70
	Powder					923776	912357	985214	965742	958724	912345	912365	923657	954782	935130.7	28440.56	
Acrylic Fleece	Liquid	Synthetic	60°C	78 min	1000	351953	324570	326580	345216	368745	325412	312085	325671	326598	302145	330897.5	19425.00
	Powder					447763	452368	452136	485213	401236	425136	412378	468521	487521	451750.8	30963.18	
Napped Fleece	Liquid	Wool	40°C	53 min	800	703023	765231	741258	701236	742103	702154	700102	702145	702314	702454	716202	23889.13
	Powder					667981	652142	645712	678546	658974	632105	671203	671230	621031	657304.7	19292.33	
Polyester Microfleece	Liquid	Synthetic	60°C	78 min	1000	626894	601235	610234	621430	678451	651201	645210	602341	612354	617851	626720.1	24598.92
	Powder					880142	895412	874523	801235	897410	896320	874236	851479	896214	874154	29511.25	
Fuzzy Merino Wool	Liquid	Wool	40°C	53 min	800	689968	685123	654785	698745	625898	689475	680123	645896	675230	680021	672526.4	22990.06
	Powder					725031	721202	710236	732548	742103	720145	701245	701259	741023	721582.8	14487.81	
Recycled Polyester	Liquid	Synthetic	60°C	78 min	1000	2800356	2845612	2845120	2745612	2657848	2845610	2974125	2901234	2874106	2610476	2810009.9	110724.29
	Powder					3142584	3316397	3289755	3183462	3283157	3233971	3311799	3281809	3282092	3146151	3247117.7	66560.92
Double-sided fleece	Liquid	Wool	40°C	53 min	800	1741706	1744118	1747408	1746915	1746232	1748134	1749632	1743255	1748025	1747527	1746295.2	2487.64
	Powder					1900166	1902699	1906336	1904279	1917011	1909605	1905635	1901570	1909238	1908526	1906506.5	4902.42
Stone Washed	Liquid	Denim	60°C	73 min	800	120261	120311	120347	120310	120296	120350	120283	120345	120348	120322	120317.3	30.87
	Powder					109814	109924	109589	109239	109183	109366	109601	109485	109353	109581	109513.5	237.96
Ripped All over	Liquid	Denim	60°C	73 min	800	4315371	4301255	4329453	4286513	4363552	4243105	4398800	4285090	4248018	4226291	4299744.8	54448.10
	Powder					4194486	4119562	4113146	4115286	4099218	4190423	4126988	4098771	4199521	4127544	4138494.5	40094.87
Acid Wash	Liquid	Denim	60°C	73 min	800	530691	529605	527777	533875	530190	533364	526710	531537	533723	529002	530647.4	2489.88
	Powder					762593	763190	755052	758005	766022	772041	767764	778400	763614	752545	763922.6	7747.56
Distressed	Liquid	Denim	60°C	73 min	800	1055497	1135246	1136038	1087581	1125426	1073858	1051568	1013367	1011626	1101892	1079209.9	46365.51
	Powder					2168747	2243057	2171994	2338339	2224539	2240345	2329773	2287051	2279251	2212970	2249606.6	58918.26
Ripped Kneec	Liquid	Denim	60°C	73 min	800	592571	592624	593289	592886	593500	593307	593124	593028	592965	592632	592972.6	332.85
	Powder					725551	733430	726253	728730	734824	733335	722570	722897	732579	729368	728933.7	4530.91
Fringed	Liquid	Denim	60°C	73 min	800	648122	651076	644541	641705	634640	646423	644935	638616	650463	643434	644395.5	5126.07
	Powder					711208	712706	710354	714968	722570	712551	721620	713243	711438	715516	714617.4	4254.83
Damaged	Liquid	Denim	60°C	73 min	800	652195	655195	644745	648570	648551	650558	643054	654593	642248	652431	649214	4651.35
	Powder					699485	695145	699608	692555	694741	692422	690952	694692	690671	694124	3297.44	

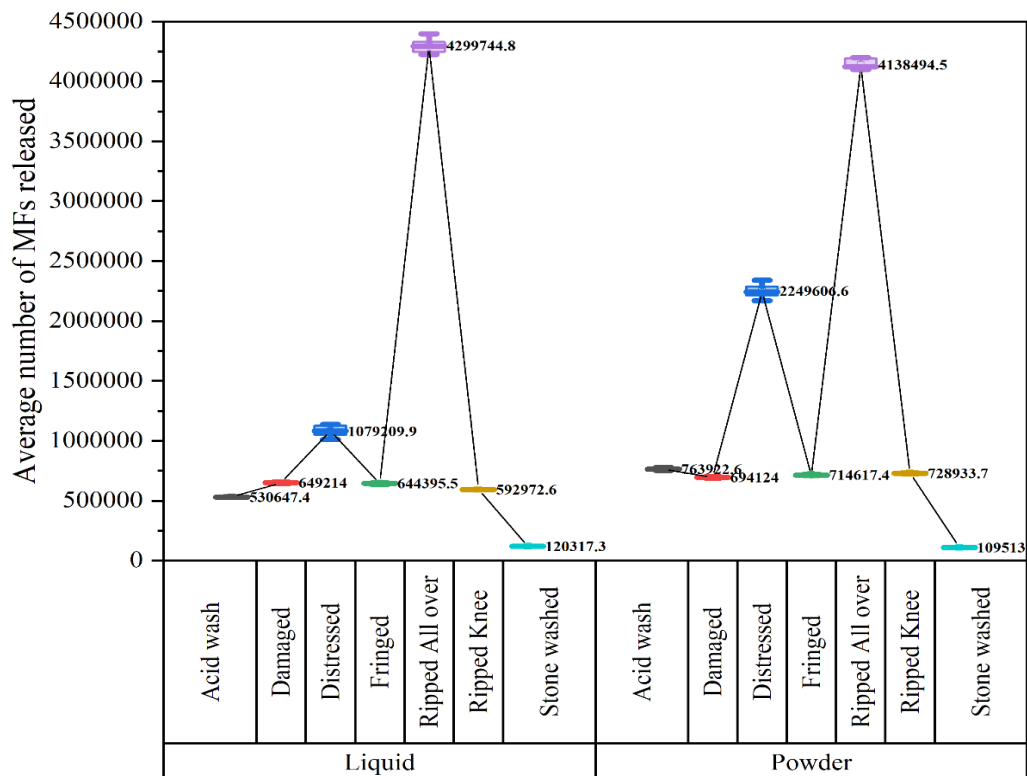


Figure 2. Distribution of the average number of MFs released during the ten wash trails of the damaged/ distressed and other types of denim jeans

3.2 Effect of detergent

Denim garments were washed using a surf excel liquid detergent (40ml) and powder detergent (40gms) with and without fabric softener (45ml) in the rinse cycle. Whereas the woolen garments were washed using eeze liquid specialty detergent (40ml) and two tablespoons (30ml) of vinegar were added as a fabric softener substitute in the rinse cycle. The effect of the detergent on the microfibers shed can be seen in Figures 1 and 2. All the fabrics were washed using the standard program suggested by the washing machine manual is used but the amount of laundry detergent is kept constant to note whether each type of cycle have a difference in the shedding and a statistically significant difference was only found in the (p-value <0.05) fuzzy woolen clothing.

About a 5 percent to 10 percent difference was observed between the liquid and powder detergent during the correlative analysis, which cannot signify that one can be prioritized over the other. A two-sample t-test was performed to find out the difference between the liquid and powder detergent and the p-value obtained was 0.068, which states that there was no significant difference. Fabric softener was also adopted to find out any variance, but the results obtained stated that no particular difference was observed in the case of these types of garments which have protruding and raw edges. Whereas, some of the previous studies [13-14] stated that the usage of fabric softeners has reduced the shedding by causing a sliding effect on the garments being laundered.

3.3 Effect of temperature

Cold water and 60°C (the most favored temperature by consumers) were used. Results obtained enumerated that an average of 5835.25 fibers were being released per filter during the 60°C temperature setting, whereas 4420.75 fibers were released when washed in cold water. These can be interpreted in such a way that cotton fibers are hydrophilic and during the laundry process the cotton fibers absorb the water and swell according to their inbuilt nature and when these fibers are prone to heightened temperature and agitation there is a highly likely chance that these fibers burst and split into to smaller fibers thus releasing more MFs.

Woolen fibers can be considered the natural hair of animals when these fibers are laundered at the highest temperatures causing damage. It is always advised that cold water should be used for laundering woolen garments. Woolen substitutes such as acrylic and polyester fills do not have any significant impact when washed in both cold and hot water as they are resistant to high temperatures. One of the major drawbacks of the temperature setting is that to obtain such high temperatures wash time is increased simultaneously, thus increasing the overall wash time which results in heightened agitation and increased MFs shedding. Yang et al. [5] conducted a study correlating the effect of washing temperature on the microfibers shedding in synthetic fibers and found that with the increase in the temperature ($\geq 60^{\circ}\text{C}$), there was a greater increase in the microfibers.

3.4 MFs generated from soiled consumer apparel

Real consumer laundry conditions were also studied to find out any persistent differences between the laboratory and consumer laundry trials. It was also observed that during real-life domestic laundry conditions metal buttons and zippers from one garment were entangling with the other garments making the raw edges of the jeans more prone to abrade thus resulting in the enhanced MFs release. From Figure 3 we can see that there was a difference in the mean values between the household laundry (more shedding) when compared to the laboratory laundry.

Further a statistical analysis was carried out to find out a p-value of 0.035, which states that there is a significant difference between the laundry types at a 5% level of significance. From Figure 3, interpretations can also be drawn out that wearing and abrasion caused during bodily movements also have an impact on the raw edges/protruding fibers. When these abraded garments are washed the laundry process also causes an enhanced level of agitation depending on the temperature and wash cycle time chosen thus resulting in a greater sheddability index than the laboratory experiments.

4. CONCLUSION

Real domestic laundry conditions were shedding significantly more number of microfibers in the laundry effluents. Although both natural and synthetic fibers are being shed in almost equal amounts natural fibers due to the

fuzzy weave structures and conscious distressing of jeans are resulting in the addition to the already existing problem. While washing these types of garments it is suggested to wash them in quick wash cycles and preferably in cold wash cycles. Some of the suggestions which can be made from the current study were that it is advisable to always modify the wash cycle according to the clothing needs which in turn reduces the agitation levels thus reducing the MFs shedding. The main barrier to consumer adoption is knowledge and awareness. Results also found that fabric softener does not play a huge role in heightening or lowering the emission, but further study is needed to fully justify and understand these types of fabrics.

Results inherently state that both consumers and manufacturers are equally responsible for microfiber pollution. Significant intervention is much needed such as encouraging consumers to use lint filters, reducing the usage of damaged or distressed clothing, usage of mesh/laundry bags while washing fuzzy garments which helps to reduce agitation levels. Further investigations can be done in the direction of home textile (mink/woolen blankets, and other furry/fluffy textile materials) items as well, which represents the sheddability index of a significant shareholder in the households. One of the important factors is that any new studies being conducted in these areas require an appropriate scope of application thus finding the ultimate solution.

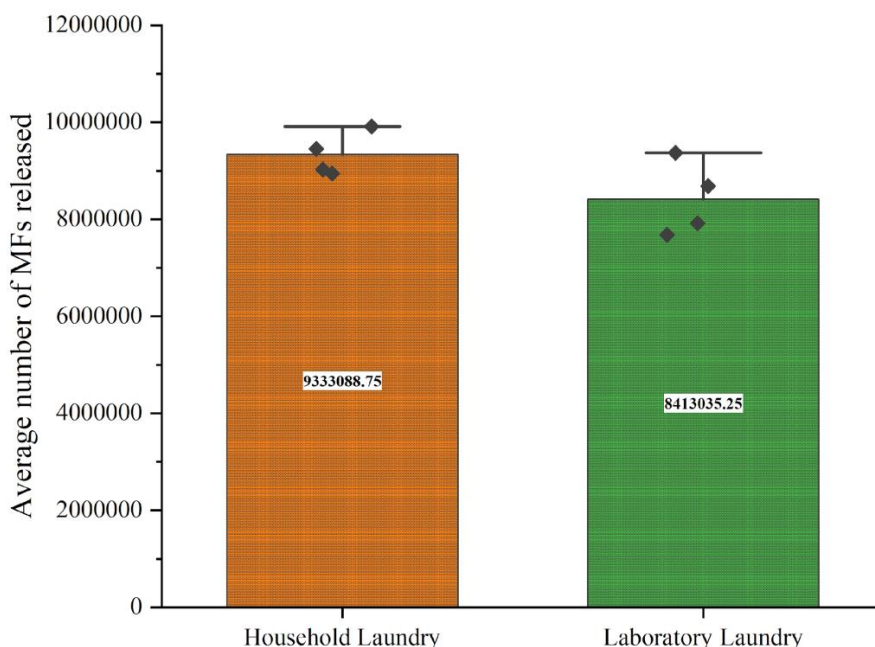




Figure 3. Distribution of MFs shedding during different laundry conditions


REFERENCES

1. De Bruin, R. 2007. Cotton/polyester and cotton/nylon warp knitted terry cloth: Why minority fibre content is important. *Journal of Family Ecology and Consumer Sciences*, 35(1), 39-46.
2. Hernandez, E., Nowack, B., Mitrano, D.M. 2017. Polyester textiles as a source of microplastics from households: a mechanistic study to understand microfiber release during washing. *Environmental Science & Technology*, 51(12), 7036-7046.
3. Napper, I.E., Thompson, R.C. 2016. Release of synthetic microplastic plastic fibres from domestic washing machines: Effects of fabric type and washing conditions. *Marine Pollution Bulletin*, 112(1-2), 39-45
4. Yang, L., Qiao, F., Lei, K., Li, H., Kang, Y., Cui, S., An, L. 2019. Microfiber release from different fabrics during washing. *Environmental Pollution*, 249, 136-143.
5. Kelly, M.R., Lant, N.J., Kurr, M., Burgess, J.G. 2019. Importance of Water-Volume on the Release of Microplastic Fibers from Laundry. *Environmental Science & Technology*, 53, 11735-11744.
6. Falco, F. De, Pace, E. Di, Gentile, G., Avolio, R., Errico, M.E., Avella, M. 2018. Quantification of microfibers released during washing of synthetic clothes in real conditions and at lab scale. *The European Physical Journal Plus*, 133(7), 1-4.
7. Cesa, F. S., Turra, A., Baroque-Ramos, J. 2017. Synthetic fibers as microplastics in the marine environment: a review from textile perspective with a focus on domestic washings. *Science of the Total Environment*, 598, 1116-1129.
8. De Falco, F., Di Pace, E., Cocca, M., Avella, M. 2019. The contribution of washing processes of synthetic clothes to microplastic pollution. *Scientific Reports*, 9(1), 1-13.
9. Kärkkäinen, N., Sillanpää, M. 2021. Quantification of different microplastic fibres discharged from textiles in machine wash and tumble drying. *Environmental Science and Pollution Research*, 28(13), 16253-16263.
10. Bruce, N., Hartline, N., Karba, S., Ruff, B., Shreya, S. 2016. Microfiber pollution and the apparel industry. *Journal of Chemical Information and Modeling*, 53(9), 1689-1699.
11. Maggipinto, M., Pesavento, E., Altinier, F., Zambonin, G., Beghi, A., Susto, G.A. 2019. Laundry fabric classification in vertical axis washing machines using data-driven soft sensors. *Energies*, 12, 1-13.
12. Zambrano, M.C., Pawlak, J.J., Daystar, J., Ankeny, M., Cheng, J. J., Venditti, R.A. 2019. Microfibers generated from the laundering of cotton, rayon and polyester based fabrics and their aquatic biodegradation. *Marine Pollution Bulletin*, 142, 394-407.
13. Lant, N.J., Hayward, A.S., Peththawadu, M.M.D., Sheridan, K.J., Dean, J.R. 2020. Microfiber release from real soiled consumer laundry and the impact of fabric care products and washing conditions. *PLoS One*, 15, e0233332.
14. Rathinamoorthy, R., Balasaraswathi, S.R. 2022. Investigations on the impact of handwash and laundry softener on microfiber shedding from polyester textiles. *The Journal of The Textile Institute*, 113(7), 1428-1437.
15. Rathinamoorthy, R., Raja Balasaraswathi, S. 2021. A review of the current status of microfiber pollution research in textiles. *International Journal of Clothing Science and Technology* 33(3), 364-387.

Investigation of Auxetic Performances of Single and Double Layer Fabrics Woven with Braid Weft Yarns of Different Structural Parameters

Mine Akgun  0000-0002-6415-7782

Fatih Suvri  0000-0001-5708-7993

Recep Eren  0000-0001-9389-0281

Tuğba Yurdakul  0000-0003-0369-3757

Bursa Uludag University / Faculty of Engineering / Textile Engineering Department, Bursa, Türkiye

Corresponding Author: Mine Akgun, akgunm@uludag.edu.tr

ABSTRACT

This study investigated the auxetic performances of single and double layer fabrics woven by using braid weft yarns with different structural parameters. Non-elastane braid weft yarns containing yarn components with different filament numbers and braid weft yarns containing elastane and conventional warp yarns were used in fabrics. To investigate the effects of weave, fabrics with single and double layer structures were woven on an industrial weaving machine. Experimental results showed that the fabrics woven with both non-elastane and elastane braid weft yarns performed an auxetic behavior by giving Negative Poisson's Ratio (NPR) values. It was observed that generally fabrics woven with braid weft yarns containing elastane could improve the auxetic performance. Fabric woven with non-elastane braid yarns of high filament numbers showed a higher NPR. When the effect of the weave on the auxetic performance was examined, a double layer fabric structure was shown to reduce the auxetic effect.

1. INTRODUCTION

Poisson's ratio (PR) is defined as the negative ratio of transverse strain to axial strain and is used to predict the deformation of engineering materials under uniaxial stress [1-3]. Materials with a negative Poisson's ratio (NPR) are also called auxetic materials. For example, when a conventional material is subjected to a tensile force, it elongates in the force axis and contracts in other axes, or when a material is subjected to a compressive force, it contracts in the force axis and expands in other axes. As opposed to materials with a positive Poisson's ratio, auxetic materials expand laterally when stretched and contract laterally when compressed [2, 4-8].

Since the Poisson's ratio is a physical parameter independent of material scales, auxetic behavior can be obtained from the molecular to macroscopic levels [2, 9, 10]. The mechanisms of auxetic materials depend on their microstructure, geometric structure, or deformation mechanisms of these structures [5, 8, 11-17].

Textile materials differ in many aspects compared to other engineering materials. For example, they may not show the same behavior in all directions under force. They can easily deform, change shape and elongate without breaking depending on their place of use. In terms of these properties, it is a unique material as to its compatibility with human movements [18]. The deformation behavior of woven fabrics when subjected to tension is an issue that should be considered in predicting the performance of fabrics during use [18, 19]. The breaking behavior of woven fabrics and their deformation under low forces are considered during these products' design and production stages, from clothing to home textiles, from textile-reinforced composites to technical textiles [18].

Deformation under tensile loading is one of the methods that can be used to determine the physical performance of fabrics. In studies [20, 21] on Poisson's ratio of various conventional fabric types, it is stated that conventional fabrics show positive PR values due to lateral contraction under tension.

To cite this article: Akgun M, Suvri F, Eren R, Yurdakul T. 2024. Investigation of Auxetic Performances of Single and Double Layer Fabrics Woven with Braid Weft Yarns of Different Structural Parameters. *Tekstil ve Konfeksiyon*, 34(4), 394-408.

Woven fabric structures are textile surfaces formed by the intersection of warp and weft yarns perpendicular to each other. In woven fabrics, both the warp and weft yarns take a crimp due to the displacement caused by the intersection of the warp and weft yarns. When the fabric is stretched in one direction, the yarns in the loading direction straighten. Straightened yarns cause other yarns to receive more crimp perpendicular to the loading direction, resulting in fabric shrinkage in the transverse direction and hence a positive PR occurs [22, 23].

Generally, there are two approaches to the production of auxetic textiles. The first involves using auxetic fibers to produce an auxetic textile structure, while the other is producing textile structures with auxetic properties using suitable yarns made from conventional fibers [2]. The literature states that different combinations of conventional yarns are used as warp and weft yarns to develop auxetic fabrics. In addition, it is stated that the benefit of using conventional yarns in forming auxetic fabrics is that they have higher structural stability than auxetic fibers [24].

It is shown in the studies that the creation of different shrinkage phenomena in woven fabric structures can be achieved by the use of weave pattern combinations with different shrinkage/contraction properties and the use of elastic/non-elastic yarns. The developed auxetic woven fabrics are based on a foldable geometric structure. The basic principle of these geometries is the different shrinkage effects. Elastic yarns are used to provide flexibility and reversibility to the fabric structure, while non-elastic yarns are used as a stabilizing component [25, 26].

In a study, the auxetic performance of a partial stretch plain weave fabric was investigated by inserting non-elastane and elastane conventional weft yarns as forming successively strips in the transverse direction of the fabric. And it was stated that this form gave the fabric a relatively similar foldable geometric structure and therefore showed an auxetic performance [27].

In a study on woven fabrics made of helical auxetic yarns (HAYs) and their essential effects on Poisson's ratio under tension, it is stated that the lower wrapping angle of the HAY and a thinner diameter of the auxetic weft yarn lead to higher auxetic behaviour of the fabric. Also this study states that the weave structure can directly affect the auxeticity of the woven fabric and the structure having longer floats results in a higher auxetic effect. It was also shown that lower tensile modulus of the warp exhibits a higher auxetic effect [28].

In a study on single and double layered bistretch auxetic woven fabrics woven with nonauxetic yarns based on the folded geometry, it is concluded that all the developed fabrics have auxetic behavior in both warp and weft

directions. In the double layered auxetic woven fabrics based on parallel in-phase zigzag foldable geometrical structure, it is shown that higher NPR effect when the fabric is stretched along weft direction than warp direction. It is stated that this behavior is different from the results obtained for single layer fabric. Also, this research concludes that the placement of weaves and weft yarn arrangements has an effect on auxetic behavior [29].

In a different study on the auxetic performance of fabrics woven on a hand-weaving loom using braid yarns, it was stated that the fabrics woven with braid weft yarn exhibited an auxetic behavior by giving negative Poisson's ratio up to a certain elongation value under tension in the warp direction. In addition, it was stated that the NPR of fabric was affected by the thickness of the braid yarn and the tightness (compactness) of the fabric [30].

In the investigation of warp directional Poisson's ratio changes of fabrics woven with elastane containing braid weft yarns with different yarn tensions and with conventional and braid warp yarns, it was stated that the fabrics with elastane containing braid weft, the NPR effect could be obtained from the fabrics woven with the conventional warp yarn, but the NPR effect could not be obtained from the fabrics woven with the braid warp yarn. Also, in fabrics woven with conventional warp yarns, it was stated that the NPR effect was obtained from fabric woven with elastane containing braid weft yarns inserted into the fabric with tension. Whereas, the fabric showed nearly zero Poisson's ratio when the braid weft yarn was inserted in slack form. [31].

This study aims to evaluate the effects of braid weft yarns with different structural parameters and also single and double layer weave structures on the auxetic performance of the fabrics. To investigate the effects of different structural parameters of the component yarns forming the braid weft yarn, non-elastane braid yarns produced with component yarns of different filament numbers and elastane braid yarns containing elastane components were used. To investigate the effect of weave structure, fabrics woven with single and double layer weaves were studied.

2. MATERIAL AND METHOD

2.1 Material

The term braid refers to the placement of the sheath yarns, made of one or more filaments released from the reels placed on the carriers in the braiding machine. They pass diagonally into each other and cross the yarn's axis diagonally without making a full rotation around each other. A basic braid structure is circular, with half of the yarn bundles moving clockwise at a certain angle to the braid yarn axis and other half moving counterclockwise directions by alternately passing over and under the first group bundles [32-34].

This study used braid yarns with different structural properties as weft yarns, and fabrics woven using single and double layer weaves were studied. The structural properties of the fabrics are presented in Table 1. Braid yarns in weft and conventional textured yarns in warp were used. All the fabric samples were produced by using 100% polyester warp and weft yarns.

Circular braid yarns (8 carriers; consisting of 8 sheath yarn components) without elastane, which are used as weft yarn in B and C coded fabric structures, were produced in Kord Endüstriyel İp ve İplik Sanayi ve Ticaret A.Ş. by attaching textured polyester and HT polyester yarns to the carrier in a 1:1 layout. To evaluate the effects of component yarn filament numbers on the auxetic performance of the fabric, the component yarns that made up the non-elastane braid yarns were composed of two different filament numbers (300/10 and 300/96 denier/filament textured polyester yarns).

The images (80 times magnification) of the braid yarns used in B and C coded fabrics under an Insize ISM-PRO digital microscope are presented in Figure 1.

Production of circular braid yarns containing elastane component (braid yarns used in X coded fabric structures) was carried out in a braiding machine with eight sheath yarns (XH110-8-8-90S Braiding Machine) (Figure 2) in Bursa Uludag University Textile Engineering Department Weaving Laboratory. Elastane braid yarns containing polyester/elastane textured yarns (150/48 denier/filament + 70 denier EL.) were employed as weft yarn seen in Figure 3.

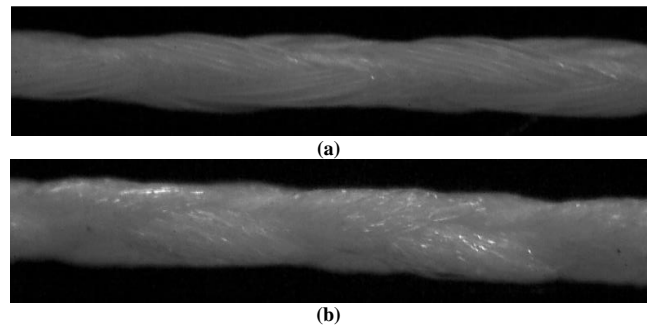


Figure 1. Microscopic images of non-elastane braid yarns (Mag: 80X) a) B coded b) C coded

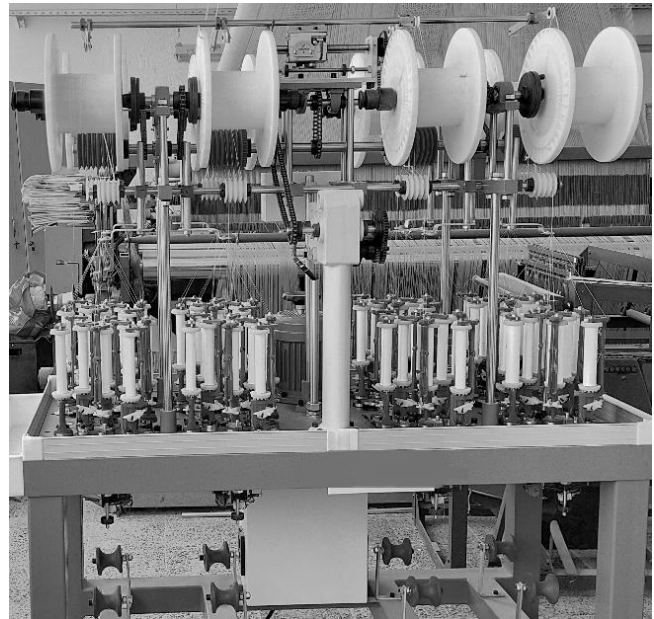


Figure 2. Braiding machine (XH110-8-8-90S)

Table 1. Structural parameters of fabrics

Fabric Code	Weave	Yarn Properties		Yarn Count [denier]		Yarn Density [thread/cm]		Yarn Crimp [%]	
		Warp	Weft	Warp	Weft	Warp	Weft	Warp	Weft
B-1	Single Layer (plain)	Textured Polyester	Circular braided yarn (non-elastane) with 8 carriers. (4x300/10 denier/filament textured polyester + 4x85/36 denier/filament HT (High Tenacity) polyester)	150	1619	66	10	13.52	6.86
B-2	Double Layer (top and bottom layer: plain)						14	16.58	8.78
C-1	Single Layer (plain)	Textured Polyester	Circular braided yarn (non-elastane) with 8 carriers. (4x300/96 denier/filament textured polyester + 4x85/36 denier/filament HT (High Tenacity) polyester)	150	1748	66	10	13.34	8.24
C-2	Double Layer (top and bottom layer: plain)						14	16.37	9.52
C-3	Double Layer (top and bottom layer: 2/1 twill)						14	12.45	11.21
X-1	Single Layer (plain)	Textured Polyester	Circular braided yarn (containing elastane) with 8 carriers. (8 x 150/48 denier/filament textured polyester (70 denier EL.))	150	2196	66	10	13.96	12.42
X-2	Double Layer (top and bottom layer: plain)						14	14.49	15.56
X-3	Double Layer (top and bottom layer: 2/1 twill)						14	15.22	17.04

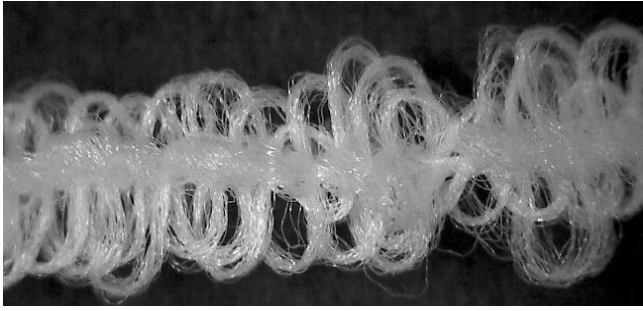


Figure 3. Microscopic images of braid yarn containing elastane (X coded) (Mag: 30X)-)

In our previous studies [30, 31], fabrics with plain weave structure, in which braid yarns were used as weft yarn, were woven on a hand weaving loom. From the results obtained, it was concluded that woven fabrics with braid yarn could show an auxetic behavior under deformation.

In this study, fabric productions were carried out on industrial weaving machines in Butik Jakar company in Bursa. Figure 4 shows the weave types used in the production of fabrics.

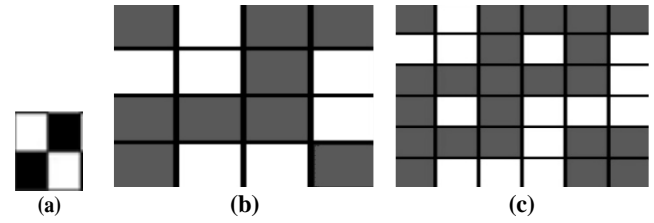


Figure 4. The weave pattern of the fabrics a) Single layer (plain) b) Double layer (top and bottom layer: plain) c) Double layer (top and bottom layer: 2/1 twill)

Photographic and microscopic (Insize ISM-PRO) (50 times magnification) images of woven fabrics with braid weft yarns are presented in Figures 5 to 7.

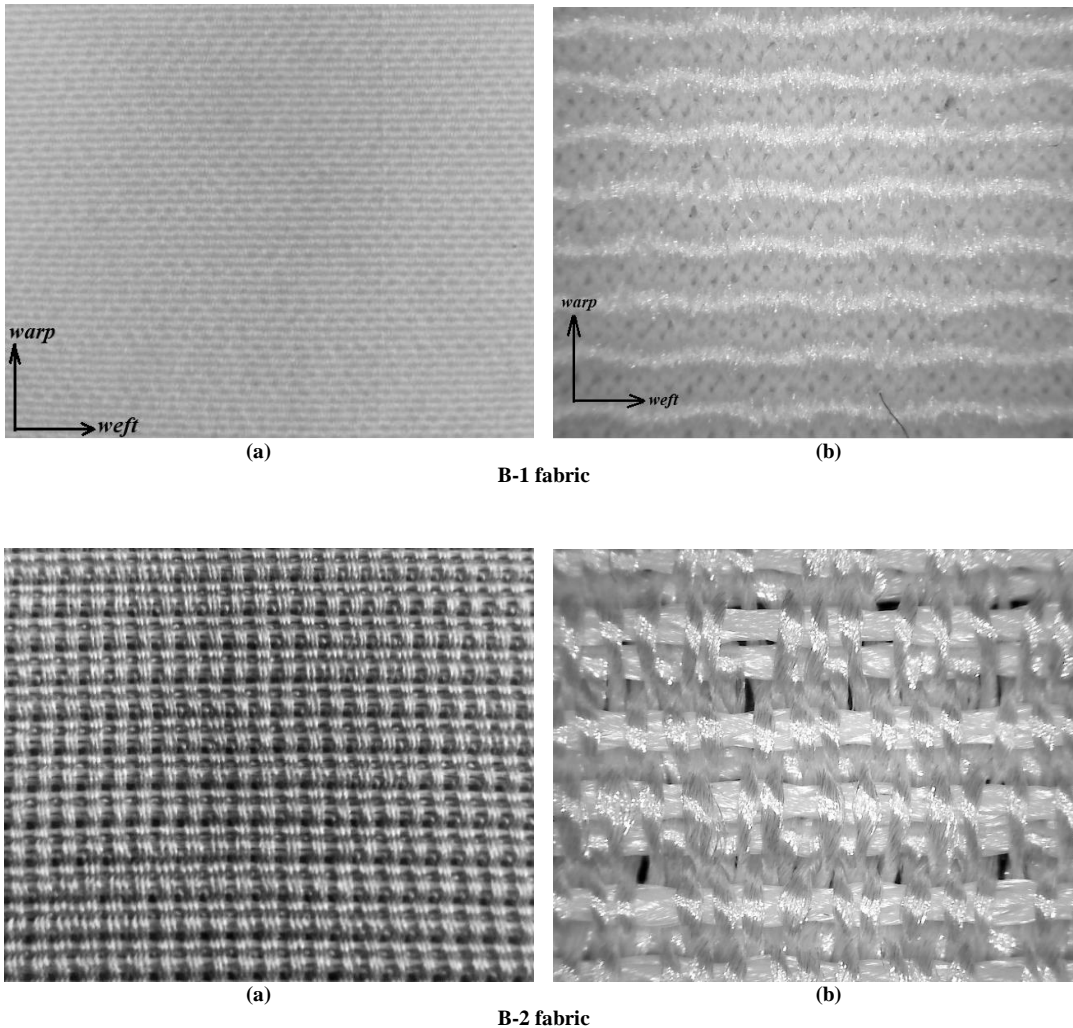


Figure 5. a) Photographic b) Microscopic (Mag: 50X) images of B coded fabrics

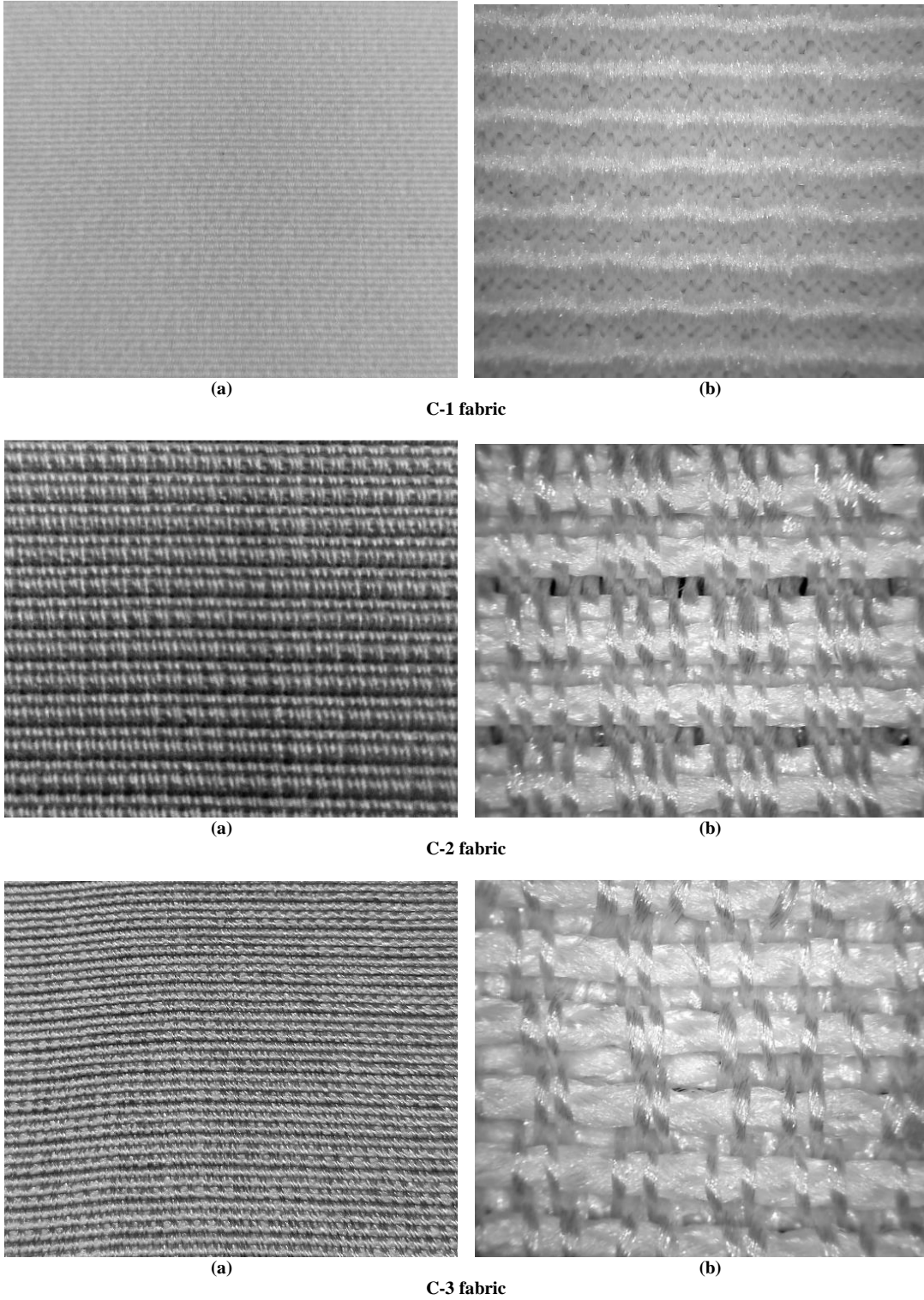


Figure 6. a) Photographic b) Microscopic (Mag: 50X) images of C coded fabrics

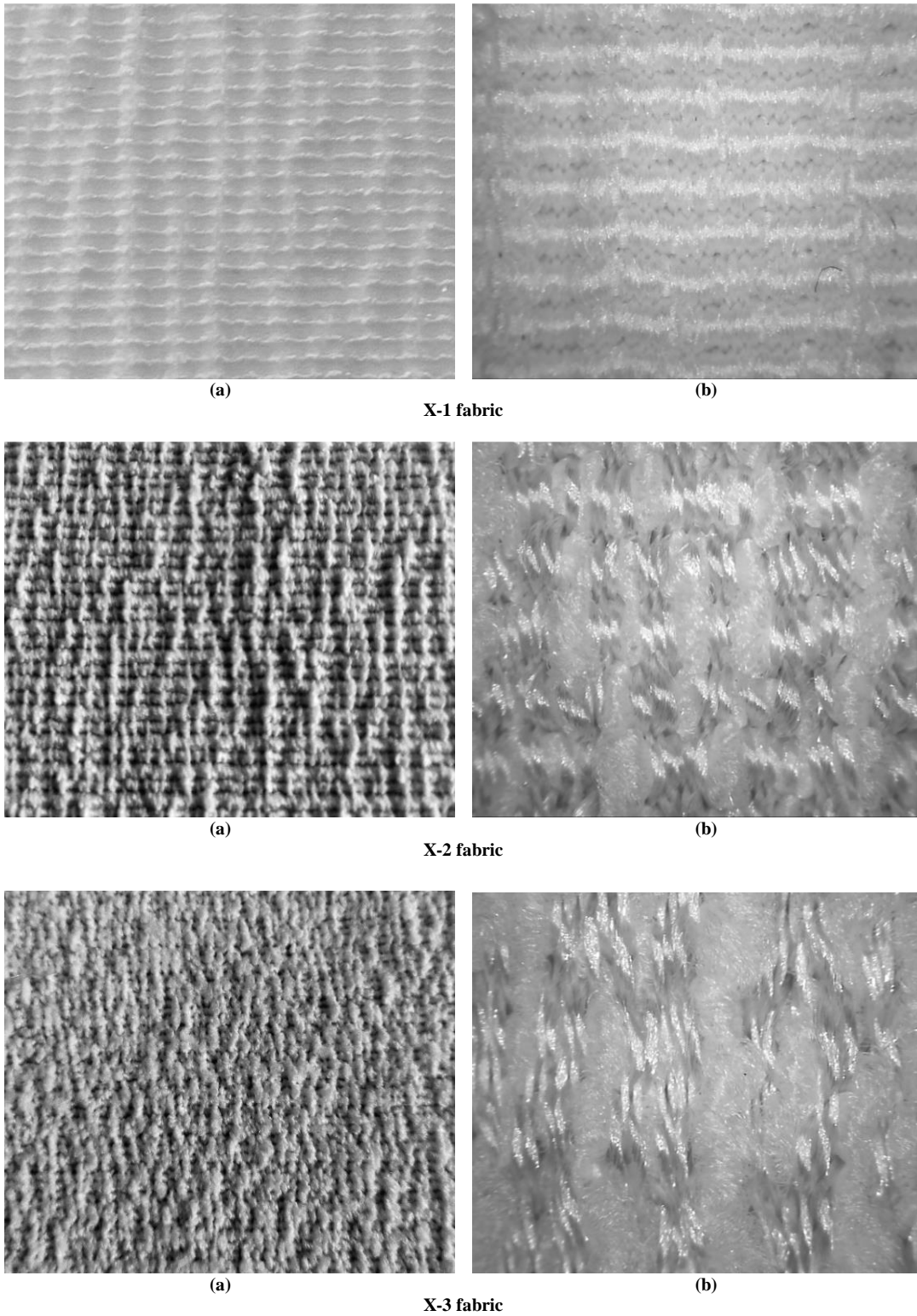


Figure 7. a) Photographic b) Microscopic (Mag: 50X) images of X coded fabrics

2.2 Method

2.2.1 Poisson's ratio measurement of fabrics

To calculate the Poisson's ratios for the evaluation of the auxetic performance of the fabrics, the fabric samples were subjected to elongation in the warp and weft directions in

the Shimadzu AG-X plus strength test device, according to the ISO 13934-1 (2013) standard test method [35]. A tensile test at a 10 mm/min speed was applied to fabric samples with a pretension obtained with 0.83 mm elongation. A computer-connected digital camera with optical zoom capability was used to record fabrics' transverse and longitudinal deformation changes under

elongation with 5 seconds intervals. A digital microscope photographed fabric samples by applying 10 times magnification (Insize ISM-PRO) (1600 x 1200 pixel resolution) with a time interval of 5 seconds (or at every 0.83 mm elongation value) until a total elongation of 20 mm (for 120 seconds) was reached during the tensile test. The setup of the testing system is presented in Figure 8.



Figure 8. Measurement setup

With the help of markers (Figure 9) placed on the fabric samples at the beginning, the changes in the width (average of x values) and length (average of y values) were calculated by measuring the distances between markers over the images taken every 5 seconds.

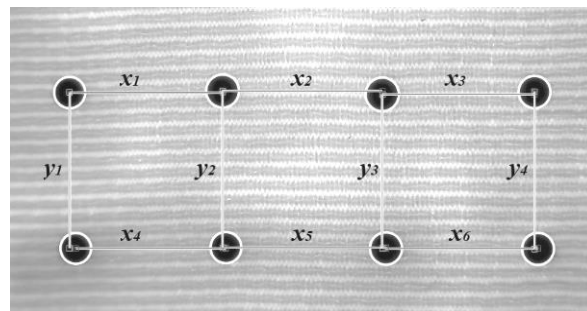


Figure 9. Placement of markers on the samples

The distances between markers placed on the fabric were measured with the help of an image processing method [36] developed using MATLAB for both the free and stretched fabric states to calculate the strains in both sample transverse and longitudinal directions. Poisson's ratio (ν) was then calculated using Equation (1) as follows [4];

$$\nu = - (\text{transverse strain} / \text{longitudinal strain}) \quad (1)$$

3. RESULTS AND DISCUSSION

3.1 Effects of the filament number of the yarn components forming the braid weft yarn on Poisson's ratio

The warp directional Poisson's ratio-elongation curves of single layer plain weave fabrics woven with non-elastane braid weft yarns (Figure 1) produced with component yarns of different filament numbers (B-1: 300/10 ve C-1: 300/96 denier/filament) are presented in Figure 10.

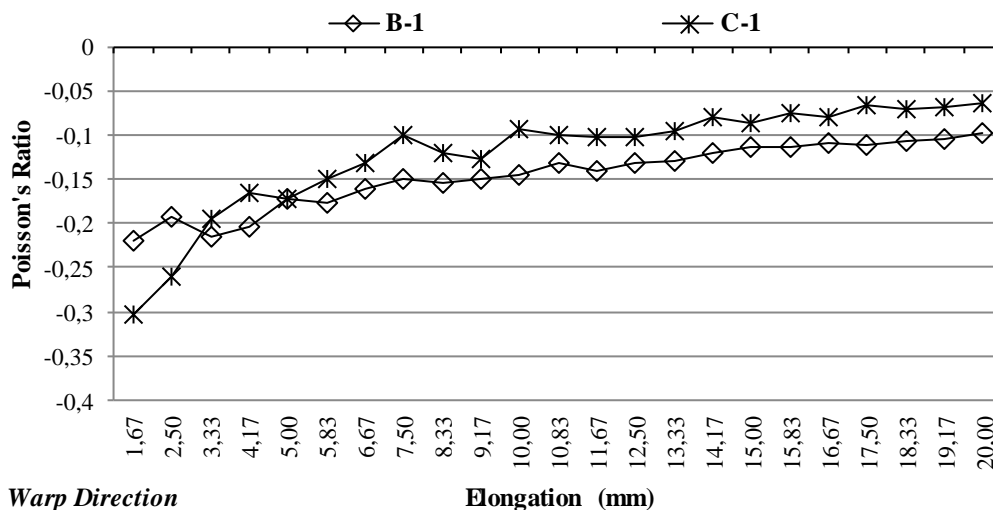


Figure 10. Poisson's ratio-elongation curve of B-1 and C-1 fabrics at warp direction

Figure 10 shows that the fabrics woven in plain weave structure with non-elastane braid weft yarns gave NPR values under 20 mm warp directional elongation. When the effect of the filament numbers of the component yarns forming the braid yarn on the auxetic performance was examined, it was seen that the C-1 fabric woven with braid yarns of high filament numbers, gave a higher NPR value than the B-1 fabric woven with low filament numbers, especially under the initial elongation values. From the results of the previous research [30], it was stated that the thickness of the braid yarn affected the auxetic performance of the fabrics, and the auxetic performance continued under higher elongation values in the fabrics woven with thick braid weft yarn compared to the fabric woven with thin braid weft yarn. A similar result was found in this study. When Table 1 was examined, it was seen that the final yarn count of the C coded braid weft yarn with high filament numbers was slightly higher than the braid yarns with low filament number. Namely, the C coded braid yarn was thicker than the B coded braid yarn. In addition, as could be seen from the images in Figure 1, the fact that braid yarn structures produced with high filament number component yarns created a more voluminous and soft structure compared to braid yarns produced with low filament number component yarns could affect the NPR of the fabrics.

The weft directional Poisson's ratio-elongation curves of single layer plain weave fabrics woven with non-elastane braid weft yarns produced with different filament number component yarns (B-1: 300/10 ve C-1: 300/96 denier/filament) are presented in Figure 11.

Figure 11 shows that the fabrics woven with non-elastane braid weft yarns gave NPR values under weft directional elongation of 5 mm. In particular, the braid weft yarns formed with component yarns of high filament numbers gave very high NPR values (≈ -1) in the C-1 coded fabric

structure, and the high NPR values continued throughout 5 mm elongation. B-1 coded fabric formed with component yarns with lower filament numbers had lower NPR values under weft directional elongation.

In weft direction, tests were carried out until 5 mm elongation because fabric structures woven with non-elastane braid weft yarns were distorted after 5 mm elongations. This distort condition might be due to more rigid and thick structure of non-elastane braid weft yarns.

3.2 Evaluation of the effects of weave structures on Poisson's ratio of fabrics

3.2.1 Evaluation of Poisson's ratios of B and C group fabrics woven with non-elastane braid weft yarns

Warp and weft directional Poisson's ratio-elongation curves of fabrics woven in single (B-1: plain weave) and double (B-2: top and bottom layer are plain weave) layer weave structures with non-elastane braid weft yarns are presented in Figure 12 and Figure 13.

In Figure 12, when the effect of single and double layer weaves on the warp directional Poisson's ratios of fabrics woven with non-elastane braid weft yarns were examined, it was seen that NPR values continued throughout 20 mm elongation in single layer structure, and up to 15 mm elongation in double layer weave structure. From the results obtained, it was seen that double layer structure and additional connection points between the layers could reduce the NPR effect.

In Figure 13, when the effect of single and double layer weaves on the weft directional Poisson's ratios of the B-1 and C-1 coded fabrics woven with non-elastane braid weft yarns was examined, it was seen that the NPR values continued throughout 5 mm elongation.

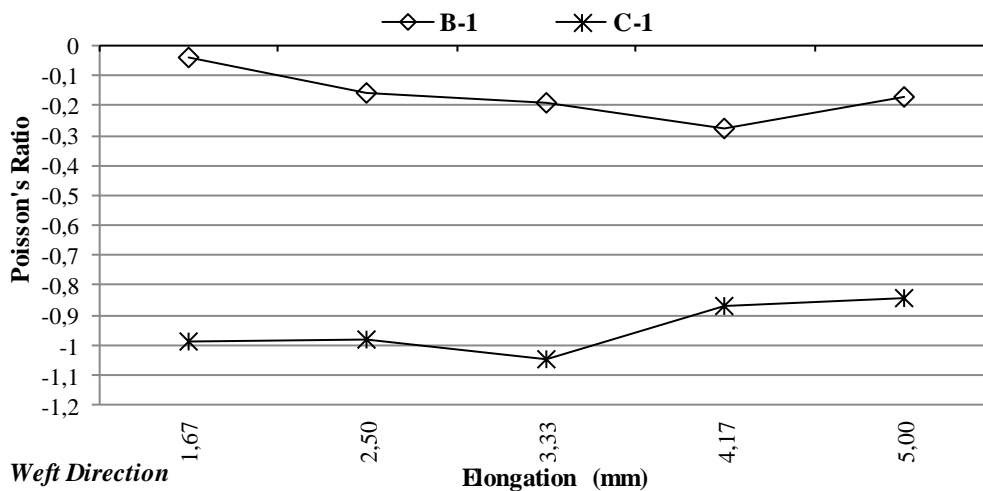


Figure 11. Poisson's ratio-elongation curve of B-1 and C-1 fabrics at weft direction

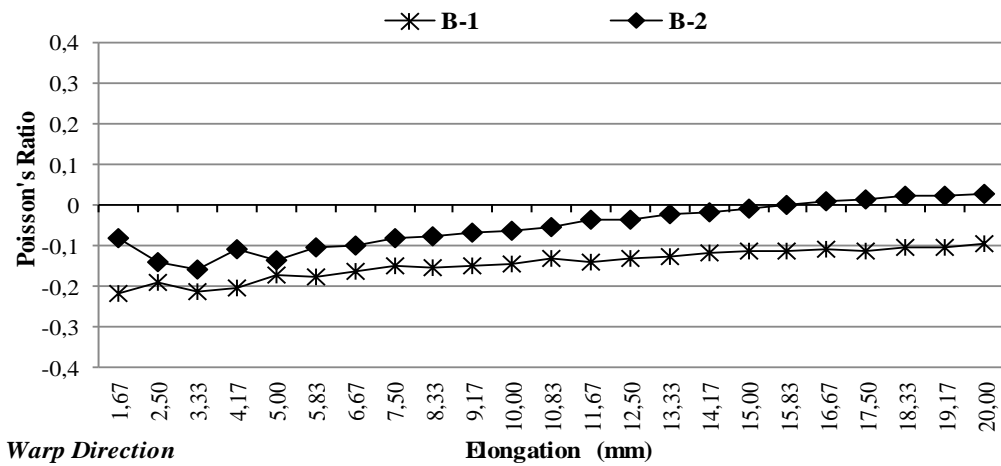


Figure 12. Poisson's ratio-elongation curve of B-1 and B-2 fabrics at warp direction

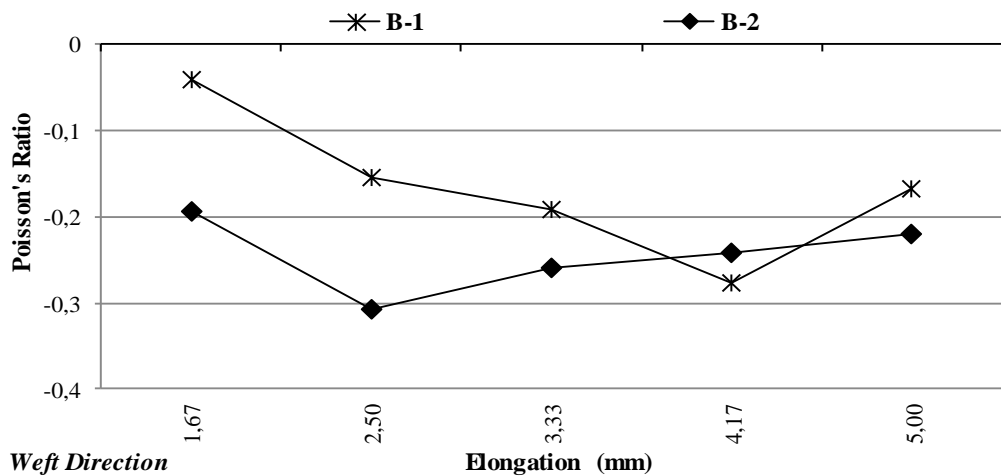


Figure 13. Poisson's ratio-elongation curve of B-1 and B-2 fabrics at weft direction

To evaluate the effects of different weave structures on auxetic performance, the warp and weft directional Poisson's ratio-elongation curves of fabrics woven with non-elastane braid weft yarns in single layer (C-1: plain weave) and double layer (C-2: top and bottom layer are plain weave; C-3: top and bottom layer are 2/1 twill weave) weave structures are presented in Figure 14 and Figure 15. In Figure 14, when the effect of single and double layer weaves on the warp directional Poisson's ratio of the fabrics woven with non-elastane braid weft yarns was examined, the C-1 coded fabric, which had a single layer plain weave structure showed NPR values throughout 20 mm elongation. The C-2 coded fabric, which had a plain weave on the top and bottom layers, showed NPR values, and Poisson's ratio approached nearly to zero at elongation values of around 20 mm. The C-3 coded fabric, which had a double layer weave structure woven in the top and bottom layer with 2/1 twill weave, gave NPR values up to around 9 mm elongation, and the Poisson's ratio turned to positive values as the elongation continued after 9 mm. The reason for this change can be the lower warp yarn crimp of 2/1 twill weave (Table 1). Figure 15 shows Poisson's ratio of single and double layer fabrics woven with non-elastane braid weft yarns. The C-1

coded single layer plain weave fabric gave a very high NPR value. In addition, this high NPR values continued throughout 5 mm elongation in weft direction. The C-2 coded fabric, which had a double layer plain weave structure, showed NPR values at initial elongation stage, and the Poisson's ratios turned to positive values as the elongation continued. NPR values were obtained for C-3 coded fabric up to 5 mm weft directional elongation but lower than single layer C-1 coded fabric.

In our previous research [30], positive Poisson's ratios were measured in the weft direction in fabrics woven with non-elastane braid weft yarn. Fabrics used in the previous research were woven on hand weaving looms. The fabrics woven on hand looms had lower warp yarn density and therefore braid weft yarns in the fabric structure did not take measurable yarn crimp. However, as seen in the fabrics examined in this study, the fabrics woven on industrial weaving machines had higher warp yarn density and caused higher crimp in braid weft yarns (Table 1). It was observed, this could cause the weft directional NPR values in fabrics woven with braid weft yarn on industrial looms.

3.2.2 Evaluation of Poisson's ratios of X group fabrics woven with elastane containing braid weft yarns

The auxetic performances of the fabrics woven with elastane containing braid weft yarns were evaluated. Warp

and weft directional Poisson's ratio-elongation curves of fabrics woven in single (X-1: plain weave) and double (X-2: top and bottom layer plain weave; X-3: top and bottom layer 2/1 twill weave) layer weave structures are presented in Figure 16 and Figure 17.

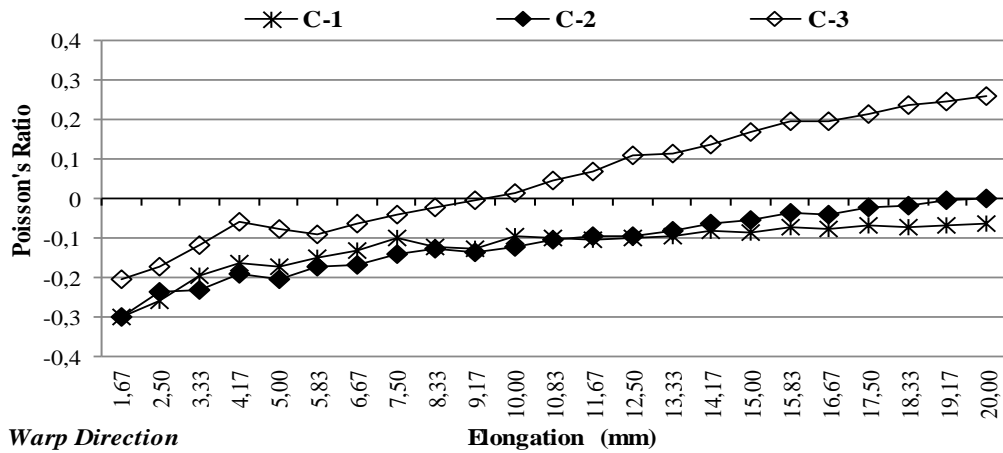


Figure 14. Poisson's ratio-elongation curve of C-1, C-2 and C-3 fabrics at warp direction

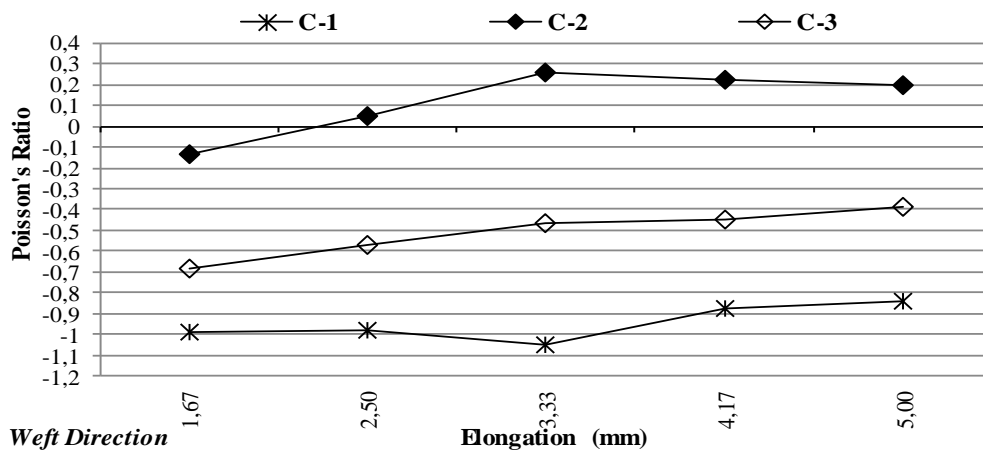


Figure 15. Poisson's ratio-elongation curve of C-1, C-2 and C-3 fabrics at weft direction

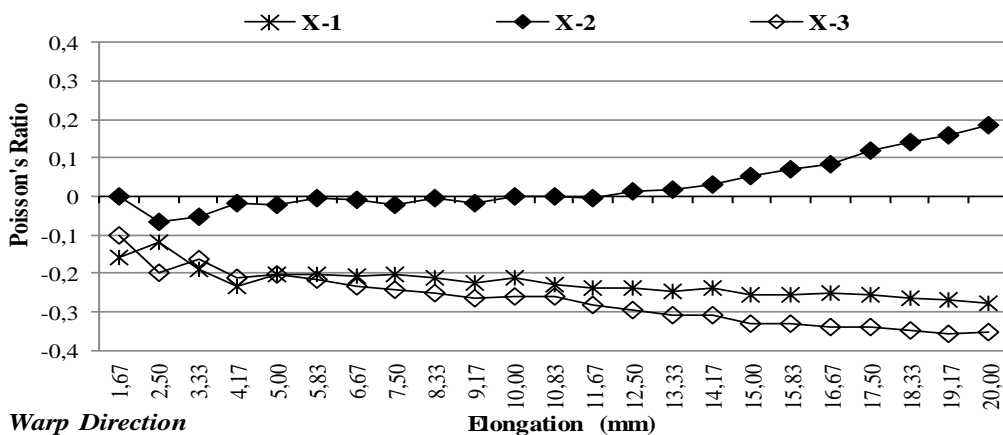


Figure 16. Poisson's ratio-elongation curve of X-1, X-2 and X-3 fabrics at warp direction

In Figure 16, X-1 (single layer fabric woven with plain weave) and X-3 (double layer fabric woven with top and bottom layer 2/1 twill weave) fabrics showed NPR effect throughout 20 mm elongation in the warp direction. X-2 fabric (double layer fabric woven with top and bottom layer plain weave) gave approximately zero Poisson's ratio values under the warp directional elongation until 11.67 mm elongation, and Poisson's ratios showed a positive trend as the elongation continued after this value. It was observed that Poisson's ratios close to zero were obtained in the double layer fabric structure (X-2) woven with elastane containing braid weft yarns, in which the plain weave structure on the top and bottom layers was used. In contrast, NPR values were produced by the fabric structure (X-3) where 2/1 twill weave caused longer yarn floats on the top and bottom layers. This result might be due to the use of a plain weave with high yarn intersections in the top and bottom layers of X-2 coded weave structure and also the formation of a tighter structure due to the effect of the elastane used in the braid weft yarn.

In Figures 14 and 16, when the warp directional Poisson's ratio-elongation curves in fabrics having non-elastane and elastane containing braid weft yarns were examined, NPR values were obtained throughout 20 mm elongation in single layer fabrics with plain weave (C-1 and X-1). However, it was observed that the effect of the weave structure was different in double layer fabrics and the properties of the braid yarns that make up the fabric had an effect on this result. While the NPR effect was observed in the C-2 coded fabric, which had a double layer weave structure woven in plain weave on the top and bottom layers with non-elastane braid yarns, nearly zero Poisson's ratios were observed in the X-2 coded fabric in the same weave structure woven with elastane containing braid yarns. This result suggests that a double layer fabric structure woven with elastane containing braid yarns and with plain weave on the top and bottom layers could limit the effect of transverse expansion under elongation. In addition, it was seen that Poisson's ratio-elongation curve tendencies of the fabrics woven with braid weft yarns

containing non-elastane and elastane components (Figure 14 and Figure 16) were different from each other. In Figure 14 and Figure 16, when the effects of the braid weft yarn structure with non-elastane and elastane yarn component on the NPR values were compared, the NPR values of fabrics woven with non-elastane braid weft yarns showed a tendency from negative to positive values under warp directional elongation. In contrast, in the fabric structures woven with elastane containing braid weft yarns (X-1 and X-3 coded fabrics), the NPR values showed a change in negative direction under warp directional elongation.

As could be seen from the NPR results of fabrics woven with elastane containing braid weft yarn, the elastane content had an improving effect on the auxetic performance of the fabrics. Fabrics woven with elastane containing weft yarn contracted in the transverse direction after the weaving process. This contraction effect could create more widening effect of the fabric in the transverse direction under the warp directional elongation of the fabrics. As a result of this, it might significantly affect to improve the auxetic performance of the fabrics.

In Figure 17, when the weft directional Poisson's ratios of the fabrics woven with elastane containing braid weft yarns were examined, it was seen that the NPR effect could be obtained from the fabrics.

To visually present the effect of the change in the transverse direction of the fabrics under elongation, the images of the transverse change of the C-1 and X-1 coded fabrics, which were chosen as the sample under different elongation values up to 20 mm are presented in Figures 18 to 20. In Figures 18-20, the distance between each marker placed on the fabric was measured by manually with the help of an Image J program. Whereas, in calculating the Poisson's ratios given in the all graphics, the distance between each marker was measured with the help of a software developed [36] in MATLAB, and the average values were taken.

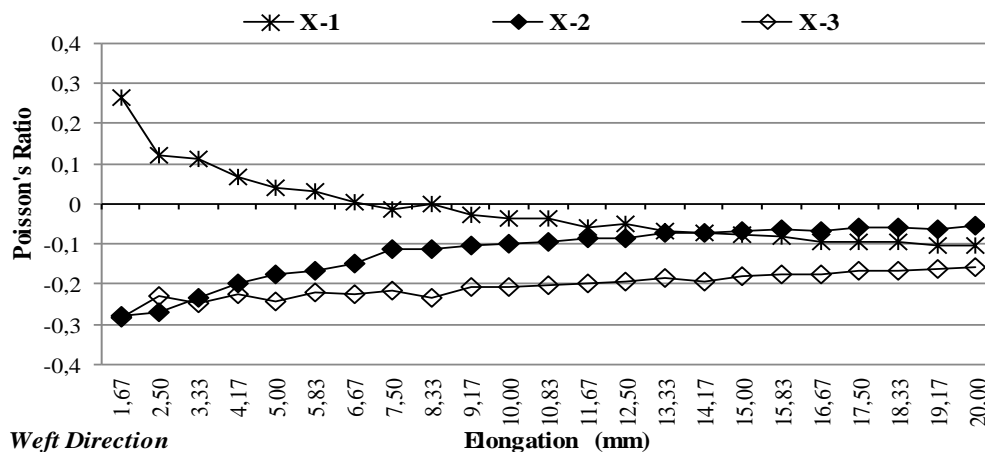


Figure 17. Poisson's ratio-elongation curve of X-1, X-2 and X-3 fabrics at weft direction

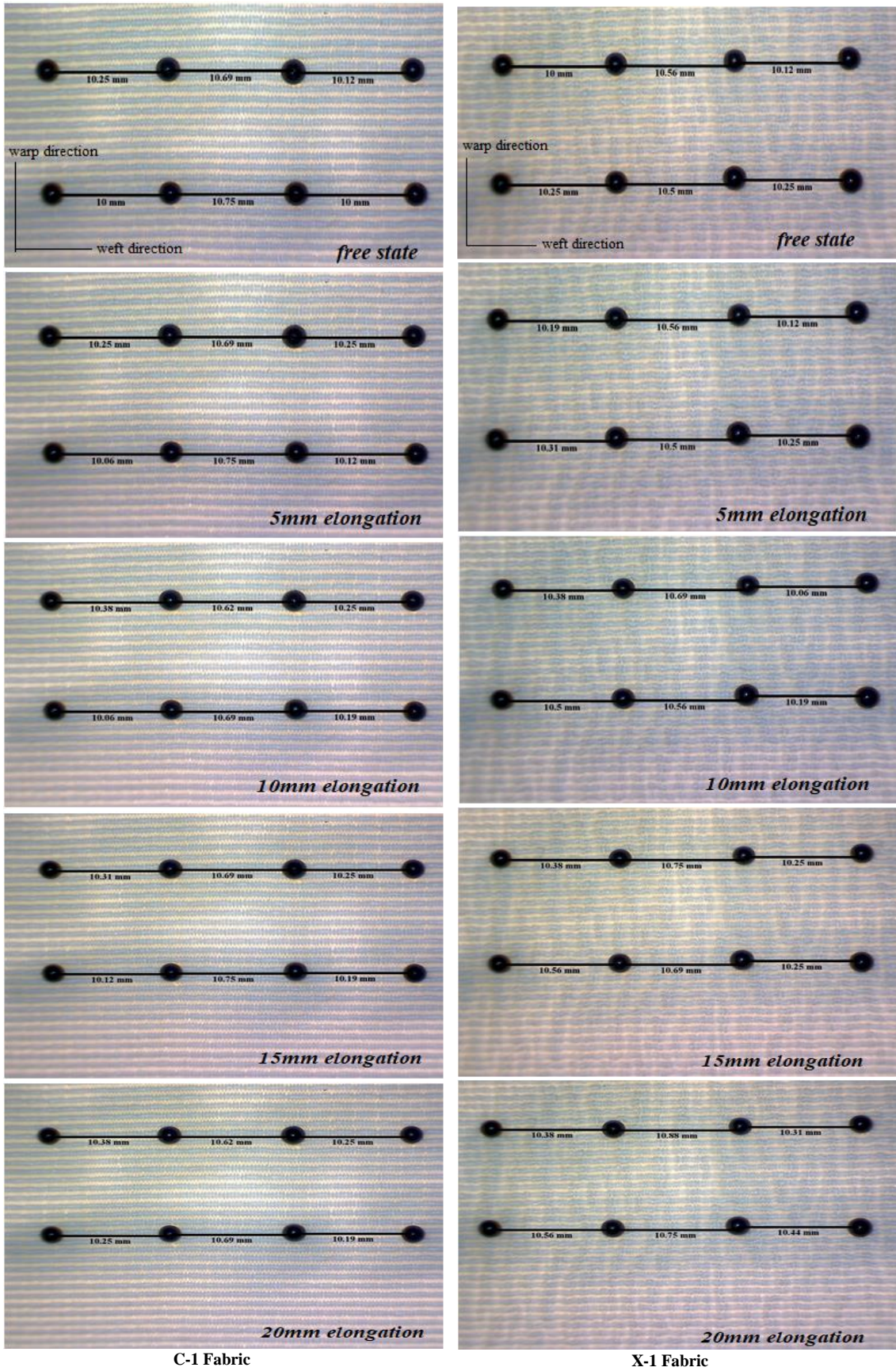
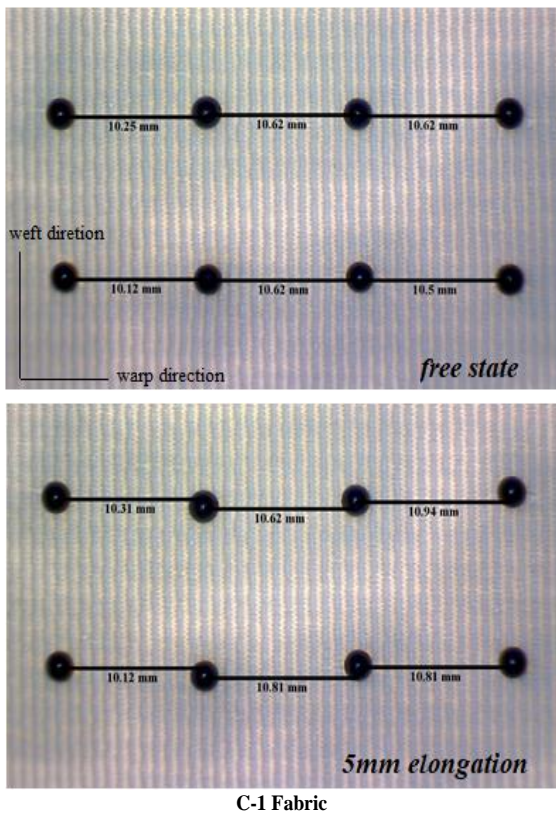
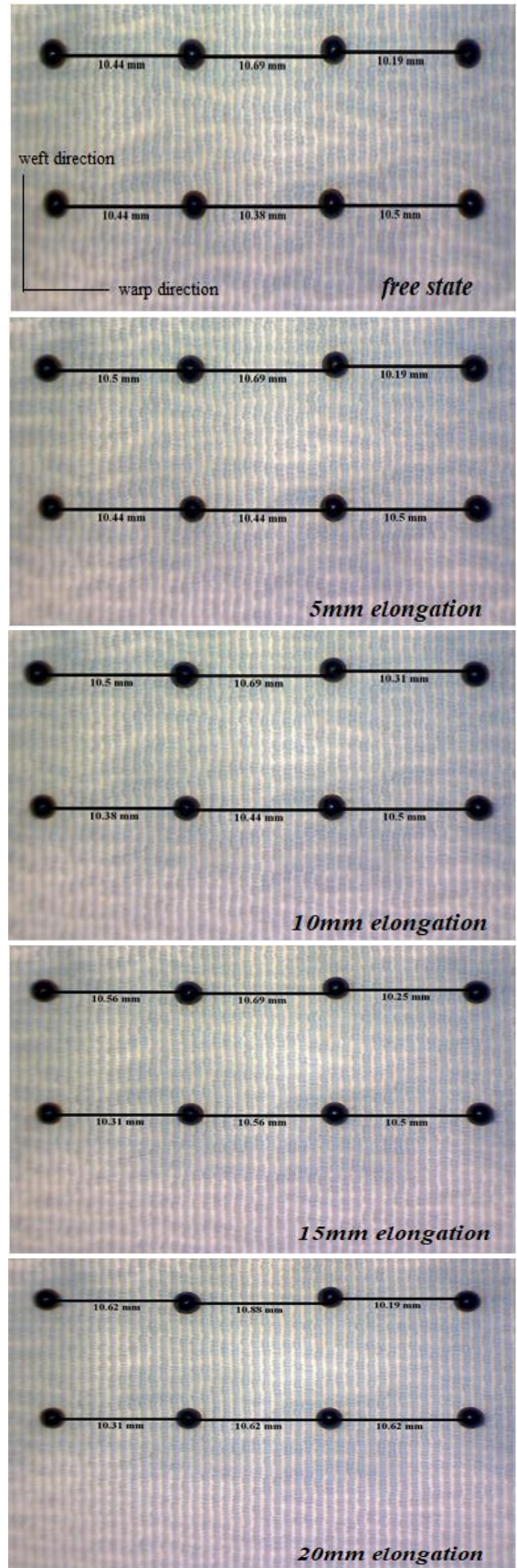


Figure 18. Changes of the C-1 and X-1 fabrics in the transverse direction under different elongation values in the warp direction



C-1 Fabric

Figure 19. Changes of the C-1 fabric in the transverse direction under different elongation values in the weft direction



X-1 Fabric

Figure 20. Changes of the X-1 fabric in the transverse direction under different elongation values in the weft direction

4. CONCLUSION

This study investigated the auxetic performances of single and double layer fabrics woven using braid yarns with different structural parameters. To investigate the effects of different structural parameters of the component yarns forming the braid weft yarn on the auxetic performance of the fabrics, the fabrics woven with non-elastane braid weft yarns having component yarns with different filament numbers and also with elastane braid weft yarns. To investigate the effect of fabric construction and weave structures, single and double layer fabrics with plain and 2/1 twill weaves were studied. In addition, the production of fabrics was carried out on an industrial weaving machine. Thus, the weavability of weft braid yarns in industrial weaving machines was observed.

Experimental results showed that the fabrics woven with non-elastane and elastane braid weft yarns both showed an auxetic performance by giving NPR values under warp and weft directional elongations. It was seen that the NPR values continued to exist throughout the 20 mm elongation, especially under warp directional elongation.

When the effect of the filament yarn number of the component yarns forming the braid weft yarn on the auxetic performance of the fabric was examined, the fabric structure woven with braid yarns consisting of component yarns with high filament numbers showed a higher NPR effect.

When a single layer plain weave fabric is compared with a double layer fabric in which the top and bottom layers are plain weave, it was seen that a double layer structure showed a reducing effect on the warp directional NPR values. It was thought that this decrease happened because of the connections between the fabric layers and connection points acted against further transverse expansion.

When the effects of non-elastane and elastane braid weft yarn structure on the NPR values of the fabrics were compared, the NPR values showed a positive tendency from negative values under warp directional elongation in fabrics woven with non-elastane braid yarns in fabric woven with single layer plain weave. On the other hand, the NPR values under elongation showed increasing absolute values in the fabric structure woven with elastane braid weft yarns. This result might be due to the elastane effect in the fabric structure. It was concluded that the fabric structure which showed more contraction in the transverse direction after the weaving process due to the effect of elastane, behaved in the opposed direction showing widening effect in transverse direction under warp directional force application.

This research has shown that fabric structural parameters and yarn construction could contribute at a significant level to the auxetic behavior of woven fabrics. In designing double layer fabrics, it must be born in mind that connections between the layers reduced auxetic effect of the fabric. For coating fabrics auxetic effect might be helpful to obtain higher covered area under tension during the processing. For some technical applications of woven fabrics auxetic behavior can be exploited and this could be considered in fabric design for such applications.

Acknowledgement

This research was supported by The Scientific and Technological Research Council of Türkiye (TÜBİTAK): Project No.119M358. The authors express sincere thanks to TÜBİTAK for their support.

The authors would like to thank Butik Jakar (Bursa) for their contribution to the production of fabrics and Kord Endüstriyel İp ve İplik Sanayi ve Ticaret A.Ş for their contribution to the supply of braid yarns.


REFERENCES

1. Ezazshahabi N, Saharkhiz S, Varkiyani MHS. 2013. Effect of fabric structure and weft density on the Poisson's ratio of worsted fabric. *Journal of Engineered Fibers and Fabrics* 8, 63–71.
2. Darja R, Tatjana R, Alenka PC. 2013. Auxetic textiles. *Acta Chimica Slovenica* 60, 715–723.
3. Yang W, Li ZM, Shi W, Xie BH, Yang MB. 2004. Review on auxetic materials. *Journal of Materials Science* 39, 3269–3279.
4. Uzun M. 2010. Negative Poisson ratio (auxetic) materials and their applications. *The Journal of Textiles and Engineers* 17(77), 13-18.
5. Carneiro VH, Meireles J, Puga H. 2013. Auxetic materials – A Review. *Materials Science-Poland* 31(4), 561-571.
6. Evans KE, Nkansah MA, Hutchinson IJ, Rogers SC. 1991. Molecular network design. *Nature* 353(6340), 124-125.
7. Evans KE, Alderson KL. 2000. Auxetic materials: the positive side of being negative. *Engineering Science and Education Journal* 9(4), 148–154.
8. Choi JB, Lakes RS. 1991. Design of a fastener based on negative Poisson's ratio foam. *Cellular Polymers* 10(3), 205-212.
9. Grima JN, Farrugia PS, Gatt R, Attard D. 2008. On the auxetic properties of rotating rhombi and parallelograms: a preliminary investigation. *Physica Status Solidi (b)* 245(3), 521–529.
10. Liu Y, Hu H. 2010. A review on auxetic structures and polymeric materials. *Scientific Research and Essays* 5(10), 1052–1063.
11. Bhullar S. 2015. Three decades of auxetic polymers: a review. *e-Polymers* 15(4), 205–215.
12. Alderson A. 1999. A triumph of lateral thought. *Chemistry & Industry* 17, 384–391.
13. Grima JN, Evans KE. 2006. Auxetic behavior from rotating triangles. *Journal of Materials Science* 41, 3193–3196.
14. Grima JN, Manicaro E, Attard D. 2010. Auxetic behaviour from connected different-sized squares and rectangles. *Proceedings of the Royal Society A: Mathematical, Physical and Engineering Sciences* 467(2121), 439–458.

15. Gaspar N, Ren XJ, Smith CW, Grima JN, Evans KE. 2005. Novel honeycombs with auxetic behavior. *Acta Materialia* 53(8), 2439–2445.
16. Attard D, Grima JN. 2008. Auxetic behaviour from rotating rhombi. *Physica Status Solidi B-basic Solid State Physics* 245(11), 2395–2404.
17. Evans KE, Alderson A. 2002. Molecular origin of auxetic behaviour in tetrahedral framework silicates. *Physical Review Letters* 89(22), 225503.
18. Hu J, Xin B. 2008. *Structure and mechanics of woven fabrics*. Cambridge: Woodhead Publications Limited.
19. Behera BK, Hari PK. 2010. *Woven textile structure: theory and applications*. Cambridge: Woodhead Publishing Limited.
20. Shahabi NE, Saharkhiz S, Varkiyani SMH. 2013. Effect of fabric structure and weft density on the Poisson's ratio of worsted fabric. *Journal of Engineered Fibers and Fabrics* 8(2), 63–71.
21. Sun H, Pan N, Postle R. 2005. On the Poisson's ratios of a woven fabric. *Composite Structures* 68(4), 505–510.
22. Shahabi NE, Mousazadegan F, Varkiyani SMH, Saharkhiz S. 2014. Crimp analysis of worsted fabrics in the terms of fabric extension behaviour. *Fibers and Polymers* 15(6), 1211–1220.
23. Ng WS, Hu H. 2018. Woven fabrics made of auxetic plied yarns. *Polymers* 10(2):226, 1-19.
24. Shukla S, Behera BK, Mishra RK, Tichý M, Kolář V, Müller M. 2022. Modelling of auxetic woven structures for composite reinforcement. *Textiles* 2(1), 1–15.
25. Zulifqar A, Hua T, Hu H. 2018. Development of uni-stretch woven fabrics with zero and negative Poisson's ratio. *Textile Research Journal* 88(18), 2076-2092.
26. Cao H, Zulifqar A, Hua T, Hu H. 2019. Bi-stretch auxetic woven fabrics based on foldable geometry. *Textile Research Journal* 89(13), 2694-2712.
27. Akgun M, Suvari F, Eren R, Yurdakul T. 2021, 18-19 June. Auxetic performance analysis of a partial stretch woven fabric structure. 8. International Fiber and Polymer Research Symposium (pp.243-245). Eskişehir, Türkiye.
28. Gao Y, Chen X. 2022. A study of woven fabrics made of helical auxetic yarns. *Applied Composite Materials* 29, 109–119.
29. Zulifqar A, Hua T, Hu H. 2020. Single- and double-layered bistretch auxetic woven fabrics made of nonauxetic yarns based on foldable geometries. *Phys. Status Solidi B* 257: 1900156.
30. Akgun M, Suvari F, Eren R, Yurdakul T. 2022. Investigation of auxetic performance and various physical properties of fabrics woven with braid yarns. *Tekstil ve Konfeksiyon* 32(3), 220-231.
31. Akgun M, Suvari F, Eren R, Yurdakul T. 2022, 4-5 November. Investigation of Poisson's ratios and some properties of fabrics woven with elastane containing braid yarn using different weft yarn tensions. 11. International Fiber and Polymer Research Symposium (pp.62-70). Gebze, Türkiye
32. Douglas WA. 1964. *Braiding and braiding machinery*. Eindhoven: Centrex Publishing Company.
33. Ko FK, Pastore CM, Head AA. 1989. *Handbook of industrial braiding*, Covington, KY: Atkins & Pearce.
34. Karaca Bayraktar, E. 1999. Investigation of effects of monofilament and braid structures of silk, polyamid 6, polyester, polypropylene sutures on some of the mechanical properties. PhD Thesis, Uludag University, Bursa.
35. ISO 13934-1. 2013. Textiles – Tensile properties of fabrics – Part 1: Determination of maximum force and elongation at maximum force using the strip method.
36. Suvari F, Akgun M, Eren R, Yurdakul T. 2021. Determination of deformation behavior of woven fabrics under stress using image processing method. *Uludağ University Journal of the Faculty of Engineering* 26(2), 661-678.

Investigation of Style and Design Characteristics of Women's Outerwear with a User-Centered Design Approach

Hatice Harmankaya¹  0000-0001-6375-7586

Meltem Özsan²  0000-0001-6217-4602

¹ Selcuk University / Faculty of Architecture and Design / Department of Fashion Design / Konya, Turkiye

² Kahramanmaraş Sutcu Imam University / Faculty of Fine Arts / Department of Textile and Fashion Design / Kahramanmaraş, Turkiye

Corresponding Author: Meltem Özsan, meltemozsan@gmail.com

ABSTRACT

This study aims to develop a design process model within the scope of the Design Thinking approach with Kansei Engineering support and to experientially apply this model. Additionally, another aim of the research is to investigate the affective/emotional preferences of female users regarding visual and functional aspects of outerwear designs, and subsequently develop alternative design model proposals in alignment with users' preferences. In this study, the 'Stanford d.school Design Thinking Model' was utilized. Research data was obtained through a survey consisting of two sections, involving the opinions of female consumers aged between 18 and 60 residing in Istanbul. The first section includes a Likert-type scale to examine users' outerwear design preferences. In the second section, a semantic differential scale was prepared to evaluate jacket, coat, and overcoat designs using Kansei words. The reliability of the measurement instrument was established through calculated Cronbach's Alpha coefficients, presented after each scale, confirming the reliability of both scales for this sample. The Kansei evaluation shows that the Design Thinking process model makes it possible to create designs that meet users' emotional needs.

1. INTRODUCTION

In the contemporary context, consumers demonstrate a heightened interest not solely in the fulfillment of product-related requirements, but also in the congruence between the visual and functional attributes of a product and their emotional and affective states. At this point, design is approached as addressing the current need as a problem. The design aims to solve an existing or anticipated problem that the designers first try to identify the problem, following which they conduct numerous studies to ascertain the solution [1]. To understand the consumer closely and meet their needs and desires in the best possible way, organizations engage in various pursuits. This is because, for all units offering products and services to the consumer, knowing the consumption habits of the customer who will purchase the new product is highly crucial. A product that can meet the expectations and needs of the consumer and is liked and accepted by the consumer, achieves success [2]. In this way, the designer can offer products that touch the user's eyes, heart, and of course, needs by using their

knowledge, experience, observations, empathy, and making correct decisions [3]. However, solutions created solely based on observation or intuition tend to remain superficial in capturing the consumer and the user cannot establish a connection with the product. Therefore, beyond traditional disciplines, design-based practices need to be adopted to protect the investments made, the effort expended, and the idea that has turned into a product. At this point, the "Design Thinking (DT)" approach comes into play to correctly perceive the problems and solve them with appropriate methodologies.

DT is an interdisciplinary thought system located at the intersection of business, design, engineering, and social sciences [4], and it is used for various purposes [5]. This situation has made it difficult to reach a consensus on the definition of DT and to agree on a single definition [6]. In general, DT provides a systematic and collaborative approach to overcoming 'wicked problems' and finding desirable solutions for users [7, 8, 9, 10, 11].

To cite this article: Harmankaya H, Özsan M. 2024. Investigation of Style and Design Characteristics of Women's Outerwear with a User-Centered Design Approach. *Tekstil ve Konfeksiyon*, 34(4), 409-423.

In wicked problems, even defining the problem itself can be difficult, let alone finding a solution. Therefore, there is a need for answers that anticipate how the problem may evolve and change, rather than seeking a single answer [3], and solutions are sought through the components of empathy, collaboration, optimism, and experimentation. In this process, external stakeholder perspectives such as users, customers, engineers, producers, and employees who decide on the feasibility of the solution are considered [12]. The DT approach employs a cognitive strategy in the process [13]. Here, a way of thinking is mentioned where the coordinated inclusion of information and stakeholder perspectives is required to transform the acquired knowledge into a new idea. This way of thinking is "moving creativity", arguing that designers not only rely on facts but also act based on intuition and assumptions [8]. Designers consider discipline and methodology as the essence of design and problem-solving processes [3]. Based on this point, DT addresses two different discourses in research [14]. The first one is "designerly thinking," and the second one is "design thinking." The "designerly thinking" discourse aims to develop a theoretical framework for transferring the practices and competencies of designers to the literature of the field. DT on the other hand, has been used to describe the characteristics of design practice that extend beyond the design context (including art and architecture) and is particularly used by those who do not have an academic background in design, especially in the field of management.

According to Tim Brown, one of the founders of the famous design firm IDEO popularized the concept of DT, it is not necessary to have professional design education to apply this approach [15]. Brown believes that individuals who possess a natural ability that can be uncovered through proper development and experience, and who are empathic, observant, curious, experimental, and optimistic, can apply this methodology. Schmiedgen et al. confirmed Brown's views by stating that DT is applied in organizations of all sizes and industries [16]. Many researchers have examined how DT provides a competitive advantage through innovation. For instance, in his study, Martin emphasized how DT facilitates knowledge development and enables businesses to generate innovative solutions, ultimately leading to a competitive advantage [17]. On the other hand, Balakrishnan views DT as a strategy that fosters creativity and suggests that effective learning practices should be developed in institutions that include design education [18].

As emphasized by most researchers, the DT approach is not only effective in stimulating students' creative abilities but also an effective strategy for generating creative solutions in the public or private sector.

In the literature, various DT approaches utilized by different disciplines can be found [5]. Herbert Simon examined the DT Process in seven stages: 1. Empathize, 2. Define, 3. Ideate, 4. Prototype, 5. Test, 6. Implement, 7. Learn [19]. Dunne and Martin evaluate the process in an iterative structure, arguing that the process starts with ideation, continues with deduction, and the idea is put into practice with testing and the results achieved with induction can be generalized [21]. As can be seen here, regardless of the number or name of the design process steps, a similar path that starts with problem definition and ends with problem-solving is followed [21]. This study benefits from the design thinking process model developed by the Hasso Plattner Institute of Design at Stanford University (d.school).

The Stanford d.school, "is a place where people use design to develop their creative potential" and it is a leader in teaching and applying DT [22, 23]. Since 2005, when it added DT courses to its engineering curriculum, the university has been teaching students how the approach works on a scientific basis and what factors ultimately contribute to the success of such innovation [24, 25, 26]. In recent years, design institutes such as d.school have become more widespread, and there have been discussions at academic institutions such as Postdam, Harvard, and MIT about how this approach can be integrated into non-design fields. Stanford School has developed a methodology for creative problem-solving that is based on Simon's (1969) proposed model. This methodology encourages creative, multidisciplinary teamwork through the DT approach [25, 27]. The model consists of six stages and as shown in Figure 1, these steps are not placed in a linear sequence. The steps can be repeated and moved forward and backward between stages based on the requirements of the findings obtained from each step. The responsibility for deciding when to move on to which stage and how the entire design process will be conducted lies with the design team [28].

In 2009 and 2010, the six-stage model was developed and transformed into a five-stage DT process model (Figure 2). This model consists of the following steps: 1. Empathize, 2. Define, 3. Ideate, 4. Prototype, and 5. Test.

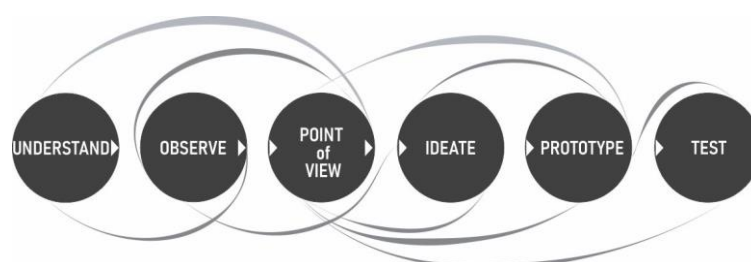


Figure 1. The Six-Stage DT Model Proposed by The Stanford d.school [29].

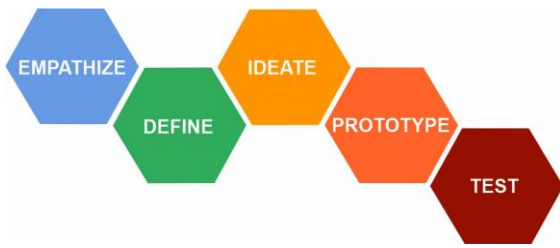


Figure 2. The Five-Stages of DT [30]

The first stage of the DT process model is related to understanding the consumer's perspective. In this stage, the designer interacts with the consumer using techniques such as observation, interviews, and others to gain common insights and develop empathy for the stakeholders of the design problem [31, 3]. In the define stage, the collected data is analyzed and shared with team members to form a perspective on the design problem. In the ideate stage, creative and feasible ideas are developed for the problem at hand. In the subsequent process, a prototype is carried out, which involves transforming ideas and concepts into tangible representations and enables feedback from users or other stakeholders. Test processes are conducted to collect this feedback and further improvements and revisions are made based on it. At this point, information is obtained about the design's ability to meet consumer expectations through user feedback, and this information is taken into consideration to achieve a better design. However, that viewing design only as a problem-solving approach may lead to a narrow perspective, states that the psychological impact of design is also significant [1]. While the designer uses the design language to add meaning to the product, the consumer also expects the design to be in harmony with their emotional expectations, along with meeting their physiological needs.

While it is unclear which technical features of the designs that are compatible with the emotions and feelings of the consumers will evoke the desired emotions and feelings, Kansei Engineering (KE) makes the human mind and heart more visible by offering a new approach to new product development [32, 33]. KE, developed by Mitsuo Nagamachi, offers a consumer-oriented approach to new product development [34, 32, 35, 36, 37]. Kansei, which has its roots in Japanese culture, refers to the impression formed in the human mind because of interaction with an object, such as emotions, feelings, thoughts, and attitudes. KE is a methodology that combines the fields of Kansei and engineering to integrate human Kansei into product design to produce products that consumers will enjoy and be satisfied with [38, 32, 39, 40].

KE utilizes customer emotions as input and seeks to find the relationship between these emotions and product features [41]. In this methodology, the design product is initially evaluated with Kansei words based on the consumer's emotional expectations. Therefore, all adjectives in the relevant field are thoroughly researched

and accumulated in a pool of words. Synonymous words are grouped, and the words that best express the meaning are selected. These identified words are paired with their antonyms. The word pairs are then used in a scale prepared for data collection in the research process [36]. The consumer rates the product image on the scale according to the values between contrasting words [42, 43, 44]. The collected data is analyzed through multivariate analysis. As a result of the analysis, statistical relationships between Kansei words and design elements can be observed. This enables the determination of the qualities and categories of design that evoke positive emotions in the consumer, thus informing the design of future products with these attributes taken into account [32].

Nowadays, most designs remain weak in achieving sufficient compatibility with consumers' needs, habits, emotions and feelings, behaviors, and preferences. Therefore, there is a need for new and improved approaches for participation in design development or new product design processes.

This study aims to develop a design process model that can be utilized for design in various fields within the context of design thinking, supported by the Kansei Engineering product design methodology. The model is intended to be experientially tested and any shortcomings identified during the process were aimed to be addressed. The advantage of this model is the testing of the compatibility of prototypes with consumer expectations. Additionally, the feelings and emotions aroused by these expectations are measured to determine which technical parameters of the product influence these emotions. As a result, designers and manufacturers can direct themselves toward creating designs that evoke desired emotions in consumers and generate new images in harmony with these emotions. In pursuit of these objectives, the research explored outerwear season trends, identified consumer expectations, and developed contemporary designs based on this information. Digital prototypes were created to examine the alignment of these designs with consumer preferences, and the Kansei Engineering product design methodology was utilized during the testing process. As a result of the findings, design elements influencing emotional expression in consumers were determined. Accordingly, alternative design model suggestions were formulated using design elements that elicit positive emotions to create products that are in complete alignment with consumer preferences.

2. MATERIAL AND METHOD

2.1 Material

In this research, a design process model was developed to identify the emotions and sentiments of consumers related to jacket, coat, and overcoat models within the category of outerwear. The aim was to demonstrate how these expectations could be incorporated into the design process.

The effectiveness of the model was then tested through practical application. The main aim of selecting outerwear in the proposed model is that the style and design differences applied to outerwear models are more long-lasting compared to other types of garments, and certain criteria dominate in terms of functionality in every season. At the same time, while certain basic technical criteria remain fixed in clothing belonging to the outerwear type, modular attachments emphasizing functionality are included. Detachable and adjustable features such as length or width can enhance product versatility and expand the range of uses for the garment. In the study, it was paid attention to reflecting current preferences and fashion trends when creating designs for jackets, coats, and overcoats.

2.2 Method

Within the scope of the research, a descriptive (survey) method was employed. This method allows for the collection of information from a broad sample group using data collection tools such as surveys and interviews [42, 43, 44]. Within this context, the study's population comprises female consumers aged between 18 and 60 residing in Istanbul, chosen due to the researcher's ease of access. According to information obtained from the 2022 address-

based population registration system, the number of women aged 18-60 residing within the borders of Istanbul is 5.107.629 [45]. However, reaching the entire population of the province would be challenging, so a sample group representing the population has been determined. The sample size of the study (Figure 3) has been calculated according to the following formula [46]:

$$n = \text{Population: } 5.107.629$$

$$z = \text{Confidence Coefficient (for a 90\% confidence interval): } 1,645$$

$$SE = \text{Standard error: } 0,05$$

The variance of the variable: 0,5

Applying the data to the formula resulted in a required sample size of 270 individuals for the desired confidence interval. For this study, a snowball sampling method was employed, reaching 347 female consumers residing in different neighborhoods of Istanbul. After excluding incomplete surveys, 342 data points were included in the analysis.

In this study, a process model applicable in the field of design was developed within the framework of the DT model with the support of KE and was presented in Figure 4.

$$\frac{n \cdot z^2 \cdot (0.5)^2}{(n-1) \cdot SE^2 + z^2 \cdot (0.5)^2} = \frac{5.107.629 \cdot (1.645)^2 \cdot (0.5)^2}{(5.107.629-1) \cdot (0.05)^2 + (1.645)^2 \cdot (0.5)^2} = 270$$

Figure 3. The formula to calculate the sample size in research

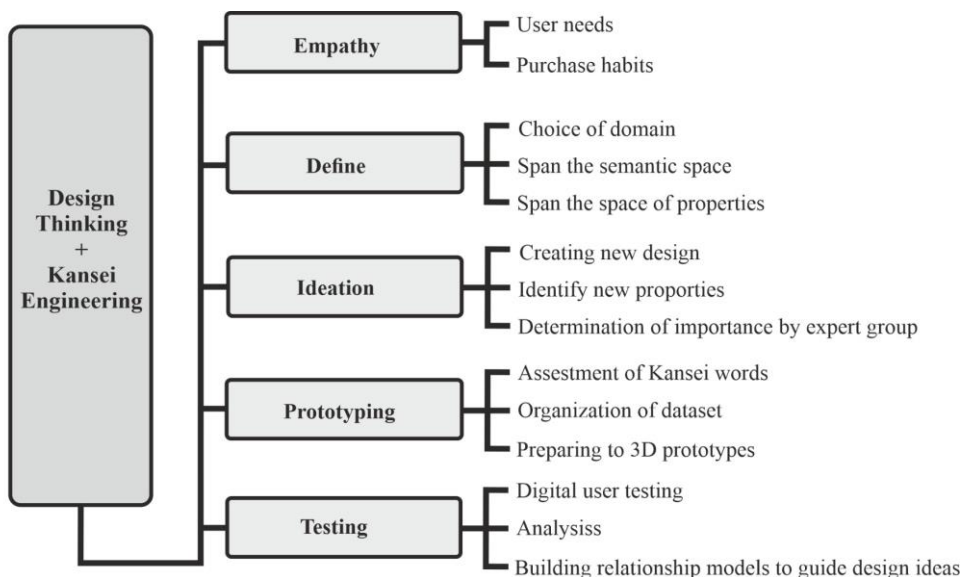


Figure 4. The general flowchart of the model

The steps of the design process model presented in Figure 4 are explained in detail in the following sections:

Phase 1: Empathy

In this stage, alongside the literature review, the preferences, expectations, and encountered issues of the

female consumers comprising the target group of the research were investigated concerning outerwear. Women's outerwear models present in the fashion market were examined. These models were categorized into three main headings: jackets, coats, and overcoats. These categories formed the design focus of the research. To measure

consumers' emotional expectations towards outerwear models and ensure that the developed designs reflect current preferences and seasonal trends, the research incorporated visual and written materials from trend seminars, fabric, and accessory swatches obtained from fashion and textile fairs, fashion trend catalogs, and fashion magazines. In this context, trends in terms of outerwear colors, fabrics, and main patterns were thoroughly investigated.

Phase 2: Define

The outerwear categories of jackets, coats, and overcoats themselves comprise numerous fundamental design attributes, and each of these design attributes further contains a multitude of subcategories. These attributes that should be present in any outerwear product generate emotions and sentiments in the consumer towards the product, subsequently influencing their preferences. Therefore, national, and international visual and written sources, fashion magazines and catalogs, as well as websites were utilized to explore the common fundamental design features and subcategories related to outerwear. These were compiled and presented in Table 1.

Phase 3: Ideation

During this stage of creating sketches for outerwear designs, the number of sketches to be generated for each type of garment was initially determined. The number of sketches was decided while considering the final number of products that would be included in the research scale. It is believed that by creating a significantly larger number of design sketches than the products included in the scale, there will be a wider range of design alternatives to choose from, increasing the chance of incorporating a diverse set of models in the study. It has been decided to create an equal quantity of jacket, coat, and overcoat models for each of the three different types of outerwear. Guided by this notion, considering consumer expectations and seasonal trends, the researcher prepared preliminary design sketches for each type of outerwear, including 15 jackets, 15 coats, and 15 overcoats. To broaden the scope of usage for the products, modular details that allow for personalization were added in addition to visual characteristics. The modular features, which can be attached or removed and have adjustable length or width, were provided by zippers, buttons, and snaps.

Table 1. Design features and parameters for outerwear

Attributes	Categories
Garment type	Jacket, Coat, Overcoat
Form/cut	Slim fit, regular fit, classic fit, oversized fit
Length	Crop, short, regular, long, extra long
Modular (length)	Basic, detachable, adjustable length
Collar design	Crew neck, stand, turnover, shawl collar, lapel neckline, v-necked
Fiber-filled	Yes, No
Hoodie	Yes, No
Shoulder pad	Yes, No
Shoulder epaulettes	Yes, No
Shoulder design	Dropped shoulder, standard structured shoulder
Sleeve model	Set-in sleeve, raglan sleeve, batwing sleeve, sleeve with gathered sleeve head, kimono sleeve, dolman sleeve
Sleeve length	Full length, bracelet, three-quarter
Modular (sleeve)	Detachable, basic, adjustable length or width
Sleeve cuffs	Standard blazer sleeve with vent and buttons closed cuff with topstitching, straight/cuffless, classic shirt cuff, classic trench coat cuff with strap, double/french, wing, circular, roll-up, ribbed/knitted, piping, button tab, sports cuff with zip
Closure type	Single-breasted button closure, Double-breasted button closure, Zipper, double-breasted zipper closure, button closure, and removable belt, snap button closure
Pocket number	Multipocket, pocketless
Pocket model	Fleto, patch, pocketless
Flap-pocket	Yes, No
Modular (pocket)	Detachable, basic
Flap-pocket design	Angled, oval
Belt	Removable belt, unbelted
Hemline	Straight, gathered, fringed
Side seam	Basic, two-side slit/zippered/snap-on



To narrow down the selection from the preliminary design sketches for each type of outerwear and determine the designs to be included in the research data collection scale, the opinions of fashion designers were sought. For this purpose, the preliminary design sketches for each garment type were numbered from 1 to 15. The fashion designers responsible for the selection were required to have active experience working as fashion designers in the design departments of established companies and possess a minimum of 5 years of experience. The views of 7 fashion designers, denoted as 'D,' who met the specified criteria, were taken into consideration. In the study, the personal information of the designers was kept confidential and coded as D1, D2, ..., and D7 with designer and distinctive serial numbers. Designers were asked to make five selections for each type of outerwear and the three most preferred jacket, coat, and overcoat designs were included in the research scale. Table 2 shows the preferences of each designer, with the code representing the designer in the row corresponding to the garment type.

Numbers have been used as labels for the outer garment design sketches prepared in the study. Additionally, colored columns have been utilized to indicate the frequencies of

the jacket, coat, and jacket models proposed by the designers for use in the study.

As shown in Table 2, most designers recommended the 2nd, 8th, and 10th jacket models. For coat models, since designer opinions converged on the 2nd and 10th models, these designs were used in the study. As for the last coat model, as designer opinions were evenly distributed, the researcher selected a design that was perceived to be distinct. For women's overcoat models, it can be observed that designers primarily recommended the 9th and 10th models. In the last overcoat model, since the vote counts were evenly distributed among different models, the researcher chose a model with distinct features to be used in the study.

Phase 4: Prototyping

The 3D digital prototypes of the three most preferred jacket, coat, and overcoat designs in line with the designers' views were prepared using the CLO 6.0 software, which offers true-to-life 3D garment simulation (Figure 5). Since the color factor is considered to have a variable effect on consumer perception, only plain beige color was used in all models.

Table 2. Designer opinions on 3D outerwear designs

	Jacket					Coat					Overcoat				
D1	2	4	6	7	8	2	3	5	13	14	1	3	5	9	10
D2	1	2	5	8	11	1	8	10	11	15	2	3	6	10	11
D3	2	8	10	14	-	2	5	8	12	13	7	9	10	15	-
D4	1	2	8	10	11	1	2	8	10	14	2	6	9	10	11
D5	2	4	8	9	13	2	5	10	12	15	1	4	7	8	9
D6	2	4	8	10	13	2	5	8	10	12	2	8	9	10	15
D7	2	5	8	10	14	3	6	10	12	13	1	9	10	12	15

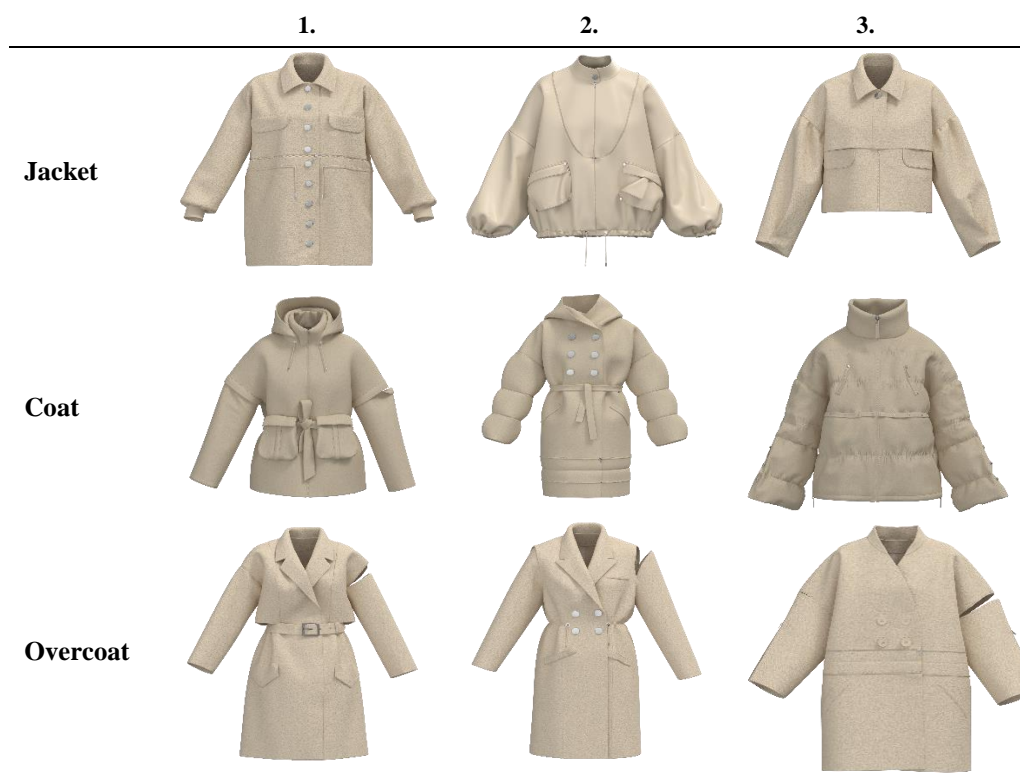


Figure 5. 3D view of determined outerwear models

At this stage, the researcher extensively investigated adjectives expressing the emotions and sensations evoked by clothing in users, utilizing a diverse range of sources. Various sources such as magazines, user forums, and shopping websites, catalogs as well as articles, theses, and conference papers, were used for this purpose. The collected words were examined, and identical or synonymous words were excluded from the pool. Next, all Kansei words were categorized into two different semantic sets as visually and functionally. Each word was paired by matching them with their opposites found in their respective word groups and Kansei word pairs (i.e. multiple emotional attributes) were created. Due to the large number of Kansei word pairs, the word pairs to be used in the study were determined with expert opinions (*The expert group consists of 5 academics who are affiliated with different universities in the field of fashion design.*). A total of 14

pairs of Kansei words representing visual meanings and 12 pairs representing functional meanings are included in the final semantic scale, as shown in Table 3.

Phase 5: Testing

Within the scope of the research, a scale was developed to measure the perceptions and emotions evoked by the created outerwear designs in consumers. The scale consists of two parts. The first part includes a Likert-type 5-point scale measuring the users' personal information and outerwear design preferences. In the second part, the perceptions and emotions evoked by the outerwear designs in participants are measured. For this purpose, a 7-point semantic differential scale (SD) has been used.

1. *Evaluate the jacket design in the image according to your emotions and feelings using adjectives representing visual and functional meanings and assign scores in a way that best aligns with your preferences.*

Table 3. The selected pairs of Kansei words

Visual assessments		Functional assessments	
K01	Random - Meticulous	K01	Unpractical - Practical
K02	Exaggerated - Simple	K02	Uncomfortable - Comfortable
K03	Classic - Modern	K03	Non-durable - Durable
K04	Similar - Unconventional	K04	Single - Multi-functionality
K05	Meaningless - Meaningful	K05	Hard to maintain - Easy
K06	Ordinary - Interesting	K06	Disturbing - Satisfying
K07	Unstylish - Stylish	K07	Incompatible - Compatible
K08	Dull - Cool	K08	Undiversifiable - Diverse
K09	Complex - Simple	K09	Mass-produced - Personalized
K10	Rough - Elegant	K10	Non-customizable - Customizable
K11	Ugly - Aesthetic	K11	Not suitable for the need - Suitable
K12	Serious - Sincere	K12	Restrictive of movement - Mobility
K13	Not my style - Totally me		
K14	Not worth the high price - Worth		



Visual assessments								
Kansei words (-)	3	2	1	0	1	2	3	Kansei words (+)
Random						X		Meticulous
Exaggerated								Simple
Functional assessments								
Unpractical								Practical
Uncomfortable								Comfortable

Figure 6. The Kansei question corresponding to the jacket model.

Figure 6 provides an overview of the semantic differential scale used in the study. As can be observed, the digital prototype front, side, and back views of each type of garment model are located at the top of the scale. In the bottom section, the Semantic Differential scale for visual and functional meanings is presented in two separate tables. There are a total of 14 pairs of Kansei words representing visual meanings and 12 pairs representing functional meanings. Figure 6 only illustrates two pairs of Kansei words, one for visual and one for functional meanings, to introduce the scale used in the study. Accordingly, the negative meaning of the word pair is placed on the left side, while the positive meaning is placed on the right side of the 7-point scale. Each interval in the table corresponds to a scoring system. The intervals closer to the word are evaluated starting from 3 and decreasing to 2, 1, and 0. Accordingly, the degree of participation in the attribute that the consumer evaluated the design in the visual is increased depending on the scoring. For scoring, first, the side is chosen from the opposite poles, and then the chosen side is marked with an "X". Each participant evaluated a total of 9 outerwear models, consisting of 3 jackets, 3 coats, and 3 overcoats, using the semantic differential scale.

The scale was administered to voluntary female consumers through both digital and face-to-face paper-based methods (mixed survey). The obtained data were examined, and answers that were incomplete or had errors were removed from the study as they could lead to incorrect results. SPSS software version 22 was utilized for data analysis. Through data analysis, the impact of the design attributes of the designed outerwear models on consumers' emotions and sentiments was observed.

3. RESULTS AND DISCUSSION

The distributions of data related to participants' expectations and opinions regarding outerwear models are presented in this section.

3.1. The participants' characteristics

The research examined the emotional expectations of female consumers towards outerwear, and as such, the opinions of 342 female consumers were gathered. The data collected solely from female participants have been analyzed and interpreted in this section. As shown in Table 4, the age range of the female participants involved in the research was 51,2% (175 individuals) between the ages of 18-25, while the lowest percentage of 2,3% belonged to the

participants aged between 51-60. 7% (24 individuals) of the participants have completed primary school, 2,6% (9 individuals) have completed middle school, 28,4% (97 individuals) have completed high school, 14,3% (49 individuals) have completed associate degree, 40,9% (140 individuals) have completed undergraduate education and 6,7% (23 individuals) have completed graduate education. When the employment status of the participants was examined, it was determined that 33,6% (115 individuals) were students and 22,5% (77 individuals) were not employed.

3.2. Participants' outerwear design preferences

Research data was obtained through a scale consisting of two sections. The first section includes a Likert-type scale to examine users' outerwear design preferences. The first section includes a Likert-type scale to examine users' outerwear design preferences. The reliability analyses of the questionnaire titled 'The Outerwear Design Preferences,' which was utilized in the research, have been conducted and are presented in Table 5.

Table 4. Descriptive statistics regarding the participants' characteristics (n=342) are as follows:

	%
Age	
18-25 yrs.	175 (51,2%)
26-30 yrs.	44 (12,9%)
31-40 yrs.	69 (20,2%)
41-50 yrs.	46 (13,5%)
51-60 yrs.	8 (2,3%)
Education	
Primary	24 (7%)
Middle	9 (2,6%)
High	97 (28,4%)
Associate	49 (14,3%)
University	140 (40,9%)
Graduate degree	23 (6,7%)
Job	
Jobless	77 (22,5%)
Official	70 (20,5%)
Worker	69 (20,2%)
Student	115 (33,6%)
Other	11 (2,3%)

Summary statistics for numerical data are presented as *mean ± standard deviation* and *median (minimum, maximum)*, while categorical data are presented as *number (percentage)*.

Table 5. Reliability results for the measurement of outerwear design preferences

	Statistical analysis score	Number of items	Cronbach's Alpha
Clothing preferences			
<i>mean±SD</i>	3,91±0,48	14	0,857
<i>M (min-max)</i>	4 (2,57-4,93)		

Summary statistics are presented as *mean ± standard deviation* and *median (minimum, maximum)* values.

According to the reliability results of a 14-item Likert-type measurement tool assessing the design features preferred by participants in outerwear (Table 5), the average total score obtained from the 14 questions was found to be $3,91 \pm 0,48$ points. The lowest score was 2,57, while the highest score was 4.93. The Cronbach's alpha (α) reliability coefficient of the scale was found to be 0,857. Here, reliability is related to how accurately the test measures the property it intends to measure, and the reliability coefficient is expected to be at least 0,70 for an acceptable value between 0 and 1 [47, 48]. In this study, it was concluded that the value obtained from the "Outerwear Design Preferences" test was above 0,70, and therefore the test was found to be reliable for this sample.

Table 6. Descriptive statistics results for the measurement of outerwear design preferences

Clothing preferences	mean	SD
Price	3,83	0,88
Brand	2,97	1,01
Benefit	4,18	0,81
Quality	4,35	0,77
Trend	3,03	1,03
Colour	3,98	0,87
Visuality	4,13	0,81
Usability	4,39	0,76
Design elements	3,89	0,88
Material	4,01	0,88
Durability	4,28	0,77
Lifespan	4,09	0,89
Ease of movement	4,41	0,80
Customizable	3,21	1,13

According to Table 6, the average score for the Price criterion in the 14-item Likert-type questionnaire measuring outerwear design preferences was found to be $3,83 \pm 0,88$. The average score for the Brand criterion was found to be $2,97 \pm 1,01$. The average score for the Benefit criterion was found to be $4,18 \pm 0,81$. The average score for the Quality criterion was found to be $4,35 \pm 0,77$. The average score for the Trend criterion was found to be $3,03 \pm 1,03$. The average score for the Colour criterion was found to be $3,98 \pm 0,87$. The average score for the Visuality criterion was found to be $4,13 \pm 0,81$. The average score for the Usability criterion was found to be $4,39 \pm 0,76$. The average score for the

Design elements criterion was found to be $3,89 \pm 0,88$. The average score for the Material criterion was found to be $4,01 \pm 0,88$. The average score for the Durability criterion was found to be $4,28 \pm 0,77$. The average score for the Garment Lifespan criterion was found to be $4,09 \pm 0,89$. The average score for the Ease of movement criterion was found to be $4,41 \pm 0,80$ and the average score for the Customizable criterion was found to be $3,21 \pm 1,13$. According to these obtained data, the highest average was found in Ease of Movement with $4,41 \pm 0,80$, while the lowest average was observed in the Brand criterion with $2,97 \pm 1,01$.

3.3. The statistical relations between Kansei words and outwears

In the second section of a scale consisting of two sections, participants evaluated the designs of jackets, coats, and overcoats using a semantic differential scale and in this step the relations between kansei words and outerwear designs was analyzed.

The Cronbach's Alpha reliability coefficients were examined for the semantic differential scale measuring emotional expectations towards outerwear designs in terms of positive and negative connotations of Kansei words related to visual and functional aspects for each model and are presented in Table 7. The lowest Cronbach's Alpha reliability coefficient for positive visual scores was found to be 0,917, and the highest was 0,956, for jackets, coats, and overcoats. For negative visual scores, the lowest Cronbach's Alpha reliability coefficient was 0,882, and the highest was 0,945, for jackets, coats, and overcoats. When the emotional expectations towards outerwear in the functional dimension were examined, the lowest Cronbach's Alpha reliability coefficient for positive functional score was found to be 0,923 and the highest was 0,958 for jackets, coats, and overcoats. For negative functional score, the lowest Cronbach's Alpha reliability coefficient was found to be 0,849 and the highest was 0,946 for jackets, coats, and overcoats.

Table 8 presents the values of the SD scale, in which participants evaluated each outerwear model, including jackets, coats, and overcoat, in terms of emotional words for their visual aspect.

Table 7. Reliability results of the scale of emotional expectations for outerwear designs (n=342)

Item		Visual KW(14)		Functional KW(12)	
		Positive (+)	Negative (-)	Positive (+)	Negative (-)
Jacket	Jacket 1.	0,917	0,857	0,923	0,849
	Jacket 2.	0,937	0,882	0,946	0,907
	Jacket 3.	0,939	0,904	0,941	0,902
Coat	Coat 1.	0,953	0,926	0,951	0,914
	Coat 2.	0,953	0,936	0,945	0,925
	Coat 3.	0,956	0,945	0,955	0,946
Overcoat	Overcoat 1.	0,944	0,911	0,953	0,902
	Overcoat 2.	0,952	0,917	0,958	0,920
	Overcoat 3.	0,955	0,941	0,955	0,936

Table 8. The comparison of the positive and negative visual scores of the three products

Aesthetic			Negative (-)		Test Statistics †		
					F	p	η^2
Jacket							
Jacket 1.	1,24±0,85 ^a	1,14 (0-3)	0,47±0,55 ^{cd}	0,21 (0-3)	128,610	<0,001	0,274
Jacket 2.	1,42±0,92 ^b	1,43 (0-3)	0,42±0,57 ^d	0,21 (0-3)	195,326	<0,001	0,364
Jacket 3.	1,20±0,91 ^a	1,07 (0-3)	0,54±0,67 ^c	0,29 (0-3)	74,717	<0,001	0,180
Test Statistics ‡	F=13,214; p<0,001; $\eta^2=0,072$		F=6,485; p=0,002; $\eta^2=0,037$				
Coat							
Coat 1.	1,17±0,96 ^a	0,93 (0-3)	0,54±0,72 ^d	0,21 (0-3)	61,738	<0,001	0,153
Coat 2.	0,94±0,92 ^b	0,68 (0-3)	0,79±0,85 ^{bc}	0,5 (0-3)	3,085	0,080	0,009
Coat 3.	1,00±0,94 ^b	0,64 (0-3)	0,70±0,85 ^c	0,29 (0-3)	12,146	0,001	0,034
Test Statistics ‡	F=14,222; p<0,001; $\eta^2=0,077$		F=16,150; p<0,001; $\eta^2=0,087$				
Overcoat							
Overcoat 1.	1,63±0,96 ^a	1,79 (0-3)	0,36±0,60 ^e	0,14 (0-3)	294,930	<0,001	0,464
Overcoat 2.	1,31±0,97 ^b	1,14 (0-3)	0,45±0,66 ^d	0,14 (0-3)	125,235	<0,001	0,269
Overcoat 3.	0,94±0,93 ^c	0,5 (0-3)	0,77±0,88 ^c	0,43 (0-3)	3,632	0,058	0,011
Test Statistics ‡	F=82,431; p<0,001; $\eta^2=0,327$		F=36,647; p<0,001; $\eta^2=0,177$				

F: Two-way repeated measures ANOVA, Effect Size (η^2), ‡Comparison within Products, †Comparison within Opinions, Summary statistics are presented as mean ± standard deviation and Median (Minimum, Maximum) values. The bold sections indicate statistical significance ($p<0,05$). $a>b>c>d>e>f$. Different letters or letter combinations within the same row indicate statistically significant differences ($p<0,05$).

According to Table 8, there is a significant difference between the means of positive and negative visual scores for three different jacket models with $F=12,108$ and $p=0,001$ confidence levels. The average positive visual scores of the 1st, 2nd, and 3rd jacket models are statistically significantly higher than the average negative visual scores. The effect sizes were found to be 0,274, 0,364, and 0,180, respectively. According to the measurements, it has been determined that the visual score averages of the 2nd jacket model are higher than the other models, while the averages of negative visual scores are lower than the other models. Therefore, it was found that the participants expressed positive emotions and feelings visually, in other words, their favorite design was the 2nd jacket model. The least favorite model was identified as the 3rd jacket.

According to Table 8, the visual positive and negative score averages of three different coat models show a significant difference at the confidence level of $p=0,001$ with $F=15,954$. At the same time, while there is no statistically significant difference between the positive and negative visual scores of the 2nd coat model, the positive visual score averages of the 1st and 3rd coat models are significantly higher than the negative visual score averages. The effect sizes are determined as 0,153, 0,009, and 0,034, respectively. The first coat model, which received the highest positive visual score average, was the one that participants focused on the most, while the negative visual score averages were statistically higher in the 2nd and 3rd coat models. Thus, it can be concluded that the participant group preferred the 1st coat model the most visually, and the 2nd coat model the least.

When the participants' emotional expectation levels were examined visually through coat models, there was a statistically significant difference in the positive and

negative visual score averages for three different coat models with $F=93,965$ and $p=0,001$. There is no statistically significant difference between the positive and negative visual scores in the 3rd coat model, while in the 1st and 2nd coat models, the average positive visual scores are significantly higher than the average negative visual scores at a statistically significant level of $F=93,965$ and $p=0,001$. The effect sizes are determined as 0,464, 0,269, and 0,011, respectively. Based on the obtained data, the visual score averages are higher for the 1st coat model, while the negative visual score averages are statistically higher for the 3rd coat model. Therefore, the most visually preferred model is the 1st coat model, while the least preferred one is the 3rd coat model (Table 8). These results indicate that participants have preferences for different design features in outerwear products and that these preferences show statistically significant differences. Additionally, these findings can assist designers in determining appropriate visual design features for a specific target audience.

Table 9 shows the evaluation of models of three different outerwear types, namely jackets, coats, and overcoats, using words expressing positive and negative emotions from a functional perspective, and the obtained data is reflected in the table. Accordingly, the mean scores of positive and negative functional aspects were found to be significantly different for the three different jacket models with $F=5,914$ and $p=0,016$ confidence levels. As a result of the analysis, the mean positive functional scores in the first, second, and third jacket models were statistically significantly higher than the mean negative functional scores. The effect sizes were found to be 0,519, 0,447, and 0,368 respectively. Accordingly, it can be observed that the mean functional scores of the first jacket model are higher than the other

models. Moreover, while there was no statistically significant difference in negative functional score averages among the jacket models, participants' preference for positive functional aspects was concentrated on the first and second jacket models. This result indicates that participants liked the first jacket model more in terms of functional aspects than the other models, and least preferred the third jacket model.

When looking at the data in Table 9, it can be observed that the average positive and negative functional scores show a significant difference in a confidence level of $F=24,343$ and $p=0,001$ for three different coat models. It was observed that the participants evaluated the coat models positively, with effect sizes found to be 0,330, 0,082, and 0,165, respectively. Accordingly, among the coat models that evoke positive emotions and feelings in terms of functionality, the first coat model had the highest average score, while in terms of negativity, the second coat model had the highest score. These results indicate that the participant group liked the first coat model the most in terms of functionality, and least liked the second coat model.

When examining the data regarding overcoat models that evoke positive and negative emotions and feelings in terms of functionality among the participants, it can be seen that the average positive and negative functional scores for three different overcoat models are significant at the level of $F=56,872$ and $p=0,001$. At the same time, the positive functional score averages in all overcoat models are statistically significantly higher than the negative score averages. The effect sizes were found to be 0,513, 0,368, and 0,127, respectively. The functional score averages of the 1st overcoat model are higher compared to the other models. The negative functional score averages, on the

other hand, are higher for the 3rd overcoat model. From these results, it has been determined that the participant group liked the 1st coat model the most in terms of functionality, and the 3rd coat model the least (Table 9).

3.4. Design options to guide new design ideas for outerwear

Participants evaluated the outerwear models, consisting of three jackets, three coats, and three overcoats, determined based on designer opinions, using Kansei word pairs representing visual and functional meanings. The evaluation results, indicating the models most liked by consumers in terms of visual and functional aspects (Most positive +) and the least liked (Most negative -), are provided in Table 10.

When examining Table 10, it can be observed that consumers favored two different models in terms of both visual and functional aspects among the jacket designs. However, for both the coat and overcoat designs, the same models were favored the most in both visual and functional aspects within their respective categories. The differentiation between the model that consumers liked the most for its visual appeal and the one they liked the most for its functionality in the jacket designs can be explained by the functional aspect of the most favored jacket featuring a modular attachment with a detachable zipper at the waistline. This modular design provides versatile usage options [49], where the design concept moves from parts to a whole or from a whole to parts. Additionally, the researcher finds the field of modular design to be vast and worth exploring, particularly for its potential to contribute to environmental conservation and balance in today's fast fashion market. This expansion in design allows for the vitality of ready-to-wear production and the limitless potential of design [50].










Table 9. Comparison of positive and negative functional scores of three products

Functional	Positive (+)		Negative (-)		Test Statistics †		
					F	p	η^2
Jacket							
Jacket 1.	1,58±0,92 ^a	1,63 (0-3)	0,30±0,48 ^c	0,08 (0-2,8)	368,537	<0,001	0,519
Jacket 2.	1,57±0,99 ^a	1,67 (0-3)	0,33±0,59 ^c	0 (0-3)	275,526	<0,001	0,447
Jacket 3.	1,40±0,98 ^b	1,42 (0-3)	0,36±0,60 ^c	0,08 (0-3)	198,410	<0,001	0,368
Test Statistics ‡	F=8,205; p<0,001; $\eta^2=0,046$		F=1,463; p=0,233; $\eta^2=0,009$				
Coat							
Coat 1.	1,39±1,01 ^a	1,46 (0-3)	0,39±0,64 ^f	0,08 (0-3)	167,766	<0,001	0,330
Coat 2.	1,04±0,96 ^c	0,75 (0-3)	0,59±0,79 ^d	0,25 (0-3)	30,647	<0,001	0,082
Coat 3.	1,21±1,02 ^b	1 (0-3)	0,51±0,80 ^e	0,08 (0-3)	67,267	<0,001	0,165
Test Statistics ‡	F=29,037; p<0,001; $\eta^2=0,146$		F=14,601; p<0,001; $\eta^2=0,079$				
Overcoat							
Overcoat 1.	1,67±1,04 ^a	1,83 (0-3)	0,27±0,53 ^e	0 (0-3)	359,722	<0,001	0,513
Overcoat 2.	1,41±1,05 ^b	1,33 (0-3)	0,33±0,61 ^e	0 (0-3)	198,790	<0,001	0,368
Overcoat 3.	1,12±1,01 ^c	0,88 (0-3)	0,53±0,78 ^d	0,17 (0-3)	49,623	<0,001	0,127
Test Statistics ‡	F=50,607; p<0,001; $\eta^2=0,229$		F=19,232; p<0,001; $\eta^2=0,102$				

F: Two-way repeated measures ANOVA, Effect Size (η^2), ‡Comparison within Products, †Comparison within Opinions, Summary statistics are presented as mean ± standard deviation and Median (Minimum, Maximum) values. The bold sections indicate statistical significance ($p<0,05$). $a>b>c>d>e>f$: Different letters or letter combinations within the same row indicate statistically significant differences ($p<0,05$).



Table 10. The emotional state results of participants toward outerwear models

		<i>Visual assessments</i>		<i>Functional assessments</i>	
		Positive (+)	Negative (-)	Positive (+)	Negative (-)
Jacket					
					
Overcoat					

Finally, the design features of the outerwear models that meet the participant's emotional expectations, or in other words, those visually and functionally favored, were compared with the Design Features and Parameters for Outerwear presented in Table 1. Using this table as a reference, the design features, and parameters of the models most favored by participants in terms of both visual and functional aspects were analyzed, resulting in the development of Table 10. In this table, since the visually most favored jacket and the functionally most favored jacket were different models, the design attributes of the visually favored jacket are listed under the 'Visual' column, while the design attributes of the functionally favored jacket are listed under the 'Functional' column. For the coat and overcoat models, since the same models were favored both visually and functionally within their respective categories, the design attributes of the most favored coat and overcoat models are provided under the 'Visual-Functional' column.

Table 11 shows that design features such as oversize fit, dropped shoulders, one-piece and long sleeves without modular features, ribbed cuffs, and multiple pockets with flaps are common preferences both visually and functionally for *jacket* models. Additionally, the adjustable

length with a detachable feature for jackets received positive functional feedback, while non-modular designs were visually favored. Designs with adjustable lengths that offer versatility and personalization to consumers should incorporate modular elements without sacrificing aesthetics. Additionally, the attachment-detachment line of the piece should be designed to be concealed, maintaining the overall appearance of the garment.

When examining the consumer Kansei-oriented design combinations for *coat* models, it's evident that features such as classic/casual-fit, long length, dropped shoulders, one-piece long sleeves, hooded stand collar, fiber-filled, zipper closure, multiple flap-covered patch pockets are dominant. Therefore, it's anticipated that these features can satisfy the usable design characteristics for coat designs. Additionally, consumers have shown a positive response towards modular elements that emphasize functionality, such as the ability to extend the coat's length, detachable sleeves, and pockets. Looking at the general design details, it can be inferred that there is no positive sentiment towards models with shoulder pads, epaulets, sleeve vents, and cuffs, indicating a lack of favorable appreciation for these details among consumers.

Table 11. The features and parameters determined for the new outerwear design

Features	Jacket		Coat	Overcoat
	Visual	Functional	Visual-Functional	Visual-Functional
Fit/form	Oversize	Oversize	Classic-fit	Classic-fit
Length	Regular	Long	Long	Extra long
Modular (length)	Basic	Detachable	Basic	Basic
Collar design	Stand	Turnover	Stand	Lapel collar
Fiber filled	No	No	Yes	No
Hoodie	No	No	Yes	No
Shoulder pads	No	No	No	No
Shoulder epaulettes	No	No	No	No
Shoulder design	Dropped	Dropped	Dropped	Dropped
Sleeve model	One-piece	One-piece	One-piece	One-piece
Sleeve length	Full length	Full length	Full length	Full length
Modular (sleeve)	Detachable	Basic	Detachable	Detachable
Sleeve cuffs	Ribbed	Ribbed	Cuffless	Cuffless
Closure type	Zipper	Single-breasted	Zipper and removable belt	Button closure and removable belt
Pocket number	Multipocket	Multipocket	Multipocket	Multipocket
Pocket model	Patch	Fleto	Patch	Fleto
Flap-pocket	Yes	Yes	Yes	Yes
Modular (pocket)	Detachable	Basic	Detachable	Basic
Flap-pocket design	Angled	Oval	Angled	Angled
Hemline	Gathered	Basic	Basic	Basic
Side seam	Basic	Two side slit	Basic	Basic

When analyzing the consumer Kansei-oriented design combinations for *overcoat* models, it's observed that features such as classic/casual-fit, extra long length, a lapel neckline, dropped shoulders, one-piece long sleeves, detachable modular sleeves, belted or tied with a sash, multiple flat pockets with flap covers, angular flap covers are generating a positive sentiment among consumers. Fiber-filled material, hood, shoulder pads and epaulets, shoulder slits, and cuffs, on the other hand, do not align with the consumer-preferred design combinations.

To incorporate consumer emotional expectations into the design process, consumer Kansei was determined and the design elements influencing these emotions were analyzed to create design combinations (shown in Table 11). The design parameters provided in this table, considering jacket, coat, and overcoat designs, are anticipated to positively fulfill consumer preferences in both visual and functional aspects when applied to newly designed outerwear. The products developed by considering user Kansei can enhance sales potential and lead to increased revenue within the applicable industry, as illustrated in this study [51].

4. CONCLUSION

In the product design process, finding suitable solutions for the consumer is essential, alongside the designer's intuition, skills, and thoughts. This is because the design process involves not only the aesthetic aspects of the product but also serves as a problem-solving method. The Design Thinking approach treats the expectations and needs of the consumer

towards a product as a problem to be solved, aiming to generate suitable solutions for the consumer. Therefore, within the framework of the Design Thinking approach supported by the Kansei Engineering methodology, a design process model has been developed and its effectiveness has been tested in this study. The combination of these two methodologies presents a unified KE-DT framework that emphasizes the customer's emotional needs. The proposed model demonstrates the importance and effectiveness of user participation in creating a design that meets emotional expectations, as observed in Tables 8 and 9. Another significant contribution of the presented model is the creation of a new design dataset by analyzing the positive emotions and feelings of consumers, as shown in Table 11. During the redesign process, using this dataset, the emotional perception and product features between the designer and the user can be effectively narrowed down. Consequently, this enables the presentation of new designs that are responsive to consumer expectations and better satisfy the psychological needs of users.

In this study, the following results were found:

- The model developed in this study has been used to measure the emotional impression that outerwear designs create on consumers. This model is not only applicable to the fashion industry but can also be used in various sectors such as automotive, mobile devices, appliances, and household items. An important feature of this model is its flexibility, allowing for repeatable applications between stages. This involves testing ideas

with user feedback early and frequently to identify any flaws or deficiencies in the product, aiming to enhance user satisfaction and cater to their expectations.

- This model incorporates the user's perspective into the design process, reducing the impact of the designer's subjective preferences and choices. Consequently, users can indirectly participate in the design process, allowing for the establishment of an effective emotional connection between the product and the user. This is a

REFERENCES

1. Ergüven A. 2021. *İyi tasarım nedir?* İstanbul, Türkiye: Hümanist.
2. Kambar R. 2016. Moda ürünlerinde güdülenmiş tüketici yenilikçiliğinin satın alma ilgilenimi üzerindeki etkisi. *Kocaeli Üniversitesi Sosyal Bilimler Dergisi (KOSBED)*, (32), 149-166.
3. Kozan E. 2021. *Tasarım odaklı düşünce*. İstanbul, Türkiye: Abaküs.
4. Leifer LJ, Steinert M. 2014. Dancing with ambiguity: Causality behavior, Design Thinking, and triple-loop-learning. In Gassmann, O. and Schweitzer, F. (Eds.) *Management of the Fuzzy Front End of Innovation*. Switzerland: Springer, 141-158.
5. Öztürk A, Korkut F. 2020. Tasarım odaklı düşünme yaklaşımı ile Stem eğitimi etkinliği geliştirme. UTAK 2020 Dördüncü Ulusal Tasarım Araştırmaları Konferansı: Tasarım ve Öngörü Bildiri Kitabı. 8-10 Eylül 2020, Ankara, Türkiye, 391-404.
6. Sürmelioglu Y. 2021. Tasarım odaklı düşünmenin gelişimi için çevrimiçi proje tabanlı bir öğretimin tasarımı ve etkililiğinin incelenmesi. (Doctoral dissertation). Retrieved from/Available from Yüksek Lisans Tez Merkezi. (695169)
7. Gropius W. 1935. *The new architecture and the Bauhaus*. London: Faber and Faber Limited.
8. Rowe PG. 1987. *Design Thinking*. London: MIT.
9. Liedtka J, Ogilvie T. 2011. *Designing for growth: a design thinking tool kit for managers*. NY: Columbia Business School.
10. Dorst K. 2011. The core of 'Design Thinking' and its application. *Design Studies*, 32(6), 521-532.
11. Luchs MG. 2015. A brief introduction to design thinking. In Luchs, M.G., Swan, K.S. and Griffin, A. (Eds.) *Design Thinking*. NJ: John Wiley & Sons, Hoboken, 1-11.
12. Lawson B. 2006. *How designers think*. Oxford: Elsevier/ Architectural.
13. Lindberg T, Meinel C, Wagner R. 2011. Design Thinking: A fruitful concept for IT development? In Plattner, H., Meinel, C. and Leifer, L. (Eds.), *Design Thinking, understand - improve - apply*. Verlag Berlin Heidelberg: Springer, 3-18.
14. Johansson-Sköldberg U, Woodilla J, Çetinkaya M. 2013. Design Thinking: Past, present and possible futures. *Creativity and Innovation Management*, 22(2), 121-147.
15. Brown T. 2008. Design thinking. *Harvard Business Review*, 186(6), 1-10. Retrieved from <https://readings.design/PDF/Tim%20Brown,%20Design%20Thinking.pdf>
16. Schmiedgen J, Rhinow H, Köppen E, Meinel C. 2015. *Parts without a whole?: The current state of design thinking practice in organizations* (Issue 97, p.8). Retrieved from <https://idw-online.de/de/attachmentdata45603.pdf>
17. Martin R. 2009. *The design of business: Why design Thinking is the next competitive advantage*. Harvard Business, Cambridge.
18. Balakrishnan B. 2021. "Exploring the impact of design thinking tool among design undergraduates: A study on creative skills and motivation to think creatively. *International Journal of Technology and Design Education*, 32(3), 1799-1812.
19. Simon HA. 1969. *The sciences of the artificial*. The MIT, Cambridge.
20. Dunne D, Martin R. 2006. Design Thinking and how it will change management education: An interview and discussion. *Academy of Management Learning & Education*, 5(4), 512-523.
21. Howard Z. 2015. Understanding design thinking in practice: A qualitative study of design led professionals working with large organizations. (Doctoral dissertation). Retrieved from/Available from Swinburne University of Technology, Swinburne Research Bank.
22. IDF (Interaction Design Foundation). 2020. The 5 stages in the Design Thinking process. Retrieved from <https://www.interaction-design.org/literature/article/5-stages-in-the-design-thinking-process>
23. d.school. 2023. Explore The Stanford D.School. Retrieved from <https://dschool.stanford.edu/>
24. Plattner H. 2010. Foreword. In Plattner, H., Meinel, C. and Leifer, L. (Eds.), *Design Thinking: Understand - Improve - Apply*, Springer-Verlag Berlin Heidelberg, v-vi. DOI 10.1007/978-3-642-13757-0.
25. Plattner H. 2012. Foreword. In Plattner, H., Meinel, C. and Leifer, L. (Eds.), *Design Thinking Research: Measuring Performance in Context*, Springer-Verlag Berlin Heidelberg, v-vi. DOI 10.1007/978-3-642-31991-4.
26. Meinel C, Leifer L. 2012. Design Thinking Research. In Plattner, H., Meinel, C. and Leifer, L. (Eds.) *Understand innovation, Design Thinking Research: Measuring Performance in Context*, Springer-Verlag Berlin Heidelberg, 1-12. DOI 10.1007/978-3-642-31991-4.
27. von Thienen JPA, Clancey WJ, Corazza GE, Meinel C. 2018. Theoretical foundations of design thinking. Part I: John E. Arnold's creative thinking theories. In Plattner, H., Meinel, C. and Leifer, L. (Eds.) *Design Thinking Research: Making Distinctions: Collaboration versus Cooperation*, Springer, 13-40.
28. Kröper M, Fay D, Lindberg T, Meinel C. 2010. Interrelations between motivation, creativity, and emotions in Design Thinking processes - An empirical study based on regulatory focus theory. Proceedings of the 1st International Conference on Design Creativity (ICDC2010), 29 November - 1 December 2010, Kobe, Japan, pp. 97-104.
29. Plattner H, Meinel C, Weinberg U. 2009. *Design Thinking, Innovation lernen*, 114p. Munich, German: mi-Wirtschaftsbuch.
30. Stanford University Institute of Design. 2012. D. School design thinking process. Retrieved from: <http://dschool.stanford.edu/>
31. Plattner H. (Ed.). 2009. d.School Bootcamp bootleg. Institute of Design at Stanford.
32. Nagamachi M. 1995. Kansei engineering: A new ergonomic consumer-oriented technology for product development. *International Journal of Industrial Ergonomics* 15, 3-11.
33. Nagamachi M. 2011. Kansei/Affective engineering and history of Kansei/Affective engineering in the world. In Nagamachi, M. (Ed.) *Kansei/Affective Engineering*, CRC Press, 1-12.
34. Nagamachi M, Ito M, Tsuji T. 1988. Image technology based on knowledge engineering and its application to design consultation. In Adams, A.S., Hall, R.R., McPhee B.J. and Oxenburgh, M.S. (Eds.), Proceedings of the 10th Congress of International Ergonomics Association, Sydney, Australia, 72-74.


positive interaction for enterprises. Because this allows for the generation of effective solutions that cater to user satisfaction and their expectations. Additionally, in the garment industry, where consumer and market demands are constantly evolving, this model can establish a reliable foundation for continuous learning throughout the process. This can lead to a reduction in trial and error, resulting in time and cost savings.

35. Nagamachi M. 1996. Kansei Engineering and its Applications. *The Japanese Journal of Ergonomics*, 32(6), 286-289.
36. Nagamachi M. 1999a. Kansei engineering and its applications in automotive design. *SAE Technical Paper Series*, 87-94.
37. Nagamachi M. 2008. Perspectives and the new trend of Kansei/Affective Engineering. *The TQM Journal*, 20(4), 290-298.
38. Nagamachi M. 1999b. Kansei engineering; the implication and applications to product development. IEEE International Conference on Systems, Man, and Cybernetics, Tokyo, Japan, 273-278. DOI: 10.1109/ICSMC.1999.816563.
39. Lokman AM, Noor NM, Nagamachi M. 2007. Kansei Engineering: A study on perception of online clothing website. Proceedings of the 10th QMOD, Helsingborg, Sweden.
40. Nagamachi M, Lokman, AM. 2011. *Innovations of Kansei Engineering*. New York, USA: CRC, Taylor & Francis Group.
41. Ahmady A. 2008. Review and classification of Kansei Engineering and its applications. Proceedings of the 4th Annual GRASP Symposium: Graduate Research and Scholarly Projects, Wichita State University, 143-144.
42. Rosenthal R, Rosnow RL. 1981. *Essentials of behavioral research: methods and data analysis*. New York: McGraw Hill.
43. Nardi PM. 2003. *Doing survey research: a guide to quantitative methods*. Boston, MA: Pearson Education.
44. Sevinç B. 2009. Survey araştırması yöntemi. In Böke K. (Ed.) *Sosyal Bilimlerde Araştırma Yöntemleri*, İstanbul: Alfa Basım Yayın, 245-284.
45. Turkish Statistical Institute (TÜİK). (2022). Population by province, single age, and sex, 2007-2022. Retrieved from <https://data.tuik.gov.tr/Kategori/GetKategori?p=nufus-ve-demografi-109&dil=2>
46. Semiz, M. 2011. *Örnekleme yöntemleri*. Konya: Dizgi Ofset.
47. Durmuş B, Yurtkoru ES, Çinko M. 2013. *Sosyal bilimlerde Spss'le veri analizi*. İstanbul, Türkiye: Beta.
48. Büyüköztürk Ş, Kılıç Çakmak E, Akgün EÖ, Karadeniz Ş, Demirel F. 2021. *Eğitimde bilimsel araştırma yöntemleri*. Ankara, Türkiye: Pegem.
49. Li X, Su J, Zhang Z, Bai R. 2021. Product innovation concept generation based on deep learning and Kansei engineering. *Journal of Engineering Design*, 32(10), 559-589.
50. Zhou F, Hu M, Zhao Y. 2020. Study on the influence of modular design of garments on market innovation. *Journal of Textile Science & Fashion Technology*, 6(3), 1-2.
51. Akgül E. 2020. Kansei tabanlı ürün tasarımı için hibrit bir yaklaşım (Doctoral dissertation). Retrieved from/Available from Yök National Thesis Center. (624977).

A Comparative Study on the Performance of Side-by-side Hollow Bicomponent Yarns

Merve Bulut¹  0000-0003-2232-6506

Merve Küçükali Öztürk²  0000-0002-2493-4532


Cevza Candan¹  0000-0003-2007-5758

Banu Nergis¹  0000-0001-6010-6497

Tuğba Zengin³  0000-0002-7799-6999

Aysun Yenice³  0000-0003-0036-7868

Rasim Boyacıoğlu⁴  0000-0002-8115-2035

Ecenur Tor⁴  0000-0002-4146-4691

¹ Istanbul Technical University, Department of Textile Engineering, Istanbul, Türkiye

² Istanbul Bilgi University, Department of Textile and Fashion Design, Istanbul, Türkiye

³ Kucukcalik Tekstil San. ve Tic. A.S., Bursa, Türkiye

⁴ KFS Kucukcalik Filament ve İplik San. ve Tic. A.S., Sakarya, Türkiye

Corresponding Author: Merve Bulut, merve.bulut@itu.edu.tr

ABSTRACT

Using hollow yarns can change and improve many qualities of fabrics including thermal, acoustic, or mechanical properties. Using technical yarns in commercial textile products has been studied extensively to bring them some sort of functionality. In this study, side-by-side 50%/50% bicomponent yarns made from different raw materials were tested and evaluated to determine their processing behaviour and performance characteristics. All yarns have co-polyester (coPET) as one component where the other component is Polyester (PET), recycled PET (rPET) and Polyamide 6 (PA6), respectively. Afterwards, the coPET component is dissolved from all yarns by alkalization, thus making the hollow yarns, and the samples were textured by heat treatment. The mechanical and physical properties were evaluated by various tests, including unevenness, crimp testing, hollow ratio, and shear test. Their thermal and thermomechanical properties were evaluated with Differential Scanning Calorimeter (DSC) analysis and Thermal Gravimetric Analysis (TGA). Also, X-ray Diffraction Analysis (XRD) analysis was carried out in order to observe the crystalline behaviour of the samples. All evaluations were done on the non-textured and textured state of the yarns to see the effect of the heat treatment. The physical and mechanical test results revealed that despite the alkalization, the textured yarns demonstrated better strength and dimensional resistance. DSC and TGA analysis showed that the alkalization and heat treatment caused an increase in the polymer mobilization, which resulted in an increase in the decomposition enthalpy and a lower decomposition temperature. As a final note, XRD results indicated that for the PET/coPET and rPET/coPET samples, the texturization process significantly increased the crystallinity of the samples, which is unexpected and therefore needs further investigation.

1. INTRODUCTION

The physical properties of textiles are critical for every imaginable scenario, since they tend to dictate many factors, such as processability, usability, lifetime, etc. Recently, functional materials, such as bicomponent yarns, have been used in traditional and commercial textile products to add a new function or feature to the product. Their unique structures and properties, as well as their

modifiability attracts considerable attention. As such, their processing parameters and final properties are being extensively studied [1]. Bicomponent fibers are manufactured by pumping two different polymers from different channels into the same nozzle. By changing the nozzle head, bicomponent fibers with different shapes and different ratios can be manufactured. These fibers can then either be spun into yarns, made into nonwovens, or used in

To cite this article: Bulut M, Küçükali Öztürk M, Candan C, Nergis B, Zengin T, Yenice A, Boyacıoğlu R, Tor E. 2024. A Comparative Study on the Performance of Side-by-side Hollow Bicomponent Yarns. *Tekstil ve Konfeksiyon*, 34(4), 424-433.

other materials such as a reinforcement material in composites. Depending on the chemical composition of the polymers, the components can be connected by only physical means and not due to a chemical reaction of some sort. This allows for neither polymer to lose its intrinsic properties. This property of bicomponent materials makes them a popular material to be used and researched, since the final product will carry the properties of both materials. The components can also be chemically bonded if the two polymers are compatible with each other, in that case the interface between the components can be utilized in order to strengthen the material [1].

In terms of the shape, bicomponent fibers can be classified into four main categories: side-by-side, shell/core, islands-in-the-sea, or segmented-pie type. Side-by-side type bicomponent fibers are made by extruding two polymers with different shrinkage or viscosity values next to each other. Their biggest advantage is that they can be used to create a permanent crimp on the material, imitating a wool yarn. When subjected to some type of heat treatment or stretching action, the mechanical difference between the two polymers causes a permanent crimp on the fiber. By adjusting the polymer type, the drawing temperature and the drawing ratio, crimp levels as high as 42% can be achieved [2]. In shell/core type fibers, the two polymers are fed individually, and the “shell” or the “sheath” part completely covers the “core” part. These fibers are mainly used to take advantage of both components; the shell part gives the visual or handle properties such as luster, dyeability, or thermal insulation whereas the core part gives mechanical properties such as high strength, stability, or it can be used to decrease the cost of the material for commercial or mass-produced products. Due to the composite-like structure of a bicomponent fiber, they can be made into a nonwoven and then mixed into a resin without the need of an additional binding agent. This has the advantage of not only eliminating a step for speeding up the production in an industrial setting, but also decreases the production cost altogether [3]. In a different approach, both components can be utilized to make a high-performance product. For example, researchers have made a poly (vinyl pyrrolidone) (PVP) and poly (D,L-lactide) (PLA) shell/core bicomponent fiber by utilizing coaxial electrospinning method. The final product had a lower tensile strength and a higher water uptake level than pure PLA. With PLA being a biodegradable polymer, the final product can be utilized to load bioactive molecules for drug delivery and tissue regeneration applications [4]. Islands-in-the-sea type is composed of a component called the islands, distributed inside the sea component [1]. In this type, the island segments inside the fiber can be dissolved in order to create a ultrafine yarn, which is highly utilizable. This type of fiber is commonly used to manufacture hollow yarns by removing one of the components. Such a fiber has been utilized in making a needle-punched nonwoven which is then made into a filtering bag. The resulting product had a

superior tensile strength, bursting strength and dust-removal efficiency than some of the commercially available products on the market [5]. In a different approach, researchers made a nonwoven sheet using a Polyamide-6 (PA6) as the island and polyethylene (PE) as the sea bicomponent fiber and then dissolved the sea component after the hydroentanglement. The resulting material had up to 25% weight loss after the dissolution of the sea polymer. Also, since the removal of the sea component enhances the fibrillation of the remaining component, the sound absorption coefficient of the nonwoven web has increased as the number of islands increase. This can be utilized to make a lightweight, cheap, and bulky acoustic application material [6]. In the segmented-pie type, two polymers that are not compatible with each other are extruded together and then rapidly cooled down to mold it into a shape that resembles a pie chart [1]. This can again be utilized to make a hollow fiber or an ultrafine fiber for different applications. A polyester/polyamide 6 segmented-pie bicomponent fiber is made into a leather base by making it into a nonwoven to be used in artificial leather production. Comparing the final product with the commercial artificial leathers in terms of their air permeability, water vapour permeability and thermal insulation proved that the nonwoven has superior properties. This is not only a cheaper alternative for the apparel industry, but also a more sustainable method of producing artificial leather and a more ethical approach to real leather [7].

Bicomponent yarns can also be manufactured as hollow yarns by using two materials with different melting temperatures or different thermal/hydroscopic properties, spinning it into a yarn, and then melting the polymer with the lower melting point afterwards or dissolving one of the components by means of a heat or water treatment either after spinning or in the fabric form. Neutral fibers such as cotton or wool can also be made into a hollow yarn by using the neutral fiber as a sheath with a generally water-soluble polymer in the middle (such as PVA), then subsequently removing the core part by a water treatment. This increases the bulkiness of the yarn with decreasing its weight at the same time [8]. Also, the air gap in the middle acts as a major insulator that increases the thermal and acoustic properties of the yarn. Using hollow yarns in the structure enhances many properties, such as yarn strength, thermophysiological comfort, moisture and air permeability, and sound absorption [9, 10]. Previous study comparing fabrics knitted with 100% cotton fiber versus a hollow cotton fiber show that fabrics with a hollow cotton fiber show better permeability, absorbency, wicking, drying and thermal resistance properties. In both studies, the hollowness of the cotton yarns is achieved by spinning a cotton & poly (vinyl alcohol)(PVA) yarn with PVA in the core, and subsequently dissolving the PVA. [11, 12]. Another study found that the mechanical strength of a hollow cotton yarn is the same as the conventional cotton yarn but it has a better elongation, while being softer and bulkier at the same time [13]. Aytac

and Gurkan Unal (2018), produced hollow yarns with cotton, viscose, wool, and polyester as the sheath and PVA in the core, with different sheath-core ratios. The hollow yarns, regardless of the material in the sheath, have shown better comfort properties and decreased pilling tendency. Also, it is found that air and water vapour permeability levels can be increased in all cases by adjusting the sheath-core ratio accordingly [14].

Also, bicomponent fibers and yarns open the road for a more greener approach, where a recycled material can be combined with a high-performance material in order to maintain its superior property while still being a more sustainable alternative [15]. Recycled PET (rPET) has been redrawn with a nano-structure titanium dioxide (nano-TiO₂) to make an antibacterial bicomponent multifilament yarn as a commercial potential to make antibacterial carpets. Here, the rPET allows for repurposing PET water bottles and bringing the necessary tensile properties whereas the TiO₂ provides the antibacteriability [16]. Textile industry, specifically coloration and printing section is a widely known environmental pollutant. A study made a core-shell type bicomponent fiber by using cotton waste as the core and colored textile waste as the sheath as a mean of creating a more sustainable material. The resulting material showed the same color retency and intensity as a single component regenerated cellulose fiber even though it already has dye material on it. This has the benefit of dyeing this fiber with using less dyestuff in order to achieve the same color effect [17].

It is evident that bicomponent materials are gaining popularity day by day due to their high modifiability and cost decreasing properties and they are rapidly finding themselves applications in commercial areas. In this study, three types of side-by-side hollow bicomponent yarns having different raw materials have been developed and compared in terms of their physical, mechanical, and thermomechanical properties. By doing so, it is aimed to contribute the literature by giving an in-depth study of the

mechanical and thermomechanical properties of side-by-side hollow bicomponent yarns manufactured from various source materials. This study also discusses the properties of both textured and nontextured yarns presenting a complete understanding of the impact of heat treatment and alkalization on yarn properties. To our best knowledge, the aforementioned points have not been thoroughly evaluated and discussed in the literature. As a final word, all of the developed yarns are intended to be used in commercial blackout curtain fabrics in an attempt to enhance the sound absorbing quality of the blackouts from bicomponent hollow yarns, in addition to their main function, namely light blocking out.

2. MATERIAL AND METHOD

2.1 Material

Six different bicomponent yarn samples were developed and evaluated by collaborating with the KFS Company operating in Türkiye. The yarns consist of PET/coPET, rPET/coPET, and PA6/coPET in both their nontextured and textured forms, making a total of six samples. Here, rPET denotes recycled polyester and coPET denotes co-polyester. The coPET components were dissolved by alkalization treatment. The properties of the raw materials were given in Table 1, and the compositions of the yarn samples are given in Table 2. All the samples are partially oriented yarns (POY). In the sample coding, samples that have “T” next to them are the textured yarns where the ones without the letter T were not texturized. The yarn counts for the non-textured yarns were taken before the dissolving of the coPET component and they are reduced to the desired yarn count by dissolving them in fabric form afterwards. The yarn counts were tested according to the TS 244 EN ISO 2060 standard and the number of filaments were determined by the firm accordingly to their in-house testing method.

Table 1. Raw material properties

Material	Viscosity (dl/g)	Moisture (PPM)	Melting Point (°C)
PET	0,66	1477,99	252,7
coPET	0,685	1487,27	238,7
rPET	0,709	1572,14	253,6
PA6	2,4	891,42	218

Table 2. Sample properties

Sample ID	Composition	Yarn Count (DN)	Number of Filaments
1	50% PET & 50% coPET	248,48	72
1T	50% PET & 50% coPET	152,52	72
2	50% rPET & 50% coPET	248,48	72
2T	50% rPET & 50% coPET	157,47	72
3	50% PA6 & 50% coPET	251,23	72
3T	50% PA6 & 50% coPET	156,91	72

2.2 Method

The nontextured and textured yarns were tested on their breaking force and elongation at break according to DIN EN ISO 2062, hot air shrinkages according to DIN EN 14621, and fat content by the NMR method. The nontextured yarns were also evaluated on their unevenness according to TS2394 standard and the textured yarns were additionally evaluated on their number of nips and nip stability, which was determined manually, and their crimp contraction and mechanical crimp retentions according to DIN 53840 standard. Their cross-sectional images were taken by Scanning Electron Microscope (SEM). The hollowness ratios of the yarns were determined with the help of a program written on MATLAB from the images taken from the SEM. The images taken from MATLAB program can be found in Figure 1. As it can be seen, the alkalization treatment dissolved the coPET component completely in all samples. The hollowness ratio of the PET, rPET, and PA6 yarns after the coPET has been melted were determined as 24,61%, 18,15%, and 38,03% respectively.

Differential Scanning Calorimetry (DSC) analysis and Thermal Gravimetric Analysis (TGA) were done on all the samples to see the effect of the texturization process on the yarns in terms of their thermomechanical properties, as well

as to see the different thermal behaviour of yarns having different raw materials. DSC analysis was carried out using a Perkin-Elmer DSC-4000 device and an average of 3mg of material. For the PET/coPET yarns, the samples were heated from 25°C to 300°C at a heating rate of 10°C/min and then the samples were cooled to 25°C at a rate of 10°C/min. The rPET/coPET yarns were heated from 0°C to 300°C at a heating rate of 10°C/min and then the samples were cooled down to 0°C at a rate of 10°C/min. The PA6/coPET yarns were heated from 20°C to 300°C at a heating rate of 20°C/min and then cooled back down to 20°C at a rate of 20°C/min. TGA was carried out using a TA Instruments SDT Q600 device using an average of 9mg of material. The tests were done in a nitrogen atmosphere with a flow rate of 100 ml/min and all the samples were tested in a temperature range of 0-650°C with a heating rate of 10°C/min.

The crystallization behaviour of the samples was investigated by X-ray diffraction (XRD) with a Bruker D8 ADVANCE device ($\lambda = 1,54060$). The 2θ scanning range was 0-55°.

3. RESULTS AND DISCUSSION

The mechanical test results for the nontextured and textured yarns can be found at Table 3.

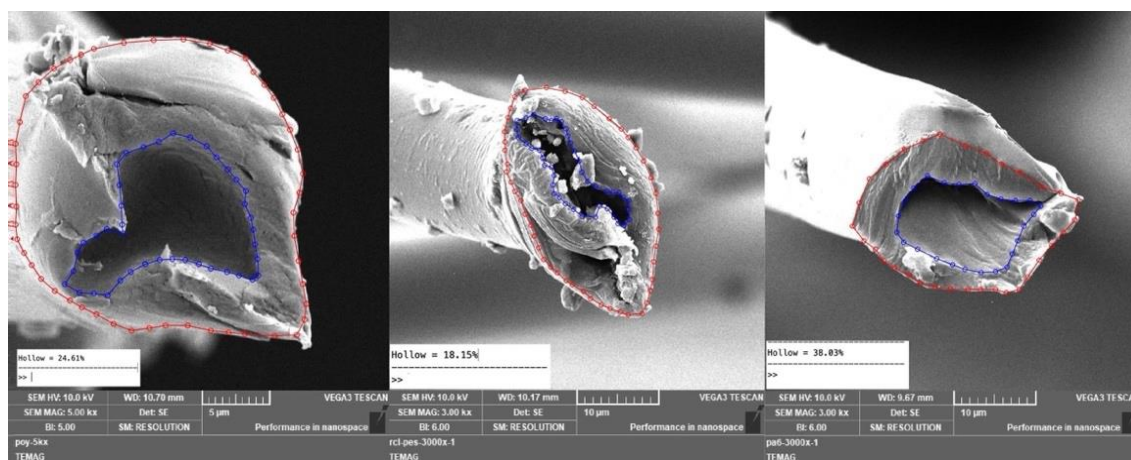


Figure 1. Hollowness ratios of the samples

Table 3. Test results for textured and nontextured yarns

ID	Breaking Force (cN)	Elongation at Break (%)	Boiling Shrinkage (%)	Fat Content	Unevenness (CV%)	Number of Nips	Nip Retention (%)	Crimp Contraction (%)	Crimp Retention
1	1,79	123,4	72	0,457	1,1	-	--	-	-
1T	3,16	22,8	72	1,245	-	80	4646	33,06	53,09
2	1,79	123,4	72	0,457	1,2	-	-	-	-
2T	2,89	25,78	72	1,81	-	52	33	32,59	54,66
3	2,15	131,27	72	0,377	1,02	-	-	-	-
3T	3,86	27,57	72	1,526	-	82	60	27,98	63,24

The textured yarns have better dimensional resistance and improved strength when compared to their nontextured counterparts. The heating during the texturization improves crystallinity and density due to a greater number of immobile polymer chains with less elongation. This enhances strength while decreasing elongation. Alkalization, however, causes a reduction in the fiber diameter which results in lower tensile properties due to finer fibers breaking apart from the structure easily. Nevertheless, the texturization seems to play a bigger role as the breaking force and elongation results show that the textured yarns are stronger than their nontextured counterparts.

The results of the DSC analysis for the PET/coPET sample, rPET/coPET sample and PA6/coPET sample can be found in Figure 2, Figure 3, and Figure 4, respectively. In all the figures, the graph on the top shows the results for the nontextured yarns and the graph on the bottom shows the results for the textured yarns.

DSC analysis performed on the nontextured and textured yarns shows a double-peaked graph, as expected from bicomponent yarns. The melting properties of PET samples are very complex depending on the experimental conditions chosen for the measurements, isothermal temperature or non-isothermal crystallization conditions, thermal history, and heating rate. The observed multiple melting endotherms are a result of the balance between melting and recrystallization and lamella thickness distribution present in the sample prior to heating. The presence of polymelt endotherms as observed with DSC is very common and is observed for many semicrystalline polymers, copolymers, and blends. When two endotherms, I and II, are present, it is confirmed that they are due to the presence of a double lamella thickness distribution produced during crystallization. The peak points of the curves during the heating stage, thus the melting temperatures, of all four of the components were compatible with the polymer properties given in Table 1.

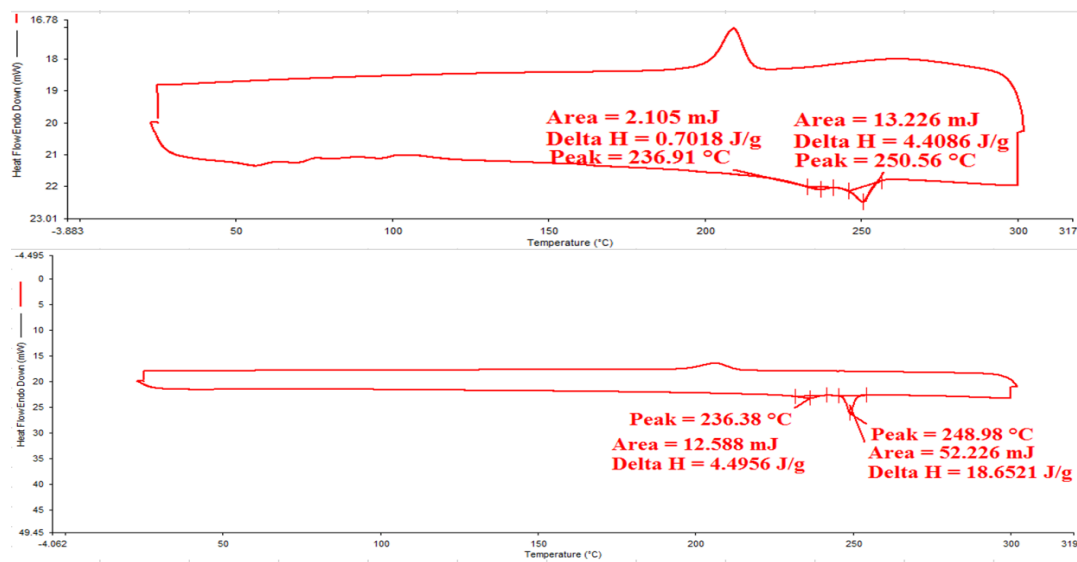


Figure 2. DSC results for nontextured and textured PET/coPET yarns.

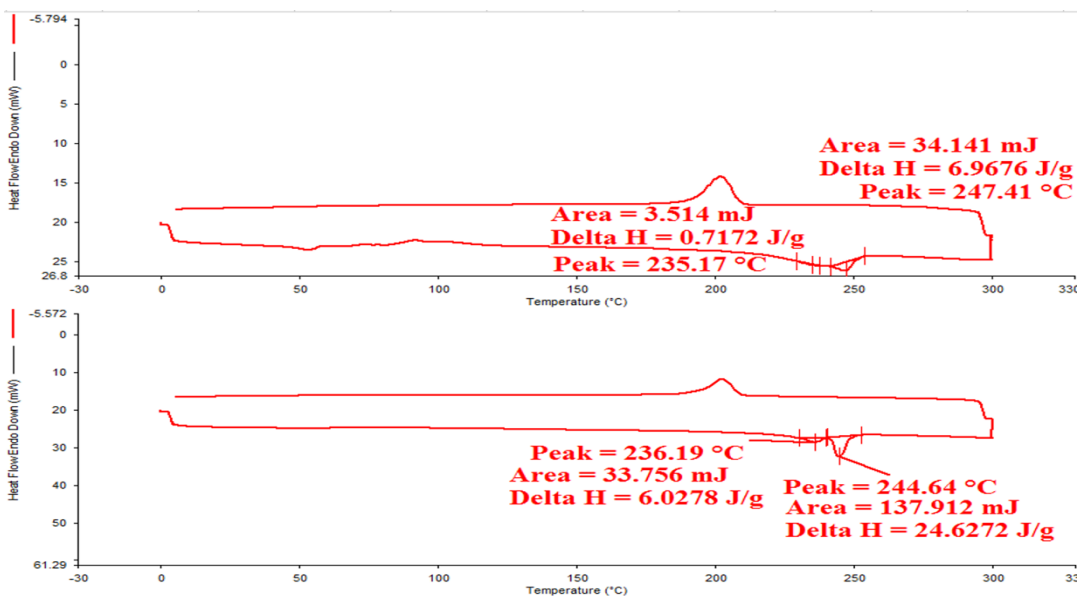


Figure 3. DSC results for nontextured and textured rPET/coPET yarns

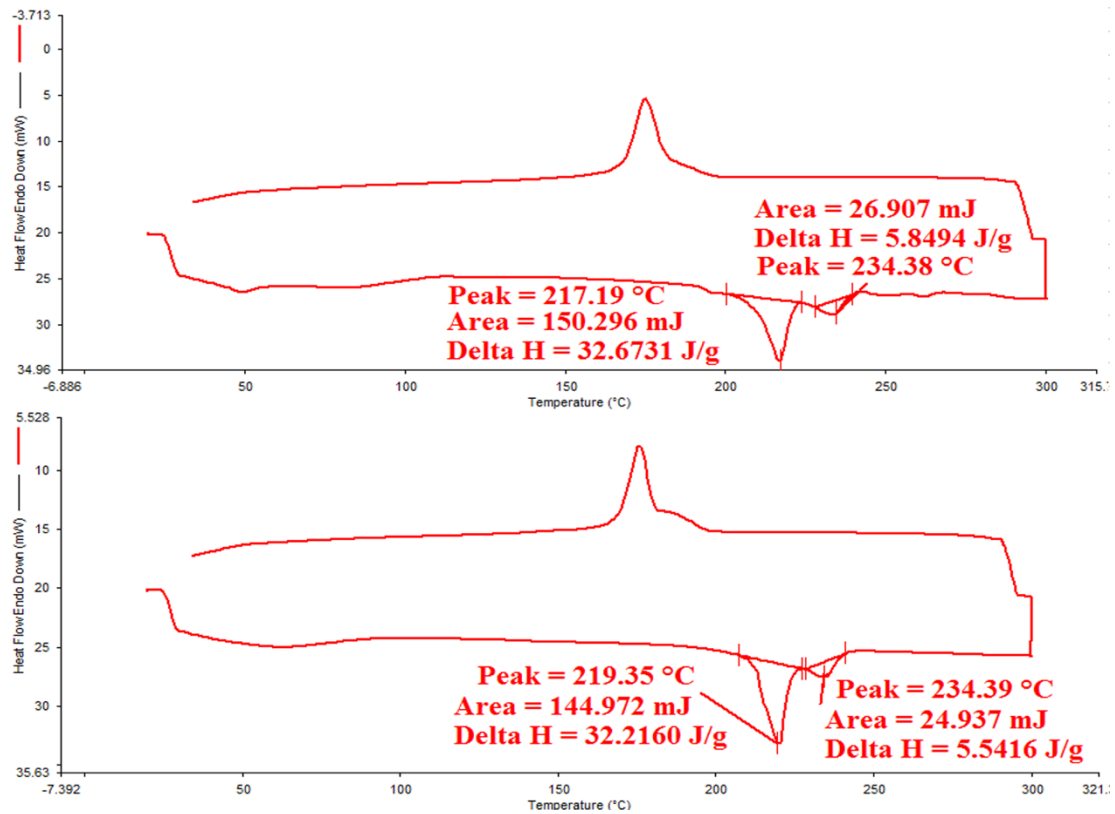


Figure 4. DSC Results for Nontextured and Textured PA6/coPET yarns.

The enthalpy (ΔH) values have had a massive increase for all samples after the texturization. The enthalpy value is dependent on the polymer content of the sample. The heat treatment done by texturization indicates that the texturing process makes it difficult for the fiber to crystallize, which led to an increase in their ΔH values.

The endothermic curves also show different trends. For the nontextured samples, the melting peak is sharper and narrower, but the curve gets wider with the texturization process. The same trend can be observed for the re-crystallization during the cooling stage. Another observation is that for PET/coPET blend, the peak of PET is narrower whereas for the rPET/coPET blend, the rPET has a broader peak. This can be correlated to the thickness difference between PET and rPET materials. PET fibers' melting temperature is higher and is more peaked than rPET fibers. This difference can be attributed to the use of virgin raw materials and the absence of contamination in the PET/coPET sample. The smaller thickness of the rPET fiber crystallites is due to thermo-mechanical deterioration during the recycling and replication stages.

The TGA graphs for the PET/coPET sample, rPET/coPET sample and PA6/coPET sample can be found in Figures 5 to 7, respectively. In all the figures, the graph on the top is for the nontextured sample whereas the graph on the bottom is for the textured counterpart of that sample. The graphs show the weight change of the samples with increasing temperature.

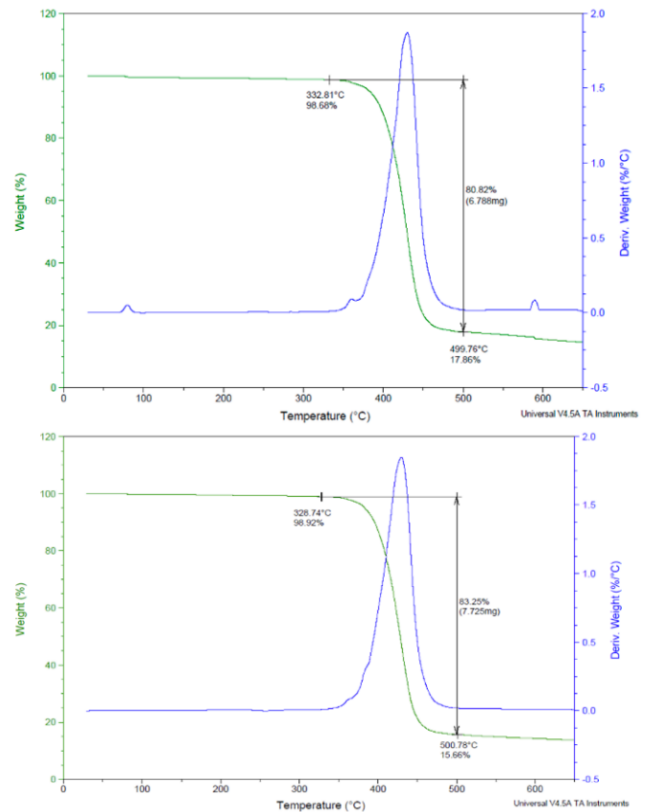


Figure 5. TGA results for nontextured and textured PET/coPET yarns.

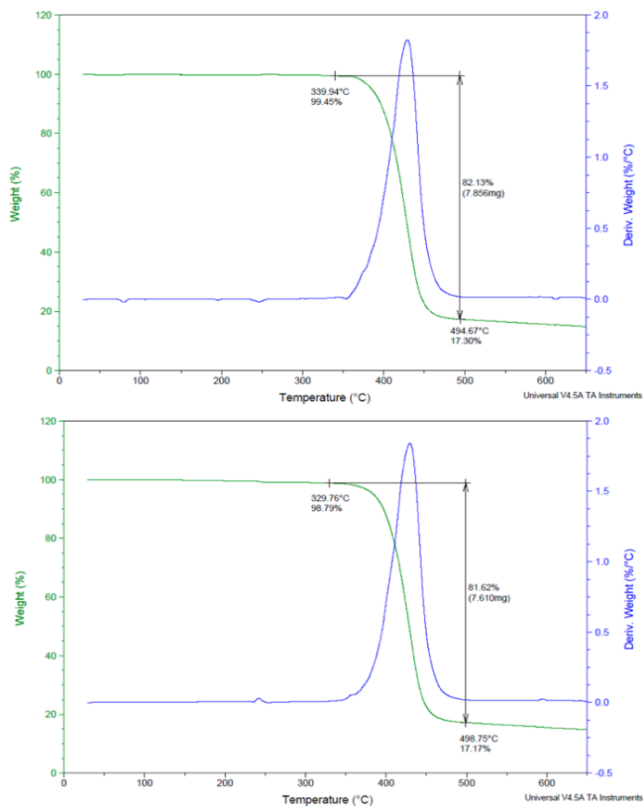


Figure 6. TGA results for nontextured and textured rPET/coPET yarns.

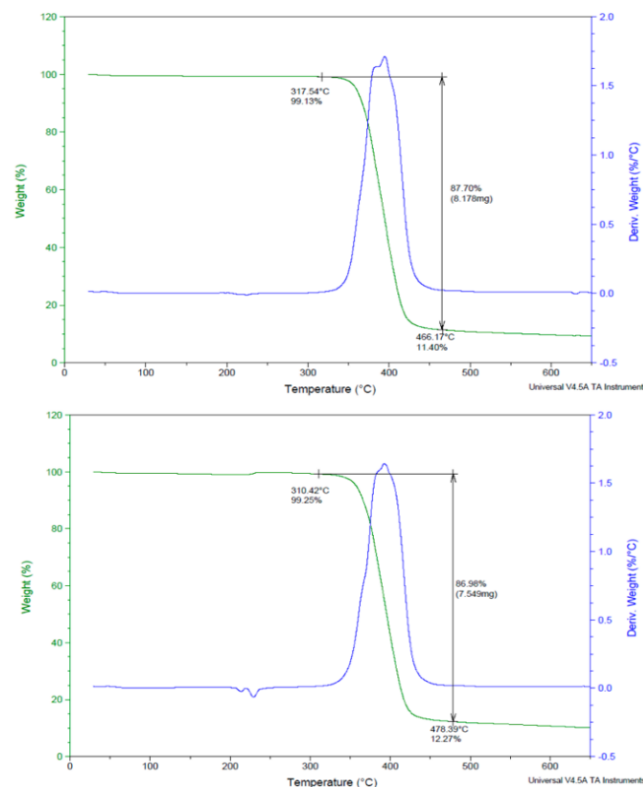


Figure 7. TGA results for nontextured and textured PA6/coPET yarns.

The starting temperature marked in the figures is the temperature at which a sharp drop in sample weight begins. When polymers are heated to sufficiently high temperatures, the weakest covalent bonds in the polymer

structure starts to break down and the polymer begins to degrade, which is called the 'decomposition temperature'. Polymers decompose before boiling. As can be seen from all figures, for all samples the materials began to decompose at lower temperatures after the texturization process. The decomposition temperature drops down from 332,81°C to 328,74°C for the PET/coPET yarn, from 339,94°C to 329,76°C for the rPET/coPET yarn, and from 317,54°C to 310,42°C for the PA6/coPET yarn. This may be due to the increase in polymer chain mobility after texturing. In addition, recycled PET showed less weight loss compared to the virgin PET sample, which can be explained by the dampness of the damaged surface of rPET [18]. For the PA6/coPET yarn, in both textured and nontextured forms, the degradation starts at lower temperatures compared to the PET/coPET and rPET/coPET yarns. This may be due to the fact that PA6 has a lower moisture content, which can be seen from the material properties at Table 1. In TGA analysis, the materials in general initially evaporates the moisture inside it, and then starts breaking down [19]. Since the moisture content of the yarn is also going to be relatively low, there is not much water content in the structure to be evaporated before the decomposition, thus the decomposition can begin at a lower temperature than the other samples.

The crystallinity and amorphism ratios of the samples according to the XRD results can be found in Table 4, and the XRD graphs of the samples are given in Figure 8, Figure 9, and Figure 10 for the PET/coPET sample, rPET/coPET sample and the PA6/coPET sample, in turn. In all of the graphs, the nontextured samples are denoted with "NT" and their textured counterparts are denoted with "T".

Table 4. XRD results.

Sample ID	Crystallinity (%)	Amorphism (%)
1	1,0	99,0
1T	14,8	85,2
2	0,7	99,3
2T	14,6	85,4
3	12,3	87,7
3T	2,7	97,3

As can be seen both from the tables and the graphs, XRD results indicate that for the PET/coPET and rPET/coPET samples, the texturization process significantly increased the crystallinity of the samples, which is an interesting result. In XRD analysis, an X-ray beam is directed onto the sample in a predetermined angle, and then the reflected scattering of the beam from the sample is measured as a function of the reflection angle. In general, if the sample has a high crystallinity, the diffraction shows as peaks whereas if the graph is smoother without any sharp peaks, the sample has a more amorphous form. But a broadened XRD pattern can also have other causes such as a non-flat material surface, high sample porosity, or a noise in the analysis itself [20]. Nevertheless, the texturization and alkalization parameters should be further investigated and studied in order to see their effect on the crystallization

since both processes may affect the polymer structure and the overall yarn behaviour after the coPET component has been removed. Previous studies on the thermomechanical analysis of polymers have proven that heat setting

parameters not only drastically effects the crystal and amorphous regions inside the structure, but also effects the mechanical properties of the final yarn as well [21].

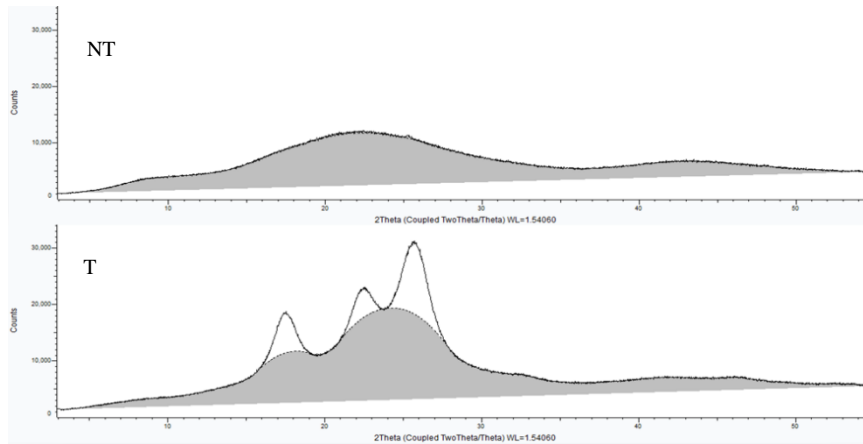


Figure 8. XRD results for nontextured and textured PET/coPET yarns.

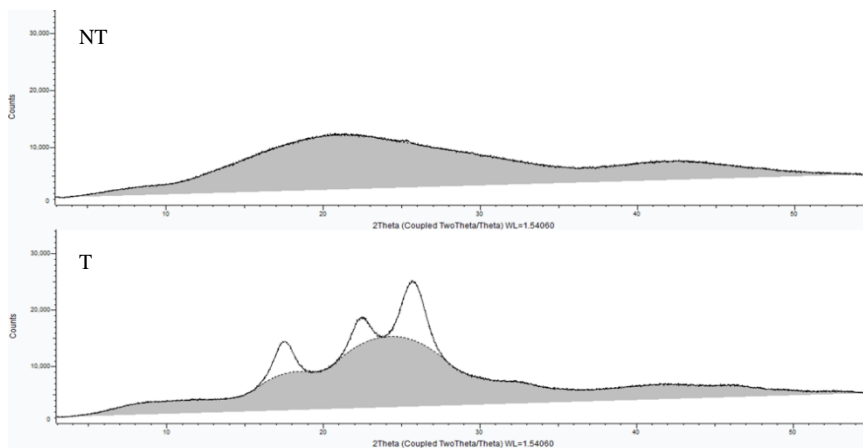


Figure 9. XRD results for nontextured and textured rPET/coPET yarns.

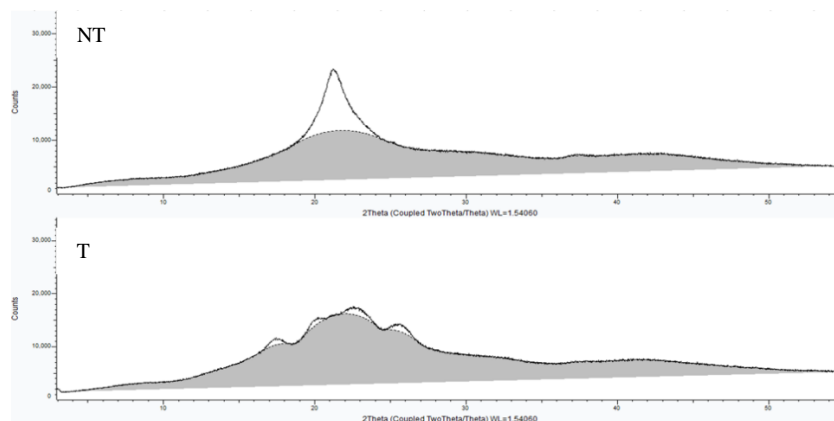


Figure 10. XRD results for nontextured and textured PA6/coPET yarns.

PA6/coPET sample shows the highest crystalline behaviour amongst all the samples in their nontextured forms. Contrary to the other samples, the PA6/coPET blend shows an opposite behaviour where the crystallinity is already at a high percentage but drops down afterwards. Crystallinity behaviour of polymers is dependant on many different properties such as the molecular weight, synthesization conditions, polymer architecture and so on. Polyethylene (PET) chains are mainly linked with dipole-dipole bonds whereas polyamides (PA) are linked with hydrogen bonds which has a dissociation energy almost ten times of a dipole-dipole bond. Also, the hydrogen bonds can be formed in a parallel form (α) or an anti-parallel form (γ) in PA6. In parallel form, the adjacent polymer chains are in the same directionality but in anti-parallel form, the chains have opposite directionality. In the parallel form, the hydrogen bonding occurs between the adjacent chains on the same sheet but in the anti-parallel form the hydrogen bonds occur between chains that are on adjacent sheets. Since the bonds between adjacent planes are stronger than bonds formed on the same sheet, the bonds are much stronger, thus increasing the crystallinity and the rigidity of the polymer [22, 23]. Nevertheless, the PA shows a different behaviour in a material context which is consistent with the other results in the study, but again it is essential to study the effects of the texturization and alkalization processes to get a better understanding of the situation.

4. CONCLUSION

This study evaluated and compared the mechanical and thermomechanical properties of three different bicomponent yarns. The tests were carried out in both the textured and nontextured forms of the samples to observe the effect of heat treatment and alkalization on the final properties. The results indicate the importance of choosing an appropriate raw material for bicomponent yarn production, since the chosen raw material carries its' intrinsic properties to the yarn stage and greatly affects the properties of the final material. It also demonstrates that alkalization and texturization have a significant impact on the properties of the polymers and the final yarns. An important result is that the textured yarns had better mechanical properties, even though they went through a heavy chemical process such as alkalization and half of the filament volume was removed. It is evident that texturization process appeared to play a more significant role than the alkalization; the heating process involved in texturization improved the crystallinity and density by increasing the number of immobile polymer chains with reduced elongation, as supported by literature [24]. This shows that hollow yarns have high mechanical strength and that they can be used in places where both insulation and strength are needed. The observed increase in the strength of all types of filaments proves that both components of a bicomponent yarn can be chosen and modified according to the desired application area and the required properties from the product without having to sacrifice from the tensile properties.

Thermomechanical analysis revealed that heat treatment and alkalization results in a higher polymer chain mobility, which caused an increase in the enthalpy values and decreased the decomposition temperature of the polymers. The unexpected rise in crystallinity seen in the XRD measurements for the PET/coPET and rPET/coPET samples following texturization may be explained by the fact that texturization includes the use of heat and mechanical processing, and the combination of these parameters may have resulted in changes in the polymer structure. According to the literature [21], mechanical deformation and orientation during texturization might impact polymer chain arrangement, potentially decreasing crystalline development. It is possible that the combination of heat and mechanical forces during texturization resulted in a unique set of conditions enabling crystalline development in the bicomponent yarns in the setting of this study. This unexpected result highlights the complex interactions of processing parameters and the need for additional research to identify the specific factors leading to the observed increase in crystallinity. Future work on the area should focus on the effect of the alkalization and texturization parameters as both processes seem to majorly affect the filament properties.

The study underlines the significance of choosing appropriate raw materials for bicomponent yarn manufacturing, since the basic characteristics of the chosen materials have a significant effect on the end result. Furthermore, the study indicates the ability of hollow yarns to improve mechanical strength and dimensional resistance even after chemical processes such as alkalization. The thermomechanical study provides helpful information on the enhanced polymer chain mobility caused by heat treatment and alkalization, which affects the yarn's enthalpy values and decomposition temperature.

Bicomponent fibers have been a popular application due to their many advantages, one of them being that they can be made into hollow yarns by removing one of the components. Hollow bicomponent yarns provide greater bulk with less weight to a textile material. They are, therefore, often used to provide acoustic or thermal insulation. Bicomponent hollow yarns are suitable candidates to replace their traditional counterparts, thanks to their modifiability, enhanced properties, and availability for a more sustainable approach. In the future, with the development of new materials and new methods, the use and importance of bicomponent yarns and products made from these yarns will increase, and thus this study contributes valuable knowledge to developing functional textiles with improved properties for future applications.

Acknowledgement

The authors gratefully acknowledge the funding by The Scientific and Technological Research Council of Turkey (TÜBİTAK) 1505 Program with the grant number 5210113.

REFERENCES

1. Zhu, S., et al., 2021. Evidence for bicomponent fibers: A review. *E-Polymers* 21(1), p. 636-653.
2. Oh, T.H., 2006. Melt spinning and drawing process of PET side-by-side bicomponent fibers. *Journal of Applied Polymer Science*, 101(3), p. 1362-1367.
3. Dasdemir, M., et al., 2011. Formation of novel thermoplastic composites using bicomponent nonwovens as a precursor. *Journal of Materials Science*, 46(10), p. 3269-3281.
4. Sun, B., B. Duan, and X. Yuan, 2006. Preparation of core/shell PVP/PLA ultrafine fibers by coaxial electrospinning. *Journal of Applied Polymer Science* 102(1), p. 39-45.
5. Guo, N.K., X. Huang, and L.X. Jing, 2014. Application Research of High-Strength Needled Filter Bag with Sea-Island Superfine Fiber. *Advanced Materials Research*, 1004-1005, p. 553-556.
6. Suvari, F., Y. Ulcay, and B. Pourdeyhimi, 2018. Influence of sea polymer removal on sound absorption behavior of islands-in-the-sea spunbonded nonwovens. *Textile Research Journal*, 89(12), p. 2444-2455.
7. Zhao, B., et al., 2019. The Application of Hollow Segmented Pie Bicomponent Spunbond Hydro-Entangled Microfiber Nonwovens for Microfiber Synthetic Leather Apparel. *AATCC Journal of Research*, 6(1_suppl), p. 45-49.
8. Uttam, D., A. Mukhopadhyay, and S.M. Istiaque, 2013. Modelling to predict thermophysiological properties of hollow/microporous yarn fabrics. *Journal of the Textile Institute*, 104(4), p. 407-413.
9. Yongfu, X., Y. Zhang, and G.Y. Yuan, 2020. Preparation and fuzzy evaluation of wool hollow yarn. *Textile Research Journal*, 90(9-10), p. 1149-1156.
10. Liu, X., et al., 2021. Sound absorption of hollow polyester woven fabric with honeycomb weave. *Applied Acoustics*, 180, p. 108148-108148.
11. Mukhopadhyay, A., S.M. Istiaque, and D. Uttam, 2011. Impact of structural variations in hollow yarn on heat and moisture transport properties of fabrics. *Journal of the Textile Institute*, 102(8), p. 700-712.
12. Celep, G. and M.E. Yükksekaya, 2017. Comparison of thermal comfort properties of single jersey fabrics produced by hollow yarns with different hollowness ratio. *The Journal of The Textile Institute*, 108(2), p. 165-171.
13. Merati, A.A. and M. Okamura, 2000. Hollow Yarn in Friction Spinning. *Textile Research Journal*, 70(12), p. 1070-1076.
14. Aytaç, İ. and P. Gürkan Ünal, 2018. The effect of core-sheath proportion on the characteristics of fabrics produced with hollow yarns: part II comfort and mechanical properties. *The Journal of The Textile Institute*, 109(7), p. 975-982.
15. Guo, Z., et al., 2021. Development of Circularly Recyclable Low Melting Temperature Bicomponent Fibers toward a Sustainable Nonwoven Application. *ACS Sustainable Chemistry and Engineering*, 9(49), p. 16778-16785.
16. Pivsa-Art, S., K. Sunyikhan, and W. Pivsa-Art, 2022. Bicomponent multifilament yarns of recycled poly(ethylene terephthalate) and nano-titanium dioxide for antibacterial carpet. *Journal of Industrial Textiles*, 51(1), p. 1034S-1047S.
17. Rosson, L. and N. Byrne, 2022. Bicomponent regenerated cellulose fibres: retaining the colour from waste cotton textiles. *Cellulose*, 29(7), p. 4255-4267.
18. Lubna, M.M., et al., 2018. Modification of Thermo-Mechanical Properties of Recycled PET by Vinyl Acetate (VAc) Monomer Grafting Using Gamma Irradiation. *Journal of Polymers and the Environment*, 26(1), p. 83-90.
19. Bendak, A., O. Allam, and L. El-Gabrie, 2010. Treatment of polyamides fabrics with cyclodextrins to improve some properties. *Open Text. J.*, 3, p. 6-13.
20. Ali, M., 2023. Qualitative Analyses of Thin Film-Based Materials Validating New Structures of Atoms.
21. Yildirim, K., et al., 2014. Twist setting temperature and time effects on morphology of polyethylene terephthalate yarn. *Tekstil ve Konfeksiyon*, 24, p. 186-194.
22. Dasgupta, S., W.B. Hammond, and W.A.G. Iii, 1996. Crystal Structures and Properties of Nylon Polymers from Theory, in *CN.* p. 139-74.
23. Zhang, M., S.M. June, and T.E. Long, 2012. 5.02 - Principles of Step-Growth Polymerization (Polycondensation and Polyaddition), in *Polymer Science: a Comprehensive Reference Volume 1-10.* p. 7-47.
24. Gupta, V. B., & Kumar, M. 1975. Changes in the Structure of Polyethylene Terephthalate Yarn on Texturing. *Textile Research Journal*, 45(5), 382- 388. <https://doi.org/10.1177/004051757504500504>

The Effect of Production Parameters of Face to Face Warp Velvet Fabric on Abrasion Resistance and Colour Properties

Yunus Emre Kayserili¹  0000-0002-5230-3439

Asım Davulcu²  0000-0002-2234-9655

¹ Ağrı University / Erzurum Yolu 4 Km 04100 Merkez, Ağrı, Türkiye

² Erciyes University /Yenidoğan Mahallesi Turhan Baytop Sokak No:1 38280 Talas, Kayseri, Türkiye

Corresponding Author: Yunus Emre Kayserili, yekayserili@agri.edu.tr

ABSTRACT

Nowadays, velvet fabrics are widely used in upper clothing, curtains and especially upholsteries. One of the most important problems encountered in them is the distancing of the piles from the surface of the fabric and the other is discoloration over time. In addition to the fabric properties, yarn and fiber properties also affect this situation. In this article, the effect of production parameters on fabric abrasion was investigated in face to face warp velvet fabrics. The abrasion resistance of 100% cotton (10, 15, and 20 thousand rpm (rotation per minute)) and 100% polyester (30, 45, and 60 thousand rpm (rotation per minute)) velvet fabrics has been tested. The fabrics were produced using 3 different weft yarn counts (150, 300, and 450 deniers for polyester and 6, 12, and 20 Ne for cotton), 3 different weft densities (20, 22, and 24 picks/cm for polyester and 11, 13, and 15 picks/cm for cotton), 3 different pile heights (2, 3, and 4 cm) and two different pile connection types (V and W), and the abrasion of the fabrics was tested with a Martindale device. The results were analyzed. In addition, The effects of production parameters on fabric color were investigated in face to face warp velvet fabrics. Cotton fabrics were dyed with reactive blue, yellow and red, while polyester fabrics were dyed with disperse blue, yellow and red. Color properties and gloss have been tested and the results were analyzed. According to the test results, the increase in weft yarn count (increasing denier/decreasing Ne) causes an increase in abrasion resistance, while the increase in pile height reduces the abrasion resistance. The W bonded fabrics were found to be more resistant to abrasion than the V bonded fabrics. The color properties of the fabrics produced were tested in spectrophotometer test devices and the effects of production parameters were analyzed. It was determined that deep colors such as blue and red have an effect on color properties, while light colors such as raw fabric and yellow velvet fabric do not have a significant effect. It was also detected that raw and yellow velvet fabrics have more gloss than blue and red velvet fabrics.

1. INTRODUCTION

1.1. Velvet Fabric Information

Velvet is a type of woven fabric with a pile surface. If the pile yarns on the fabric surface are given from the weft direction, this fabric type is defined as weft velvet, and if the pile yarns on the fabric surface are given from the warp direction, this fabric type is defined as warp velvet. Generally, weft velvet fabrics are used in the clothing industry, and warp velvet fabrics are used in home textiles [1].

1.2. Production Parameters of Velvet Fabric

The most important parameter that creates velvet fabrics is the pile layer on the fabric surface, other important parameters are the warp and weft yarns that make up the ground. Besides these parameters, the type of yarn (cotton, linen, viscose, pes), yarn production methods (ring, open end), twist in the yarn (T/m) used in the pile and on the ground are important. In addition, many parameters such as the ground weave (plain, twill, satin), pile connection type (V, U, W), creating pile from weft or warp (weft, warp velvet), pile height and pile density in the fabric are among the factors affecting the structure of the velvet fabric [2, 3].

To cite this article: Kayserili YE, Davulcu A. 2024. The effect of production parameters of face to face warp velvet fabric on abrasion resistance and colour properties. *Tekstil ve Konfeksiyon* 34(4), 434-447

ARTICLE HISTORY

Received: 23.05.2023

Accepted: 20.05.2024

KEYWORDS

Velvet fabric, pile loss, abrasion resistance, color properties, gloss, fabric production parameters

1.3. Production Techniques Used in Velvet Fabrics

1. Weft Velvet
2. Warp Velvet
 - a) Warp velvet production with a single layer system
 - b) Warp velvet production with face to face system
 - Single shuttle warp velvet production
 - Double shuttle warp velvet production

Since face to face double shuttle warp velvet is used within the article, only face to face production will be emphasized among the velvet production methods [2, 3].

Double shuttle face to face warp velvet production

It is the system used in modern warp velvet fabric. In this system, the ground warp beams can be prepared separately. Pile warp beams are only used in dobby looms. The pile is fed from the creel on jacquard looms [4]. A pile surface is formed by cutting the pile warps that connect between two fabrics with the help of a knife [1]. Weft insertion is done on both fabrics at the same time. Two separate sheddings are opened on the loom, one for the top and the other for bottom fabric. In this way, it is possible to weave more fabric at the same time.

Van de Wiele, Gsken and Gnne are the machines that weave warp velvet fabric. Van de Wiele is the best known company producing the machines that weave warp velvet fabric. There are crankshaft, beating up and rapier in the main parts. In these machines, weft insertion is done with rapiers. The rapiers are driven by parts consisting of the crankshaft and gearbox. The female rapier brings the weft from the weft scissors to the half of the fabric, and the male rapier transfers the weft to the other end of the fabric. Velvet weaving machines generally work with a negative weft transfer system. The beating up ensures the compression of the weft during the weaving process [5].

1.4. Pile Connection Types Used in Velvets

V Connection Type: The pile connection formed on one weft is called V connection. The weft yarn continues by skipping one by one. V connection is preferred when a tight pile layer is desired on the fabric [6].

U Connection Type: The pile connection formed on two weft yarns is called U connection. It is produced to obtain sparse pile velvet fabrics compared to V connection [6].

W Connection Type: The pile connection formed on three wefts is called W connection. It is the preferred connection type in the production of sparse pile velvet fabrics. The best

result is obtained (on ground fabric) with plain weave connection [6].

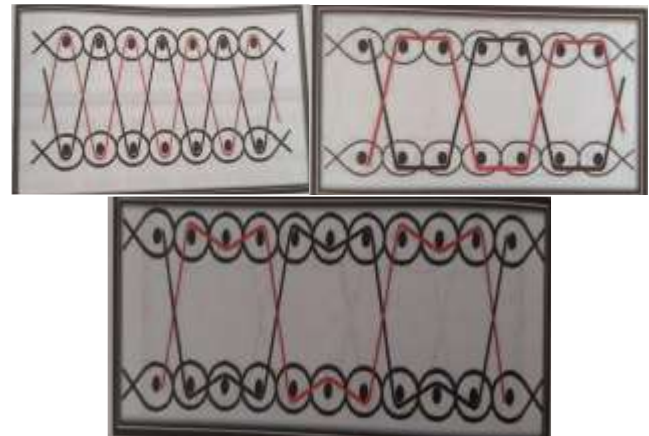


Figure 1. V connection type (left), U connection type (middle), W connection type (right) for face to face Warp Velvet

2. MATERIAL AND METHOD

2.1. Materials and Devices

2.1.1. Fabrics: Table 1 and Table 2 give information on velvet fabrics made of 100% polyester and cotton in different constructions. 8 pieces of 100% polyester and 8 pieces of 100% cotton velvet fabric were produced by changing the dark-colored parameters over the main fabric written in light colors in the table.

2.1.2. Chemicals: In the dyeing process, disperse dyestuff (blue 56, yellow 211 and red 167), reactive dyestuff (blue 221, yellow 145 and red 21), water, salt, soda, acid and dispersant were used [16].

2.1.3. Devices

Martindale fabric abrasion device is a device with 8 abrasive heads, each head uses a 12 kpa weight for abrading, a 140 mm felt and standard fabric chamber, 38 mm sample and foam insertion head, and a electronic display. In addition, 38 mm and 140 mm cutters are available separately from the device as spares [30, 31, 32].

Drying oven, (Thermal brand) is a device with an independent safety thermostat that can dry at the desired temperature between 0-200°C. The volume of the device is 53 liters. The inner surface of the device is stainless steel, and the temperature indicator is digital.

Table 1. Polyester fabric properties.

%100 Polyester Fabric Sample: 1-8 Production Method: Face to face weaving	
Yarn type and count used in weft	300/72 polyester (150/72-450/432 denier)
Yarn type and count used in warp	300/288 denier polyester
Yarn type and count used in pile	300/288 denier polyester
Weft density	20 picks/cm (22-24 picks/cm)
Warp density	25 picks/cm
Pile height	2 mm (3-4 mm)
Pile connection type	W (V)
Produced machine type	Vtr Vande Wiele

Table 2. Cotton fabric properties

%100 Cotton Fabric Sample: 9-16 Production Method: Face to face weaving	
Yarn type and count used in weft	6/1 Ne cotton (12-20 Ne)
Yarn type and count used in warp	30/2 Ne cotton
Yarn type and count used in pile	28/2 Ne cotton
Weft density	15 picks/cm (11-13 picks/cm)
Warp density	19 picks/cm
Pile height	2 mm (3-4 mm)
Pile connection type	V(W)
Produced machine type	Vtr Vande Wiele

Table 3. Polyester and cotton velvet fabrics codes

Polyester Fabrics	Codes	Cotton Fabrics	Codes
Polyester/20 (picks/cm) density/300 denier weft/2 mm pile height/W pile connection (Sample 1)	P/20 pck/300 D w/2 p h/W p c	Cotton/15 (picks/cm) density/6-1 Ne weft/2 mm pile height/V pile connection (Sample 9)	C/15 pck/6-1 Ne w/2 p h/V p c
Polyester/22 (picks/cm) density/300 denier weft/2 mm pile height/W pile connection (Sample 2)	P/22 pck/300 D w/2 p h/W p c	Cotton/13 (picks/cm) density/6-1 Ne weft/2 mm pile height/V pile connection (Sample 10)	C/13 pck/6-1 Ne w/2 p h/V p c
Polyester/24 (picks/cm) density/300 denier weft/2 mm pile height/W pile connection (Sample 3)	P/24 pck/300 D w/2 p h/W p c	Cotton/15 (picks/cm) density/6-1 Ne weft/3 mm pile height/V pile connection (Sample 11)	C/15 pck/6-1 Ne w/3 p h/V p c
Polyester/20 (picks/cm) density/150 denier weft/2 mm pile height/W pile connection (Sample 4)	P/20 pck/150 D w/2 p h/W p c	Cotton/15 (picks/cm) density/6-1 Ne weft/4 mm pile height/V pile connection (Sample 12)	C/15 pck/6-1 Ne w/4 p h/V p c
Polyester/20 (picks/cm) density/450 denier weft/2 mm pile height/W pile connection (Sample 5)	P/20 pck/450 D w/2 p h/W p c	Cotton/11 (picks/cm) density/6-1 Ne weft/2 mm pile height/V pile connection (Sample 13)	C/11 pck/6-1 Ne w/2 p h/V p c
Polyester/20 (picks/cm) density/300 denier weft/3 mm pile height/W pile connection (Sample 6)	P/20 pck/300 D w/3 p h/W p c	Cotton/15 (picks/cm) density/12-1 Ne weft/2 mm pile height/V pile connection (Sample 14)	C/15 pck/12-1 Ne w/2 p h/V p c
Polyester/20 (picks/cm) density/300 denier weft/4 mm pile height/W pile connection (Sample 7)	P/20 pck/300 D w/4 p h/W p c	Cotton/15 (picks/cm) density/20-1 Ne weft/2 mm pile height/V pile connection (Sample 15)	C/15 pck/20-1 Ne w/2 p h/V p c
Polyester/20 (picks/cm) density/300 denier weft/2 mm pile height/V pile connection (Sample 8)	P/20 pck/300 D w/2 p h/V p c	Cotton/15 (picks/cm) density/6-1 Ne weft/2 mm pile height/W pile connection (Sample 16)	C/15 pck/6-1 Ne w/2 p h/W p c

Table 4. Polyester and cotton velvet fabrics samples

Sample 1 polyester (raw)		L* 74.65	L* 9.38	L* 33.86	Sample 9 cotton (raw)		L* 64.38	L* 35.05	L* 38.84	
	30000 rpm	45000 rpm	60000 rpm	10000 rpm		15000 rpm	20000 rpm			
	Mass loss 2.34%	Mass loss 3.48%	Mass loss 6.19%	Mass loss 27.00%		Mass loss 28.15%	Mass loss 30.75 %			
Sample 2 polyester (raw)		L* 73.40	L* 5.49	L* 26.41	Sample 10 cotton (raw)		L* 60.27	L* 37.10	L* 39.46	
	30000 rpm	45000 rpm	60000 rpm	10000 rpm		15000 rpm	20000 rpm			
	Mass loss 1.42%	Mass loss 2.66%	Mass loss 4.28%	Mass loss 29.34%		Mass loss 30.85 %	Mass loss 33.77 %			
Sample 3 polyester (raw)		L* 73.29	L* 3.75	L* 26.26	Sample 11 cotton (raw)		L* 60.59	L* 24.25	L* 34.02	
	30000 rpm	45000 rpm	60000 rpm	10000 rpm		15000 rpm	20000 rpm			
	Mass loss 1.30%	Mass loss 2.32%	Mass loss 3.44%	Mass loss 28.49%		Mass loss 29.57 %	Mass loss 31.07 %			
Sample 4 polyester (raw)		L* 74.74	L* 12.12	L* 29.19	Sample 12 cotton (raw)		L* 61.40	L* 36.36	L* 35.12	
	30000 rpm	45000 rpm	60000 rpm	10000 rpm		15000 rpm	20000 rpm			
	Mass loss 3.70%	Mass loss 8.46%	Mass loss 13.87 %	Mass loss 29.25 %		Mass loss 30.25 %	Mass loss 31.57%			
Sample 5 polyester (raw)		L* 75.18	L* 13.75	L* 31.38	Sample 13 cotton (raw)		L* 63.85	L* 38.09	L* 40.69	
	30000 rpm	45000 rpm	60000 rpm	10000 rpm		15000 rpm	20000 rpm			
	Mass loss 1.98%	Mass loss 3.59%	Mass loss 4.77 %	Mass loss 27.13%		Mass loss 30.38%	Mass loss 34.62 %			
Sample 6 polyester (raw)		L* 75.14	L* 5.29	L* 28.45	Sample 14 cotton (raw)		L* 64.30	L* 27.63	L* 38.42	
	30000 rpm	45000 rpm	60000 rpm	10000 rpm		15000 rpm	20000 rpm			
	Mass loss 3.16%	Mass loss 4.43 %	Mass loss 7.17 %	Mass loss 32.59 %		Mass loss 35.42 %	Mass loss 38.66%			
Sample 7 polyester (raw)		L* 72.82	L* 4.98	L* 27.93	Sample 15 cotton (raw)		L* 65.00	L* 37.04	L* 43.35	
	30000 rpm	45000 rpm	60000 rpm	10000 rpm		15000 rpm	20000 rpm			
	Mass loss 5.02%	Mass loss 6.47 %	Mass loss 9.28 %	Mass loss 36.62%		Mass loss 38.52%	Mass loss 41.33%			
Sample 8 polyester (raw)		L* 73.32	L* 6.62	L* 30.59	Sample 16 cotton (raw)		L* 67.28	L* 38.78	L* 47.69	
	30000 rpm	45000 rpm	60000 rpm	10000 rpm		15000 rpm	20000 rpm			
	Mass loss 5.07%	Mass loss 8.31%	Mass loss 11.21%	Mass loss 3.93%		Mass loss 5.77 %	Mass loss 7.42 %			



Digital weighing is a laboratory type precision scale of 210 g capacity, Ohaus pioneer type, with internal calibration, glass protection that can be opened from three sides, an LCD display, and a weighing 4.5 kg.

Spectrophotometer device, Konica Minolta CM-3600D is used for reflectance measurement. The device, which works in D/8° sphere geometry, works with quality control or prescription software connected to the computer.

Laboratory type dyeing machine, Thermal brand is a sample dyeing machine with 12x180 cc tube number, 380 V 50/60 Hz heat and time control, 5200 W power and a 26 lt internal volume.

Gloss meter, Konica Minolta MG 268A is an ultra compact and portable gloss meter that can measure all glossy surfaces from matte to high gloss with three angles of 20°, 60° and 85°. All features such as language settings, calibration, measurement and statistics can be performed with two operating keys.

2.2. Experimental

2.2.1. Abrasion process

The device was operated according to the determined number of rotations (10-15-20 thousand rotations for cotton and 30-45-60 thousand rotations for polyester), and the weight loss of the test samples was determined at the end of the rotation. (% Abrasion) $\text{Mass loss (\%)} = (m_1 - m_2) / m_1$ was determined as the m_1 sample weight before test (grams), the m_2 sample weight after the test (grams) [28, 29, 34].

2.2.2. Dyeing process

16 samples (8 cotton and 8 polyester) of cotton fabrics were dyed with reactive blue 221, yellow 145 and red 21, and polyester fabrics were dyed with disperse blue 56, yellow 211 and red 167 in a laboratory dyeing machine (Thermal).

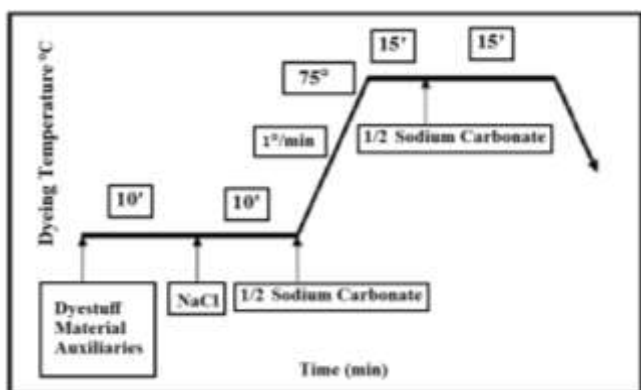


Figure 2. Reactive dyeing of cotton fabrics

2.2.2.1. Dyeing cotton velvet fabric

The dyeing process was carried out with 100% cotton fabric samples (10 g), with 1% dyeing in the sample dyeing machine (Thermal) at a flotte ratio of 1:10 according to the

impregnation method. Dyeing was carried out in separate tubes of 25gr/lt soda and 60gr/lt salt reactive yellow 145, red 21 and blue 221 at 75°C for 60 minutes. The dyeing diagram is shown in Figure 2 [12, 13, 14].

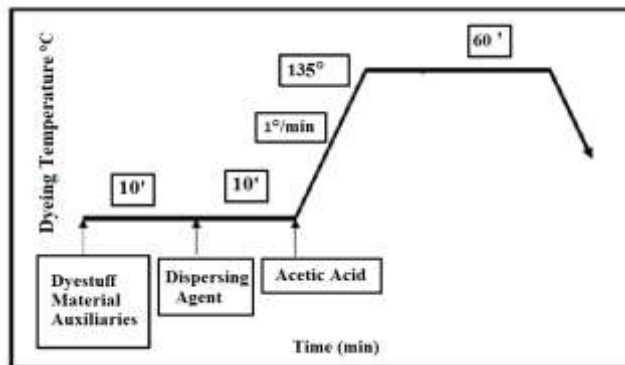


Figure 3. Disperse dyeing of polyester fabrics

2.2.2.2. Dyeing polyester velvet fabric

The dyeing process was carried out with 100% polyester fabric samples (10 g), with 1% dyeing in the sample dyeing machine (Thermal) at a flotte ratio of 1:10 according to the exhaustion method. Dyeing was carried out in disperse yellow 211, red 167 and blue 56 tubes in separate tubes at 135°C for 60 minutes. The dyeing diagram is shown in Figure 3 [9, 19, 20, 33].

2.2.3. Gloss measurement

The light emanating from the light source inside the device was reflected from the velvet fabric surface at a certain angle (such as 20, 60 and 85°) and reached the sensors on the other side of the glossmeter. Thus, the ratio of the amount of light reflected from the velvet fabric surface to the amount of light coming from the device source was measured. The resulting numerical value has been converted to a Gloss Unit (GU), which is a luminance unit. A flat black glass with a refractive index value of 1.567 was used for calibration purposes according to ASTM D523 standards. The measured value for this standard is 100 Gloss Units (GU). It is used for 85° low gloss (matt), 60° medium gloss and 20° high gloss in gloss angles.

2.2.4. SPSS 20 statistics program

Percent abrasion resistance values obtained with the Martindale test device were evaluated separately for 100% cotton velvets and polyester velvets. Density-number of rotation, pile height- number of rotation, weft yarn count-number of rotation and pile connection type- number of rotation relationships were evaluated with SPSS two-way anova analysis for 100% cotton and polyester fabrics using the percent abrasion results in Martindale. L (lightness) values obtained with spectrophotometer devices were evaluated separately for 100% cotton velvets and polyester velvets. Density-color, pile height-color, weft yarn count-color and pile connection type-color relationship were evaluated with SPSS two-way anova analysis for 100% cotton and polyester fabrics using L results in a spectrophotometer.

3. RESULTS AND DISCUSSION

3.1. Investigation of Parameters Affecting the Abrasion Resistance of 100% Cotton Velvet Fabrics

3.1.1. Effect of weft density on abrasion

In Figure 4, the increase in the weft density as 11, 13 and 15 picks/cm values increased the abrasion resistance of the velvet fabrics at 10, 15 and 20 thousand rotations and caused less mass loss. It is thought that the interaction of pile yarns with weft and warp yarns increases with increasing density. The closer the weft and warp yarns are to each other, the better the pile yarns will be attached to the fabric ground. In the literature [7,21] shirting fabrics were exposed to abrasion resistance and similar results were found when the density increased. The results showed that fabrics using 2 yarn sets (weft and warp) and velvets using 3 yarn sets (weft, warp and pile) overlapped with each other.

In the Post Hoc test, there were close values between 11 and 13 picks/cm for weft density in the subsets, there was no significant difference ($p=0.070>0.05$) but there was a significant difference between 11 and 15 picks/cm values and 13 and 15 picks/cm values in the subsets ($p=0.00<0.05$).

3.1.2. Effect of weft yarn count on abrasion

In Figure 5, the increase in the weft yarn count as 6, 12 and 20 Ne weft yarn count values decreased the abrasion resistance of the velvet fabrics in 10, 15 and 20 thousand rotations and caused more mass loss. It is thought that the connection of the pile yarns with the fabric ground decreases with the thinning of the weft yarns. For the same density value, increasing the weft yarn count (thinning the yarns) will create more gaps between the weft yarns. This gaps will reduce the pile-ground connection. The abrasion resistance increases as the yarn used for weft and warp in woven fabrics becomes thinner and the twist increases [22, 35, 36]. However, the thinning of the weft and warp yarns on the ground reduced the connection of the pile yarns and increased the amount of abrasion.

In the Post Hoc test, there was a significant difference in 6, 12 and 20 Ne values in the subsets ($p=0.00<0.05$).

3.1.3. Effect of pile height on abrasion

In Figure 6, with the increase pile height as 2, 3 and 4 mm values the abrasion resistance of velvet fabrics in 10, 15 and 20 thousand rotations decreased. As the pile height increases, the connection distance of the pile yarns with the fabric ground increases and these free ends abrade more. In literature, when pile heights increase by 0.5–1.0, 2.0–4.0 mm, the abrasion first increases and then decreases to reach

the optimum value so it is thought that the abrasion may increase with the increase in pile height. With the available data, it is not known in which interval the optimum value is. However, it is thought to be between 1.0 and 2.0 mm. In order to determine the optimum pile height in abrasion, it will be more accurate to examine the abrasion by making studies with very repetitive, close to each other and wide range pile heights [23, 37].

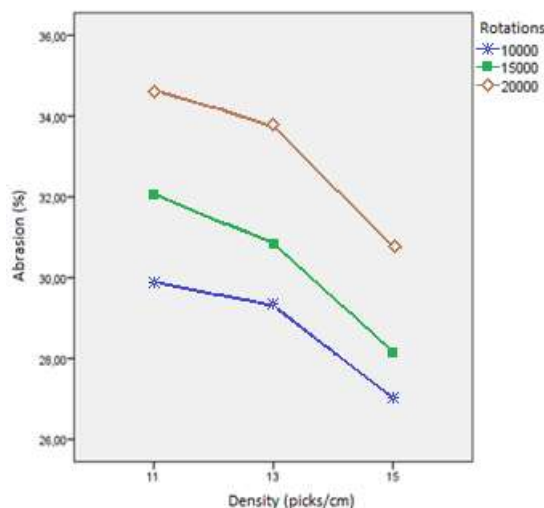


Figure 4. Weft density variation-(%) abrasion in cotton velvets. (comparison sample 9-10-13)

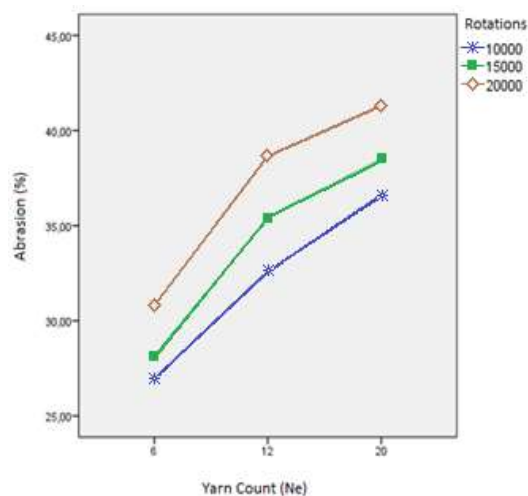


Figure 5. Weft yarn count variation-(%) abrasion in cotton velvets. (comparison sample 9-14-15)

There was a significant difference in the subsets of 2, 3 and 4 mm values used in the Post Hoc test ($p= 0.00<0.05$).

3.1.4. Effect of pile connection type on abrasion

In Figure 7, V and W connection types used in 100% cotton warp velvets, V connection pile velvets abraded more, while W connection pile fabrics abraded less. This result is thought to be that the W connection makes a better stronger

connection to the velvet fabric ground compared to the V connection and therefore is abraded less. While pile connection type W is more difficult to move away from the fabric ground because it attaches to the fabric ground from two separate points, the pile connection type V connects to the fabric ground from a single point, it is easier to move away from the fabric ground. In literature, it was concluded that plain fabrics are less abraded than twill and satin fabrics [8,24,25]. As the reason for this, it was explained that the increase in the number of connections between the weft and warp yarns reduces the abrasion.

Before examining the effect of the parameters that make up polyester velvet fabrics on abrasion, when the effect of cotton fabrics on abrasion as raw material compared to polyester fabrics was examined, it was seen that cotton fabrics exposed more abrasion in literature [26,27].

3.2. Investigation of Parameters Affecting the Abrasion Resistance of 100% Polyester Velvet Fabrics

3.2.1. Effect of weft density on abrasion

In Figure 8, the increase in the density values as 20, 22 and 24 picks/cm increased the abrasion resistance of velvet fabrics at 30, 45 and 60 thousand rotations and caused less mass loss. As in cotton velvets, the interaction of pile yarns with ground yarns increases with the increase in density in polyester velvets, and accordingly, less abrasion is observed.

In the Post Hoc test, there was a significant difference in the subsets of 20, 22 and 24 picks/cm values ($p=0.00<0.05$).

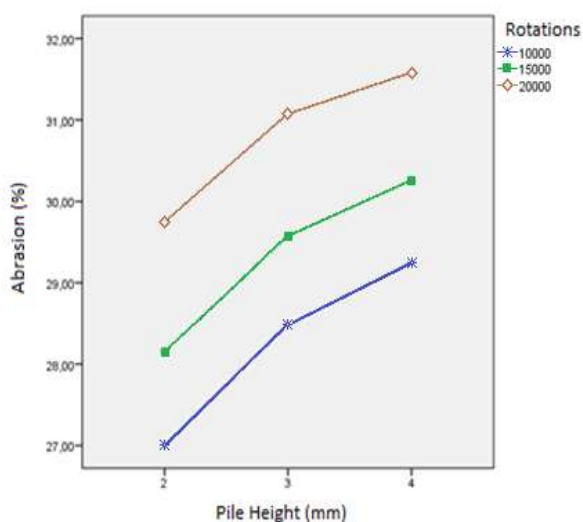


Figure 6. Pile height variation-(-%) abrasion in cotton velvets (comparison sample 9-11-12)

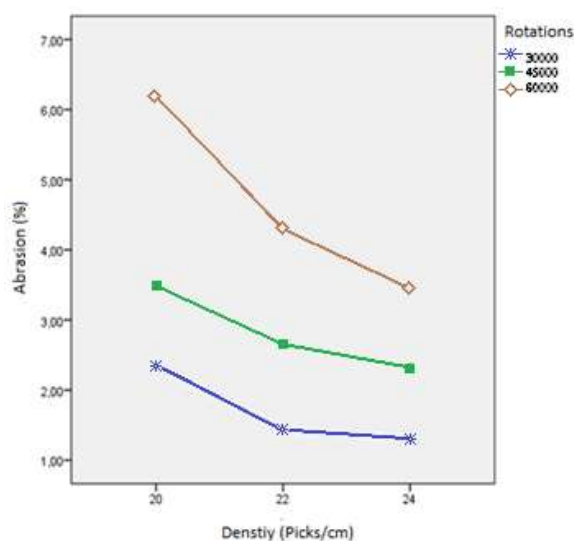


Figure 8. Variation of weft density-(-%) abrasion in polyester velvets. (comparison sample 1-2-3)

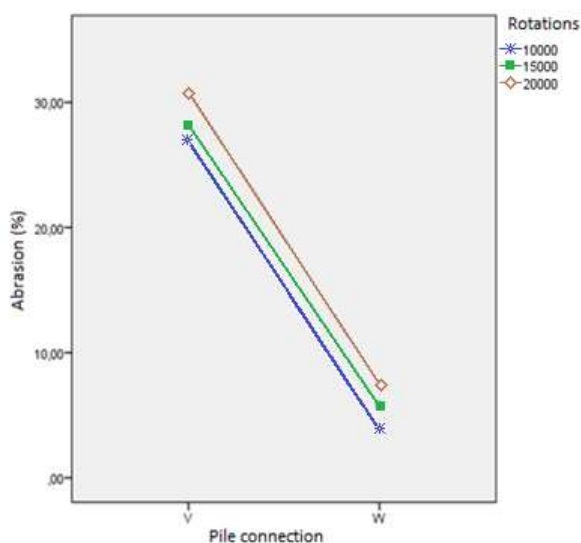


Figure 7. Pile connection variation-(-%) abrasion in cotton velvets. (comparison sample 9-16)

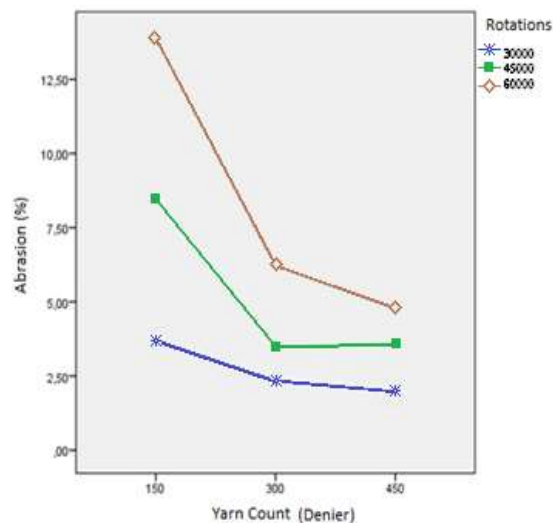


Figure 9. Weft yarn count change-(-%) abrasion in polyester velvets. (comparison sample 1-4-5)

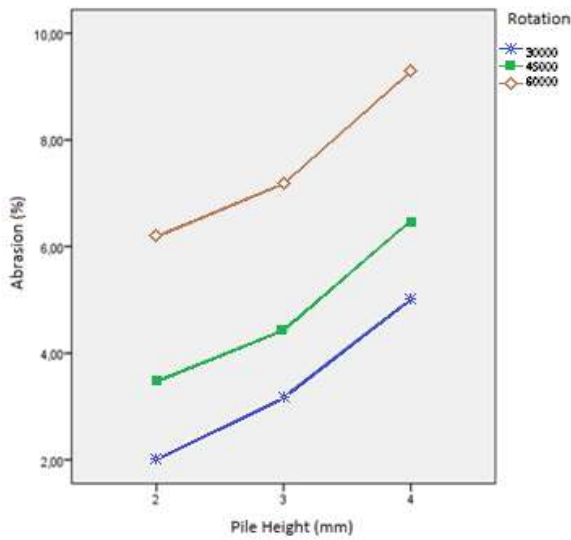


Figure 10. Pile height variation-(-) abrasion in polyester velvets (comparison sample 1-8)

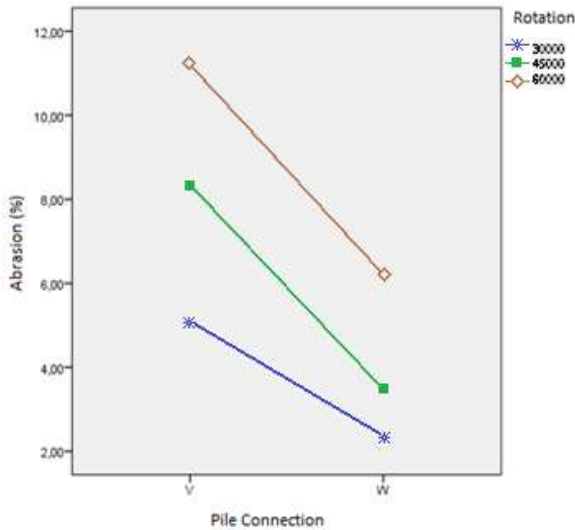


Figure 11. Pile connection variation-(-) abrasion in polyester velvets (comparison sample 1-6-7)

3.2.2. Effect of weft yarn count on abrasion

In Figure 9, the increasing weft yarn count values as 150, 300 and 450 denier increased the abrasion resistance of the velvet fabrics at 10, 15 and 20 thousand rotations and caused less mass loss. As in cotton velvets (decreasing Ne), the increasing yarn count (increasing denier) of the weft yarns in polyester velvets has led to an increase in the connection of the pile yarns with the ground and a decrease in abrasion. The change in raw material only changed the abrasion resistance values. While cotton velvets had a lot of

abrasion at low rotations, polyester velvets had much less abrasion.

In the Post Hoc test, there was no significant difference between the subsets at 300 and 450 denier values ($p=0.130>0.05$). There was a significant difference between 150 and 300 and 300 and 450 denier weft yarn counts in the subsets ($p=0.00<0.05$).

3.2.3. Effect of pile height on abrasion

In Figure 10, the increasing pile height values as 2, 3 and 4 mm decreased the abrasion resistance of the velvet fabrics at 30, 45 and 60 thousand rotations and caused more mass loss. As the pile height increases, the connection distance of the pile yarns with the fabric ground increases and these free ends abrade more. The increase in pile height in cotton velvet fabrics decreased the abrasion resistance. A similar situation was observed in polyester fabrics.

In the Post Hoc test, there was a significant difference in the 2, 3 and 4 mm values used in the subsets ($p=0.00<0.05$). As the pile height increased, a statistically significant increase was observed in the percentage abrasion resistance values.

3.2.4. Effect of pile connection type on abrasion

In Figure 11, V and W connection types used in 100% polyester warp velvets, V pile velvets abraded more, while W pile fabrics abraded less. It is similar to the result of W pile connection, which is one of the pile connection types made for cotton velvets, in the form of better connecting to the fabric and less abrasion compared to the V connection.

3.3. Investigation of Parameters Affecting the Color Properties of 100% Cotton Velvet Fabrics

The interaction test between the weft density, weft yarn count, pile height, pile connection type and color independent variables and the dependent variable L^* (lightness) in cotton velvets are examined in the F value (ANOVA table) the color factor has a very large effect compared to other independent factors. Among the factors affecting the L^* value, other factors besides the color factor are negligible. Color measurements were made by carding the piles in the same direction. The effect of pile connection type and pile height is slightly higher on the L^* value compared to weft density and weft yarn count.

In the post hoc test, the color had a significant effect on the L^* value (significance value $0.000<0.05$).

Table 5. Martindale (abraison percentage) test results of polyester and cotton velvet fabrics.

Codes		30,000 rotations	45,000 rotations	60,000 rotations	Codes	10,000 rotations	15,000 rotations	20,000 rotations	
P/20 pck/300 d w/2 p h/W p c	Mean	2.34	3.48	6.19	C/15 pck/6-1 Ne w/2 p h/V p c	Mean	27.005	28.157	30.755
	SD	0.38	0.206	0.405		SD	0.157	0.799	1.186
	%CV	16.242	5.928	6.538		%CV	0.58	2.837	3.855
P/22 pck/300 d w/2 p h/W p c	Mean	1.426	2.663	4.289	C/13 pck/6-1 Ne w/2 p h/V p c	Mean	29.341	30.852	33.778
	SD	0.026	0.388	0.227		SD	0.236	1.04	0.747
	%CV	1.858	14.585	5.29		%CV	0.804	3.373	2.211
P/24 pck/300 d w/2 p h/W p c	Mean	1.304	2.321	3.445	C/15 pck/6-1 Ne w/3 p h/V p c	Mean	28.49	29.574	31.078
	SD	0.076	0.157	0.459		SD	0.235	0.304	0.198
	%CV	5.849	6.777	13.316		%CV	0.827	1.028	0.638
P/20 pck/150 d w/2 p h/W p c	Mean	3.701	8.467	13.879	C/15 pck/6-1 Ne w/4 p h/V p c	Mean	29.252	30.254	31.575
	SD	0.164	1.09	1.07		SD	0.124	0.208	0.596
	%CV	4.421	12.868	7.712		%CV	0.426	0.687	1.888
P/20 pck/450 d w/2 p h/W p c	Mean	1.982	3.594	4.778	C/11 pck/6-1 Ne w/2 p h/V p c	Mean	29.889	32.07	34.625
	SD	0.16	0.484	0.075		SD	0.517	0.334	1.142
	%CV	8.059	13.457	1.577		%CV	1.731	1.04	3.298
P/20 pck/300 d w/3 p h/W p c	Mean	3.164	4.438	7.179	C/15 pck/12-1 Ne w/2 p h/V p c	Mean	32.597	35.427	38.669
	SD	0.237	0.088	0.148		SD	0.272	0.611	0.658
	%CV	7.484	1.989	2.067		%CV	0.835	1.725	1.703
P/20 pck/300 d w/4 p h/W p c	Mean	5.024	6.474	9.288	C/15 pck/20-1 Ne w/2 p h/V p c	Mean	36.624	38.526	41.332
	SD	0.19	0.335	0.291		SD	0.74	1.162	0.195
	%CV	3.785	5.167	3.133		%CV	2.021	3.015	0.471
P/20 pck/300 d w/2 p h/V p c	Mean	5.07	8.317	11.214	C/15 pck/6-1 Ne w/2 p h/W p c	Mean	3.932	5.778	7.43
	SD	0.386	0.226	0.916		SD	0.14	0.073	0.276
	%CV	7.614	2.714	8.169		%CV	3.562	1.272	3.71

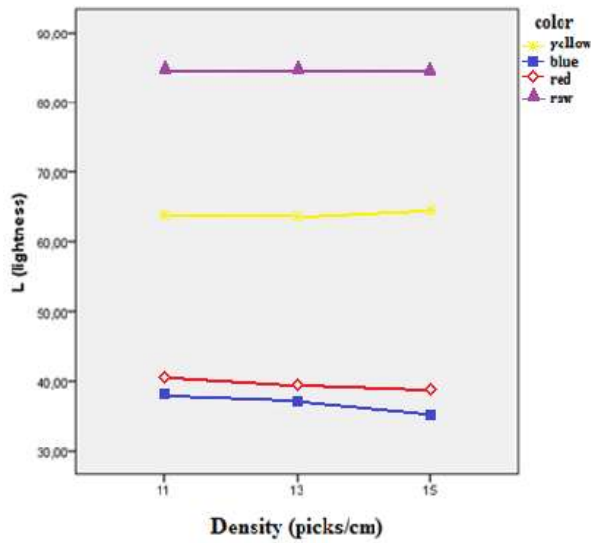


Figure 12. Weft density - L* in cotton velvets.9-10-13 (comparison sample 9-10-13)

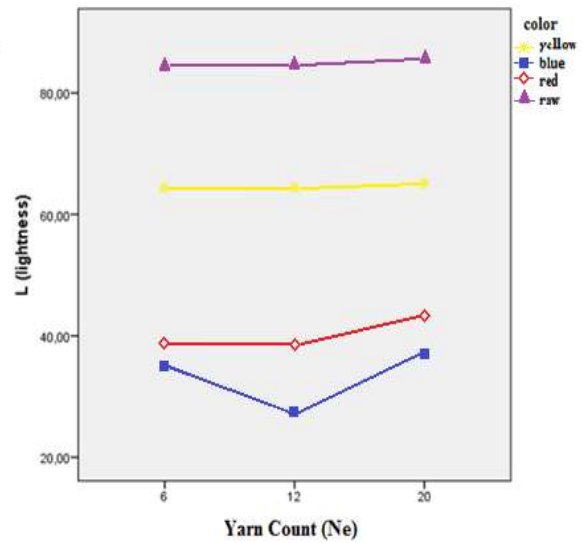


Figure 13. Weft yarn count - L* in cotton velvets. (comparison sample 9-14-15)

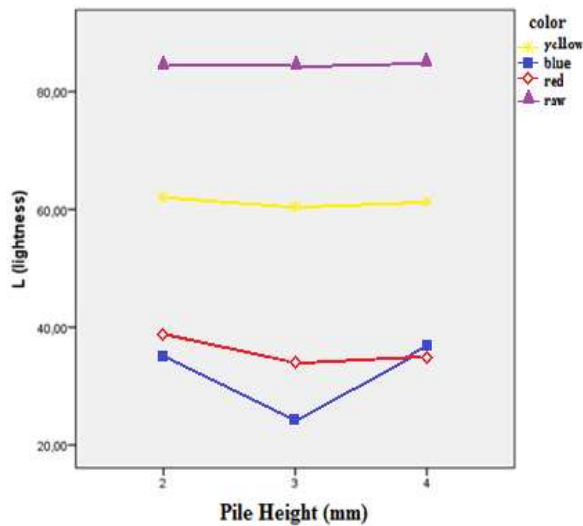


Figure 14. Pile height - L* in cotton velvets. (comparison sample 9-11-12)

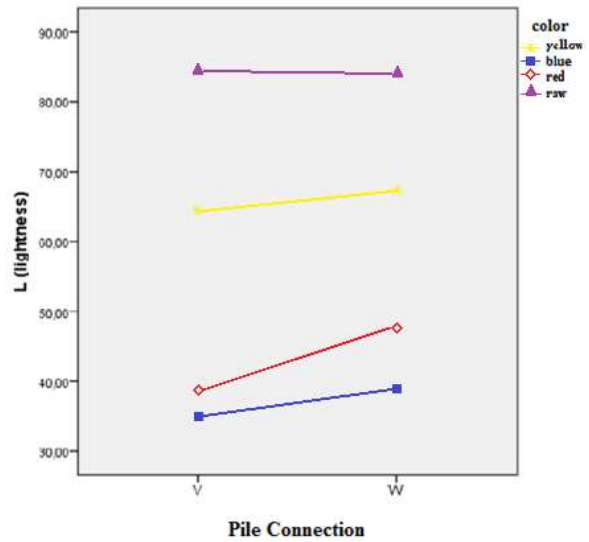


Figure 15. Pile connection - L* in cotton velvet. (comparison sample 9-16)

In Figures 12, 13, 14 and 15 the L* values of 100% cotton raw velvet fabrics are close to each other and vary between 83 and 84. Weft density, weft yarn count, pile height and pile connection type parameters have little effect on the L* value. A similar situation was observed in yellow cotton velvet fabrics. L* values were found to vary between 61 and 65. The effect of the production parameters on the L* value is more pronounced in red and blue cotton velvet fabrics. However, since this effect did not appear in a significant way in the graphics, no interpretation could be reached.

3.4. Investigation of Parameters Affecting the Color Properties of 100% Polyester Velvet Fabrics

In polyester velvets, as in cotton velvets, the relationship between weft density, weft yarn count, pile height, pile

connection type and color was tried to be determined. While all other variables constitute the independent variables, L* was examined as the dependent variable. The F value (ANOVA table) of the interaction test between the variables show that the color factor has a great effect compared to other independent factors, as in cotton velvets. Among the factors affecting the L* value, besides the color factor, other factors are much less important. The same measurement method was used for cotton velvets and polyester velvets, and color measurements were made by carding the piles in the same direction. The effect of pile connection and pile height is slightly higher on the L* value than weft density and weft yarn count parameters.

In the post hoc test, the color had a significant effect on the L* value (significance value $p=0.000 < 0.05$).

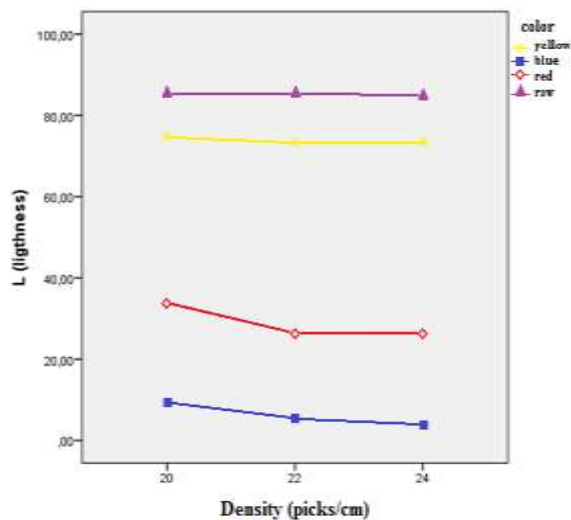


Figure 16. Weft density - L* in polyester velvet. (comparison sample 1-2-3)

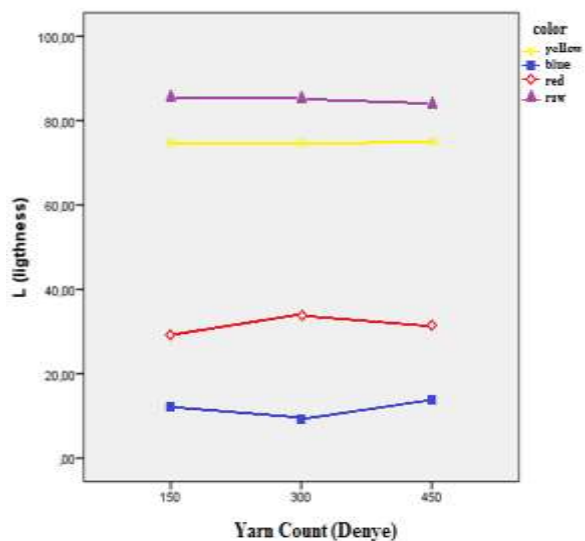


Figure 17. Weft yarn count - L* in polyester velvet. (comparison sample 1-4-5)

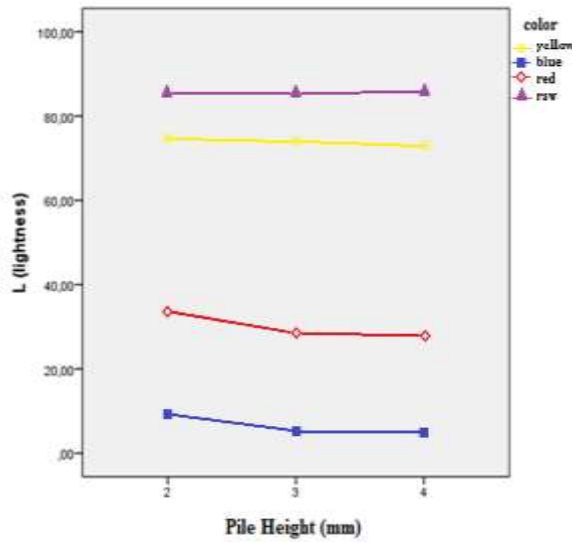


Figure 18. Pile height - L* in polyester velvet. (comparison sample 1-6-7)

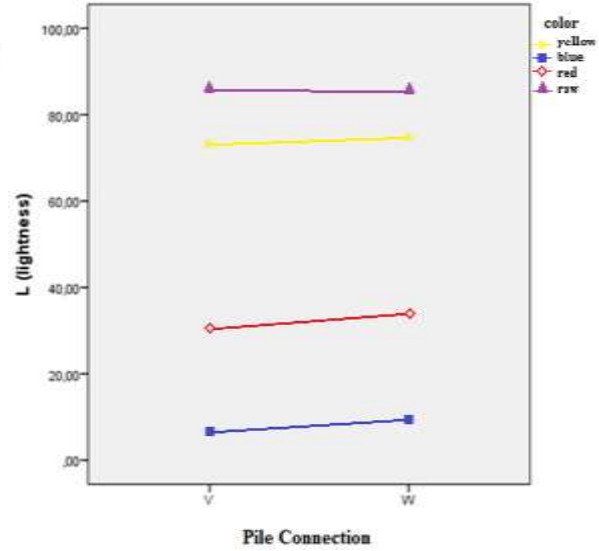


Figure 19. Pile connection - L* in polyester velvet. (comparison sample 1-8)

In Figures 16, 17, 18 and 19 the L* values of 100% polyester raw velvet fabrics are close to each other and vary between 85 and 86. Since an undyed textile material reflects almost all of the incident light, it appears white under white light. In general, the structure of synthetic fibers is smoother than that of natural fibers and natural fibers often tend to curl. Because of this, more uniform reflection occurs on the surfaces of synthetic fibers and therefore they are more shiny [11]. Weft density, weft yarn

count, pile height and pile connection type parameters have little effect on the L* value. A similar situation was observed in yellow polyester velvet fabrics and L* values varied between 73 and 74. The effect of the production parameters examined on the L* value is more pronounced in red and blue polyester velvet fabrics. However, this effect did not cause a change in the direction of decrease or increase as seen in the graphs.

Table 6. Spectrophotometer test results of cotton velvet fabrics.

		L*	a*	b*	C*	h		L*	a*	b*	C*	h	
C/15 pck/6-1 Ne w/2 p h/V p c	yellow	64.38	28.05	69.51	74.96	68.03	C/11 pck/6-1 Ne w/2 p h/V p c	yellow	63.85	27.26	70.14	75.25	68.76
	blue	35.05	-0.61	-28.23	28.24	268.76		blue	38.09	-1.07	-28.81	28.83	267.89
	red	38.84	54.74	-3.35	54.84	356.49		red	40.69	54.42	-5.59	54.74	354.12
	raw	84.46	0.30	8.92	8.93	88.07		raw	84.38	0.15	7.92	7.92	88.93
C/13 pck/6-1 Ne w/2 p h/V p c	yellow	60.27	30.17	73.63	79.58	67.74	C/15 pck/12-1 Ne w/2 p h/V p c	yellow	64.30	26.68	68.13	73.17	68.62
	blue	37.10	-0.29	-28.30	28.30	269.41		blue	27.63	0.65	-26.44	26.45	271.42
	red	39.46	54.52	-3.99	54.69	355.81		red	38.42	54.60	-3.74	54.74	356.08
	raw	84.07	0.15	8.05	8.05	88.95		raw	84.58	0.05	7.91	7.91	89.67
C/15 pck/6-1 Ne w/3 p h /V p c	yellow	60.59	31.53	72.25	78.83	66.42	C/15 pck/20-1 Ne w/2 p h/V p c	yellow	65.00	28.28	70.58	76.04	68.18
	blue	24.25	2.49	-28.58	28.69	274.99		blue	37.04	-1.22	-28.62	28.65	267.58
	red	34.02	56.99	2.65	57.05	2.66		red	43.35	53.28	-7.04	53.76	352.47
	raw	84.39	0.23	8.80	8.80	88.52		raw	85.62	-0.56	6.03	6.05	95.36
C/15 pck/6-1 Ne w/4 p h/V p c	yellow	61.40	31.03	72.39	78.76	66.80	C/15 pck/6-1 Ne w/2 p h/W p c	yellow	67.28	22.74	63.26	67.23	70.23
	blue	36.36	-0.65	-28.92	28.93	268.70		blue	38.78	-0.20	-27.24	27.24	269.56
	red	35.12	56.55	0.31	56.56	240.32		red	47.69	50.69	-7.87	51.30	351.17
	raw	84.97	0.24	8.70	8.70	88.45		raw	84.03	0.50	9.01	9.02	86.82

Table 7. Spectrophotometer test results of polyester velvet fabrics.

		L*	a*	b*	C*	h			L*	a*	b*	C*	h
P/20 pck/300 D w /2 p h/W p c	yellow	74.65	2.97	105.60	105.65	88.39	P/20 pck/450 D w /2 p h/W p c	yellow	75.18	1.42	104.18	104.19	89.22
	blue	9.38	10.28	-29.96	31.68	288.95		blue	13.75	10.85	-32.96	34.70	288.22
	red	33.86	56.92	29.32	64.06	27.21		red	31.38	57.94	34.65	67.51	30.88
	raw	85.35	-0.33	0.16	0.38	154.04		raw	84.17	-0.42	0.54	0.69	127.75
P/22 pck/300 D w /2 p h/W p c	yellow	73.40	5.08	107.75	107.87	87.30	P/20 pck/300 D w /3 p h/W p c	yellow	74.15	3.54	106.96	107.02	88.11
	blue	5.49	10.77	-27.17	29.23	291.51		blue	5.29	11.48	-27.93	30.20	292.32
	red	26.41	57.23	38.32	68.87	33.81		red	28.45	57.93	37.90	69.23	33.19
	raw	85.43	-0.33	0.46	0.57	126.15		raw	85.34	-0.32	0.16	0.36	154.09
P/24 pck/300 D w /2 p h/W p c	yellow	73.29	5.41	108.79	108.92	87.15	P/20 pck/300 D w /4 p h/W p c	yellow	72.82	5.54	107.20	107.34	87.04
	blue	3.75	7.19	-21.11	22.30	288.80		blue	4.98	9.39	-27.26	28.84	289.02
	red	26.26	57.07	37.48	68.28	33.29		red	27.93	55.69	35.07	65.83	32.14
	raw	85.00	-0.37	0.24	0.44	147.68		raw	85.74	-0.36	0.14	0.39	158.44
P/20 pck/150 D w /2 p h/W p c	yellow	74.74	3.10	104.39	104.43	88.30	P/20 pck/300 D w /2 p h/V p c	yellow	73.32	3.78	104.95	105.02	87.95
	blue	12.12	10.85	-34.49	36.17	287.54		blue	6.62	10.38	-28.82	30.64	289.85
	red	29.19	58.14	37.39	69.13	32.75		red	30.59	56.41	30.82	64.28	28.66
	raw	85.38	-0.26	0.09	0.28	161.00		raw	85.88	-0.32	0.32	0.48	141.59

3.5. Investigation of Parameters Affecting Gloss Values of 100% Cotton Velvet Fabrics

3.5.1. Effect of fabric construction on gloss

Gloss values of cotton velvet fabrics are shown in Table 9. The increasing pile height (2, 3 and 4 mm) caused a decrease in gloss values in all three angles (20°, 60° and 85°) in both undyed and reactive yellow 145, red 21 and blue 221 dyed velvet fabrics. As the pile height decreases, a flatter pile surface is formed and it is thought that this pile surface reflects light better.

In addition, the gloss value of W pile fabrics in pile connection types was higher than the gloss value of V pile velvet fabrics in all three angles. The change in other production parameters (weft density, weft yarn count) did not have a significant effect on gloss values. In our opinion, since the ground is seen more clearly in W pile velvets, it reflects the light better and looks brighter than V pile velvets.

3.5.2. Effect of color change on gloss

Gloss values of cotton velvet fabrics in Table 9, gloss values of raw and reactive yellow 145 dyed velvet fabrics were found to be higher at all measurement angles (20°, 60° and 85°) than gloss values of velvet fabrics dyed with reactive red 21 and blue 221 colors.

3.6. Investigation of Parameters Affecting the Gloss Value of 100% Polyester Velvet Fabrics

3.6.1. Effect of fabric construction on gloss

Gloss values of polyester velvet fabrics in Table 10, the increase in pile height (2, 3 and 4 mm) caused a decrease in gloss values of raw and disperse dyed velvet fabrics in all three angles (20°, 60° and 85°). In addition, the gloss value of W pile fabrics in pile connection types is higher than gloss value of V pile velvet fabrics in all three angles. The change in other production parameters (weft density, weft yarn count) did not cause a significant change in gloss values. The same comment made for cotton fabrics in 3.7.1 is valid for polyester fabrics.

Table 9. Glossmeter test results of cotton velvet fabrics.

	Red			Blue			Yellow			Raw		
	20°	60°	85°	20°	60°	85°	20°	60°	85°	20°	60°	85°
C/15 pck/6-1 Ne w/2 p h/V p c	0.10	0.30	0.47	0.00	0.20	0.27	0.40	0.93	0.53	1.00	1.87	0.70
C/13 pck/6-1 Ne w/2 p h/V p c	0.10	0.30	0.47	0.00	0.23	0.33	0.40	0.93	0.63	1.00	1.67	0.50
C/15 pck/6-1 Ne w/3 p h/V p c	0.10	0.30	0.43	0.00	0.17	0.47	0.40	0.97	0.53	1.00	1.90	0.63
C/15 pck/6-1 Ne w/4 p h/V p c	0.10	0.30	0.50	0.00	0.27	0.47	0.40	0.87	0.50	1.00	1.73	0.50
C/11 pck/6-1 Ne w/2 p h/V p c	0.17	0.33	0.40	0.00	0.30	0.40	0.40	0.93	0.43	1.00	1.67	0.23
C/15 pck/12-1 Ne w/2 p h/V p c	0.10	0.37	0.53	0.00	0.23	0.50	0.40	0.90	0.50	1.00	1.67	0.53
C/15 pck/20-1 Ne w/2 p h/V p c	0.10	0.33	0.20	0.00	0.20	0.20	0.40	1.00	0.60	1.00	1.63	0.37
C/15 pck/6-1 Ne w/2 p h/W p c	0.20	0.40	0.33	0.10	0.30	0.47	0.50	1.00	0.57	1.00	1.77	0.50



Table 10. Glossmeter test results of polyester velvet fabrics.

	Red			Blue			Yellow			Raw		
	20°	60°	85°	20°	60°	85°	20°	60°	85°	20°	60°	85°
P/20 pck/300 D w /2 p h/W p c	0.10	0.20	0.20	0.00	0.00	0.13	0.70	1.00	0.20	1.20	1.63	0.20
P/22 pck/300 D w /2 p h/W p c	0.00	0.10	0.20	0.00	0.00	0.13	0.67	0.83	0.20	1.13	1.47	0.20
P/24 pck/300 D w /2 p h/W p c	0.03	0.10	0.10	0.00	0.00	0.13	0.70	0.93	0.23	1.20	1.47	0.23
P/20 pck/150 D w /2 p h/W p c	0.07	0.10	0.00	0.00	0.00	0.10	0.63	1.00	0.20	1.20	1.73	0.33
P/20 pck/450 D w /2 p h/W p c	0.10	0.10	0.10	0.00	0.00	0.20	0.80	1.23	0.33	1.17	1.70	0.33
P/20 pck/300 D w /3 p h/W p c	0.10	0.10	0.17	0.00	0.00	0.17	0.67	1.00	0.20	1.20	1.63	0.20
P/20 pck/300 D w /4 p h/W p c	0.00	0.10	0.20	0.00	0.00	0.03	0.60	0.87	0.10	1.10	1.57	0.20
P/20 pck/300 D w /2 p h/V p c	0.03	0.10	0.17	0.00	0.00	0.00	0.60	0.97	0.17	1.00	1.37	0.23

3.6.2. Effect of color change on gloss

Gloss values of polyester velvet fabrics in Table 10, the gloss values of undyed and disperse yellow 211 dyed velvet fabrics were found to be higher in all three angles (20°, 60° and 85°) compared to the gloss values of velvet fabrics dyed with disperse red 167 and blue 56 colors. It is stated in the literature that color change is not effective on gloss. In this study, both 100% cotton and 100% polyester velvet fabrics were glossier in light-colored velvet fabrics than in dark-colored fabrics.

4. CONCLUSION

According to the test results of 100% cotton and polyester face to face warp velvet fabrics, it was found that the increase in weft yarn count (increasing denier/decreasing Ne), increases the abrasion resistance, while the increase in pile height decreases the abrasion resistance. When the pile connection type was examined, W-connected fabrics were more difficult to abrade than V-connected fabrics. It has been determined that polyester velvet fabrics are more difficult to abrade than cotton velvet fabrics. As expected, the increase in the number of rotations increased the amount of abrasion on both cotton and polyester velvet fabrics. In the selection of velvet fabrics to be used as upholstery, it is recommended to choose high density

fabrics with polyester mid-height pile instead of cotton, very high pile and loose density fabrics in terms of wear.

After dyeing, it was seen in the statistical tests that the production parameters for 100% cotton and polyester fabrics did not have a significant effect on the fabric color properties, L*. While the color properties of blue and red velvet fabrics had an effect on L*, it was found that the raw and yellow ones did not have a significant effect.

Gloss values of 100% cotton and polyester fabrics, gloss decreases in the case of increasing the pile height and using V pile connected velvet, while gloss increases in W pile fabrics. The brightness value of light-colored cotton and polyester velvet fabrics was higher than the dark-colored ones. In the literature, it is stated that the brightness of the fabric depends on the surface appearance rather than the color of the fabric. In the study, the color had an effect on the brightness of the fabric. It is shown in Table 9 and Table 10.

In the selection of velvet fabrics to be used as upholstery, it is recommended to use light colors instead of dark colors in order to prevent the color from fading over time and to prefer light colors in terms of gloss.

REFERENCES

- Özen MS, Akalın M. 2012. *Weaving Technology*, Marmara University, Istanbul 1st edition: Generation Printing, 698 pp.
- Kadolph SJ. 2007. *Textiles*, Iowa State University, Tenth Edition: Pearson Prentice Hall, New Jersey, 496 pp.
- Erdogan S. 2008. Comparison of Velvets from Past to Present in terms of Fabric Structure. Marmara University, Institute of Fine Arts, Master Thesis, Istanbul, 172 pp.
- Adanur S. 2001. *Handbook of Weaving*, Auburn University, Alabama, U.S.A: Department of Textile Engineering, 437 pp.
- Yıldiran S. 2012. Preparation of Jacquard Velvet Upholstery Fabric from Design to Manufacturing and Tests. Haliç University, Institute of Social Sciences, Master Thesis, Istanbul, 172 pp.
- Şeber, B. 2003. Fabric Structure Information Two Layer Fabric Knitting. Istanbul: Birsen Publishing House, 137 pp.
- Mansour M, Peter RL. 1973. Comparison of physical properties of fabrics woven from open end and ring spun yarns. *Textile Research Journal* 43(3), 154-166.
- Önder E, Kalaoğlu F, Özipek B. 2003. Influence of varying structural parameters on the properties of 50/50 wool/polyester blended fabrics *Textile Research Journal* 73(11), 980-984.
- Aniş P, Eren HA. 2003. Dyeing of polyester cotton blends: Applications and new approaches, *Journal of Uludağ University Faculty of Engineering and Architecture* 8(1), 131-139.
- Yeşil Y. 2010. Estimation of Color Values in Melange Fiber Blends by Developing a New Algorithm. Çukurova University, Graduate School of Natural and Applied Sciences, PhD Thesis, Adana, 273 pp.
- Akgün, M, Alpay HR, Becerir B. 2012. Evaluation of the relationships between fabric structural parameters and reflectance values. *Journal of Uludağ University Faculty of Engineering and Architecture* 17(1), 93-106.
- Yanq Y, Li S. 2002. One-step dyeing of polyester/cotton with disperse/reactive dyes. *Textile Chemist and Colorist & American Dyestuff Reporter* 32(3), 38-45.
- De Giorgi MR, Cadani E, Maricca D, Ve Pires A. 2000. Dyeing of polyester fibers with disperse dyes in supercritical CO₂, *Dyes and Pigments* 45,75-79.

14. Mangut M. 2006. Investigation of Changes in Surface Color Properties of 100% Polyester and 100% Cotton Woven Fabrics after Repeated Washing and Ironing Processes, Uludağ University, Institute of Science, PhD Thesis, Bursa, 333 pp.
15. Alpay HR, Becerir B, Akgün M. 2005. Assessing reflectance and color differences of cotton fabrics after abrasion. *Textile Research Journal* 75(4), 357-361.
16. Anış P. 2005. Textile Pretreatment. Alpha Bookstore, Bursa, 224 pp.
17. Kaswell ER. 1953. Textile Fibers, Yarns and Fabrics, Reinhold Publishing Corporation, Newyork. 552 pp.
18. Özcan, Y. 1978. Textile Fiber and Dyeing Technique, Fatih Publishing House, İstanbul, 600 pp.
19. Perkins WS. 1996. Textile Coloration and Finishing. Carolina Academic Pres, North Carolina, 240 pp.
20. Trotman ER. 1975. Dyeing and Chemical Tecnology of Textile Fibres, Charles, Griffin and Company Limited, 709 pp.
21. Tayyar AE, Sarı F, Yağız İ. 2011. The effects of structural parameters on the wear resistance of shirting fabrics *Textile and Engineer* 18 (84), 23-26.
22. Can Y, Kırtay E. 2009. Investigation of yarn properties affecting the abrasion resistance of cotton plain fabrics. *Süleyman Demirel University, Journal of the Institute of Science* 13 (3), 297-304.
23. Koç E, Zervent B, Atay A. 2004. Investigation of the parameters affecting the pile strength of warp velvet fabrics. *Textile Technology Journal* 103(1), 179-189.
24. Kaynak HK, Topalbekiroğlu M. 2008. Influence of fabric pattern on the abrasion resistance property of woven fabrics. *Fibres and Textiles in Eastern Europe* 16 (1-66), 54-56.
25. Kadem FD, Oğulata RT. 2014. Investigation of the effect of fabric construction on pilling and abrasion in yarn-dyed cotton fabrics. *Çukurova University Journal of Engineering and Architecture Faculty* 29(1), 89-97.
26. Kumpikaite E, Ragaisiene A, Barburski M. 2010. Comparable analysis of the end-use properties of woven fabrics with fancy yarns. Part II: Abrasion resistance and mass. *Fibres and Textiles in Eastern Europe* 18(4-81), 43-45.
27. Levy MJ, King RR. 1980. Pile upholstery fabrics construction characteristic and abrasion resistance. *Journal of Consumer Studies and Home Economics* (4), 167-177.
28. Dilsiz D. 2001. The effect of certain weaving factors on raw woven fabric performances and their degree of influence. Master Thesis, Çukurova University Institute of Science and Technology, Adana, 103 pp.
29. Eriçi E. 2018. Investigation of wear properties of fabrics woven in different weaves with different yarns. Master's thesis, Uludag University Institute of Science and Technology, Bursa, 49 pp.
30. Babaarslan O, İlhan İ. 2005. An experimental study on the effect of pile length on the abrasion resistance of chenille fabric. *Journal of Textile Institute* 96(3), 193-197
31. Ülkü S, Örtlek HG, Ömeroğlu S. 2003. The effect of chenille yarn properties on the abrasion resistance of upholstery fabrics. *Fibres and Textiles* 11:3(42), 38-41.
32. Kaynak HK, Topalbekiroğlu M. 2007. Investigation of the effects of tissue type on abrasion and pilling resistance in woven fabrics. *Textile and Apparel* 17(1), 40-44.
33. Sarıduman S. 2005. An Investigation on the Properties of Various Weft Cord Velvet Fabrics Produced Industrially. Çukurova University, Institute of Science and Technology, Master Thesis, Adana, 169 pp.
34. Erem AD. 2006. Investigation of Chenille Yarn Parameters Affecting Usage Performance and Abrasion Resistance of Upholstery Fabrics. Istanbul Technical University, Institute of Science and Technology, Master Thesis, Istanbul, 89 pp.
35. Özdemir Ö, Çeven EK. 2004. Influence of chenille yarn manufacturing parameters on yarn and upholstery fabric abrasion resistance. *Textile Research Journal* 74(6), 515-520.
36. Kalaoglu F, Demir E. 2001. Chenille yarn properties and performance of chenille upholstery fabrics. *Textile Asia* (3), 37-40.
37. Şekerden F. 2011. The effect of pile height and weight on water absorbency, abrasion and pilling resistance of terry woven fabrics. *Electronic Journal of Textile Technologies* 5(2), 18-25.
38. Mokrzycki WS, Tatol M. 2011. Colour difference ΔE - A survey. Faculty of Mathematics and informatics University of Warmia and Mazury, Sloneczna 54, Olsztyn, Poland, 28 p.

The Effect of Softeners on Needle Penetration Forces of Fabrics

Gamze Gülşen Bakıcı¹  0000-0002-4241-7096

Deniz Mutlu Ala¹  0000-0002-5864-308X

Zeynep Nihan Kır²  0000-0002-6072-8787

¹Çukurova University, Adana Vocational School of Organized Industrial Site, Department of Textile-Clothing-Shoes and Leather, Adana, Türkiye

²Eksoy Chemical Industry, R&D Department, Adana, Türkiye

Corresponding Author: Gamze Gülşen Bakıcı, gamzegulsenbakici@gmail.com

ABSTRACT

This study aims to investigate the effects of various softeners (polyether-modified silicone, amino-modified silicone, and fatty acid ester) on denim fabric, with a particular focus on their needle penetration forces (NPFs). The softening finish was applied according to the impregnation method, followed by the assessment of NPF using the L&M sewability tester. Fabrics subjected to softener treatments typically exhibit reduced NPF values compared to the reference fabric. Denim fabrics treated with polyether-modified silicone exhibited statistically significant differences in NPF values in both the weft and warp directions compared to the reference fabric. The lowest needle penetration force (NPF) values were observed in the warp direction of fabrics treated with polyether-modified silicone. The highest NPF values in both the weft and warp directions were observed in fabrics treated with fatty acid ester softeners.

1. INTRODUCTION

Finishing encompasses the final stages of the textile processing sequence, aiming to enhance visual appeal, tactile experience, or other aesthetic qualities of textiles, as well as to introduce additional functionalities such as water repellency or flame retardancy. Softening is recognized as a widely used chemical textile finishing method. Virtually all types of clothing and home furnishings textiles are finished with softeners. A softener is described as an additive that, when applied to textile materials, enhances their texture, making them more pleasant to the touch [1]. Textile softeners can be grouped based on their ionic properties into anionic, cationic, amphoteric, and nonionic softeners containing silicones [2]. Silicone softeners can be categorized into three groups: Reactive Silicone Polymers, Non-Reactive Silicone Polymers, and Organo-Functional Silicone Polymers [3]. This study utilized amino-modified silicone compounds and polyether-modified silicone compounds, both of which belong to the organo-functional silicone polymers group. Additionally, a fatty acid ester

softener was used to assess and compare sewability properties. Fabric softeners are frequently used to enhance the handle quality of textiles, contributing to properties such as anti-static behavior, water repellency and sewability. The quality of garment seams depends on several factors, including seam strength, seam slippage, seam puckering, seam appearance, seam efficiency, and NPF. The process of softening textile fabrics typically involves reducing the coefficient of friction between the fibers, filaments, and yarn [1]. A low coefficient of friction positively affects the sewability of the fabric. Softeners provide lubrication to the fibers, reduce the coefficient of friction, enhance fabric smoothness, and may potentially decrease the glass transition temperature of the polymer. The lubricating properties of the softeners enhance the sewability of the fabric by minimizing friction between the sewing needle and the yarn in the fabric. Sewability is commonly defined as the ability with which fabric components can be effectively seamed without causing damage. One of the parameters used to assess the sewability of the fabric is the NPF. A high NPF indicates

ARTICLE HISTORY

Received: 19.02.2024

Accepted: 28.05.2024

KEYWORDS

Softener, needle penetration force, denim, sewability

To cite this article: Gülşen Bakıcı G, Ala DM, Kır ZN. 2024. The effect of softeners on needle penetration forces of fabrics. *Tekstil ve Konfeksiyon* 34(4), 448-453.

increased fabric resistance, making the fabric more prone to damage. Therefore, NPF plays a crucial role in predicting potential damage during the sewing process [4]. Fabric construction, fiber type, yarn count, yarn density, fabric weight, loop length, finishing processes applied to the fabrics, sewing needle, and machine parameters all play a role in the sewability of fabrics and NPF values [5-8]. Different methods, such as seam strength, seam slippage, and seam pucker, are used to determine the sewing quality of fabrics [9-17]. Measuring the NPF values of fabrics with the L&M sewability tester is another method used to determine the sewing quality of fabrics. Recent studies on NPF can be summarized as follows: Ala & Gülşen Bakıcı (2019) investigated the sewability (based on NPF) of 1 × 1 rib knitted fabrics, which were produced with separate yarn ends. It was found that the number of separate ends and the stitch density have an influence on the NPF values of 1 × 1 rib knitted fabrics [4]. Boz et al. (2022) determined the sewing direction, needle point form, needle number, and sewing speed as variables and performed the sewability test using the L&M Sewability test device. According to the acquired data, the needle number emerged as the primary factor responsible for needle damage during sewing [18]. Atta et al. (2021) developed a new feature to be added to state-of-the-art sewing machines by studying the effect of NPF on the motor current. They revealed a correlation of 0.91 between the L&M test results and the results obtained with the proposed technique [19]. Gülşen Bakıcı (2019)

introduced varying quantities of sewing facilitator chemicals into the dye bath of 100% polyester fabric to examine its sewability characteristics. Consequently, an increase in the chemical concentration in the dye bath led to a decrease in NPF values in both the weft and warp directions, resulting in an improvement in the fabric's sewability [20]. The aim of this study is to investigate the effect of different types of softeners on NPF values of denim fabric.

2. MATERIAL AND METHOD

2.1 Material

The sewability properties of 100% cotton denim fabrics were measured using different softeners. The properties of the fabric used in the study are given in Table 1.

Polyether-modified silicone, amino-modified silicone, and fatty acid ester softeners, each characterized by distinct chemical compositions and sourced from Eksoy Chemical Industry, were employed in the softening finishing treatments of the fabrics (Table 2). The concentrations of these softeners were meticulously adjusted to achieve homogeneity, taking into account the quantities of solid constituents present. Auxiliary chemicals were sourced from Merck Chemical Industry. Particle sizes and zeta potentials were measured using the Malvern ZetaSizer Nano ZS instrument.

Table 1. The properties of the fabrics

Fabric	Weaving type	Weight (g/m ²)	Linear density		Yarn density (yarns/per cm)	
			Weft	Warp	Weft	Warp
Denim (100% cotton)	2/1 Z twill	340	Ne 20/2	Ne 30/2	10	12

Table 2. Properties of softeners

Softener Code	Softener Type	View	pH	Concentrate (g/L)	Solid Content	Particle Size
P1	Polyether-modified silicon	Yellow liq.	7.3	5	65	103.5
P2	Polyether-modified silicon	Yellow liq.	6.5	5	65	105.2
P3	Polyether-modified silicon	Viscous liq.	5.6	5	65	168.3
P4	Polyether-modified silicon	Colorless liq.	6.2	20	16	34.1
P5	Polyether-modified silicon	Colorless liq.	6.6	20	16	172.5
P6	Polyether-modified silicon	Yellow liq.	7.5	25	14	51.5
P7	Polyether-modified silicon	Viscous liq.	8.4	25	14	23.9
A8	Amino-modified silicon	Colorless liq.	6.5	50	7	24.81
A9	Amino-modified silicon	White liq.	7.9	50	7	67.1
A10	Amino-modified silicon	White liq.	6.7	50	7	2530
A11	Amino-modified silicon	White liq.	5.7	50	7	487.0
A12	Amino-modified silicon	Colorless liq.	6.4	30	12	74.2
F13	Fatty acid ester	White liq.	5.2	50	28	190.0
F14	Fatty acid ester	Cream liq.	7.9	50	28	75.0
F15	Fatty acid ester	Cream liq.	3.2	50	28	128.0

2.2 Method

The pH of the softener solutions was adjusted to 5.5. The softener finishing process was applied to the fabrics

employing the impregnation method. This process involved a 1-dip 1-nip cycle within a softener bath, performed using a padding machine to achieve an approximate 85% wet pick-up. The denim fabrics were dried at a temperature of



130°C in the Forlab drying machine. After conditioning of the denim samples under standard atmospheric conditions (20±2°C and 65±4% RH), Needle Penetration Force (NPF) values were determined using the L&M sewability tester (Figure 1).

Each of the five samples, measuring 35 mm × 350 mm, were prepared in both the weft and warp directions. Two tests were performed on each sample. Needle Penetration Force (NPF) represents the average force exerted during 100 needle penetrations in a sewability test. Two tests were conducted on each of the 5 weft and 5 warp samples prepared for each fabric, resulting in a total of 10 tests in both the weft and warp directions. Given that each test represents the average of 100 needle penetrations, the Needle Penetration Force (NPF) values in both the weft and warp directions for each fabric were derived from the mean value of 1000 needle penetrations. Using a Nm90/14 sewing needle (SES), the apparatus allowed the needle to penetrate the fabric at a rate of 100 penetrations per minute along the long edge of the sample. The force values resulting from the needle penetrating the sample were measured in gram-force (gf).



Figure 1. L&M sewability tester

3. DISCUSSION

The measured Needle Penetration Force (NPF) values of the reference fabric, without any softener, and the fabrics treated with fifteen different softeners are presented in Figure 2. Typically, fabrics treated with softeners exhibited reduced NPF values compared to the reference fabric. Among the fabrics treated with polyether-modified silicone,

P1, P2, and P7 showed decreased Needle Penetration Force (NPF) values in both the weft and warp directions. Due to their chemical structure, polyether-modified silicones impart hydrophilic properties to the fabric and penetrate its inner regions, thereby providing internal softness. Their inherent capacity for internal softening is particularly influential. Consequently, lower Needle Penetration Force (NPF) values have been observed in fabrics treated with polyether-modified silicones. Among fabrics treated with amino-modified silicone, A8 and A9 exhibited the highest Needle Penetration Force (NPF) values in both the weft and warp directions. Unlike polyether-modified silicones, amino-modified silicones do not provide inner softness to the fabric; instead, they form a surface coating on the fabric. This coating imparts surface smoothness and slipperiness. The effectiveness of amino-modified silicones in producing a slippery texture depends on the particle size, with larger particle sizes providing better surface coverage and a smoother tactile sensation. In contrast, smaller particle sizes result in reduced surface slipperiness. For this reason, the NPF values of the fabrics treated with A8 and A9 softeners, which have smaller particle sizes, were higher than those of the other treatments. Analysis of the Needle Penetration Force (NPF) values of fabrics treated with fatty acid esters revealed that the F15 softener exhibited the lowest value. However, upon examining the fabrics treated with fatty acid esters, no definitive conclusion can be drawn regarding the relationship between NPF values and particle size.

The Needle Penetration Force (NPF) values of denim fabric demonstrate a normal distribution in both the weft and warp directions. Homogeneity of variances was assessed using the Levene test, and the results are presented in Table 3. The p-values for NPFwarp and NPFweft were calculated as 0.010 and 0.007, respectively, indicating non-uniform variances. Since the variances are unequal, the Welch test was conducted to determine whether there are differences between the groups (Table 4). As shown in Table 4, a statistically significant difference was observed in the mean Needle Penetration Force (NPF) values of fabrics treated with softeners in both the warp and weft directions (p-value=0.000 <0.05). Consequently, it can be concluded that there are differences in the average NPF values among the fabric groups in both the weft and warp directions.

Table 3. Homogeneity of variances test results

Dependent variable	Levene Statistic	df1	df2	p-value
NPFwarp	3.873	3	156	.010
NPFweft	4.221	3	156	.007

Table 4. Welch Test

Dependent variable	Statistic	df1	df2	P-value	Level of significance
NPFwarp	68.944	3	37.414	.000	significant
NPFweft	10.305	3	36.639	.000	significant

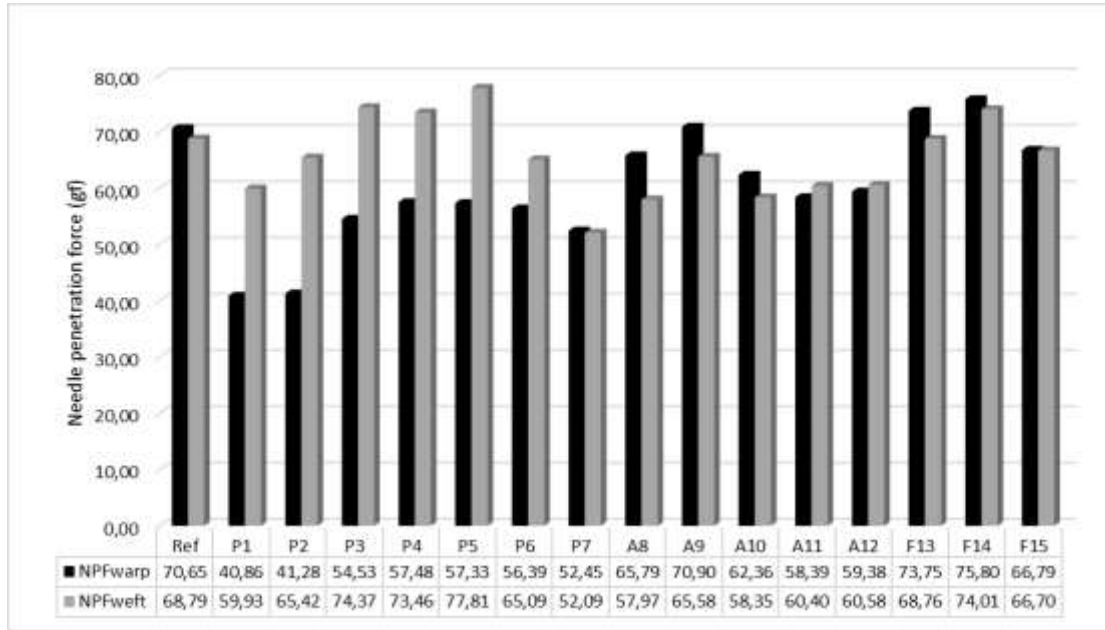


Figure 2. NPF means of denim fabrics finished with softeners

Subsequently, Tamhane's post hoc test was performed to assess group differences, and the results are presented in Table 5. When evaluating the NPF values in the warp direction as the dependent variable, it was observed that the mean NPF values differed significantly between the reference fabric and the fabric treated with polyether-modified silicone. However, no statistically significant difference was observed in the average NPF values between the reference fabric and fabrics treated with amino-modified silicone or fatty acid ester. Thus, the reference fabric, along with fabrics treated with amino-modified silicone and fatty acid ester softeners, were statistically grouped together, whereas the fabric treated with polyether-modified silicone was classified separately.

When the NPF values in the weft direction were evaluated as the dependent variable, no statistical differences were observed between the reference fabric and those treated

with other softeners. However, the average NPF values in the weft direction for fabrics treated with amino-modified silicone were found to differ from those of fabrics treated with polyether-modified silicone and fatty acid-treated fabrics.

3.4 Correlations

The relationship between NPF values in the weft and warp directions, particle size and zeta potential was examined using Spearman Correlation Analysis. The results are given in the Table 6. The correlation between particle size and NPF values in both the warp and weft directions is not considered significant. In the warp direction, the relationship between NPF values and zeta potential is found to be significant, indicating a strong negative correlation (correlation coefficient = -0.903). Conversely, in the weft direction, the relationship between NPF values and zeta potential is not considered significant.

Table 5. Multiple comparison results

Dependent Variable: NPFwarp					Dependent Variable: NPFweft				
(I) softener type	(J) softener type	Mean Difference (I-J)	Std. Error	Sig.	(I) softener type	(J) softener type	Mean Difference (I-J)	Std. Error	Sig.
REF	Polyether-modified silicon	19.17786*	3.288	0.001	REF	Polyether-modified silicon	1.914	3.944	0.998
	Amino-modified silicon	7.288	3.356	0.267		Amino-modified silicon	8.216	3.953	0.320
	Fatty acid ester	-1.476	3.253	0.998		Fatty acid ester	-1.029	3.962	1.000
Polyether-modified silicon	REF	-19.17786*	3.288	0.001	Polyether-modified silicon	REF	-1.914	3.944	0.998
	Amino-modified silicon	-11.89006*	1.652	0.000		Amino-modified silicon	6.30209*	1.650	0.001
	Fatty acid ester	-20.65352*	1.431	0.000		Fatty acid ester	-2.942	1.672	0.403
Amino-modified silicon	REF	-7.288	3.356	0.267	Amino-modified silicon	REF	-8.216	3.953	0.320
	Polyether-modified silicon	11.89006*	1.652	0.000		Polyether-modified silicon	-6.30209*	1.650	0.001
	Fatty acid ester	-8.76347*	1.582	0.000		Fatty acid ester	-9.24447*	1.693	0.000
Fatty acid ester	REF	1.476	3.253	0.998	Fatty acid ester	REF	1.029	3.962	1.000
	Polyether-modified silicon	20.65352*	1.431	0.000		Polyether-modified silicon	2.942	1.672	0.403
	Amino-modified silicon	8.76347*	1.582	0.000		Amino-modified silicon	9.24447*	1.693	0.000

Table 6. Spearman Correlation Analysis

Variables		NPFwarp	NPFweft
Particul size	Correlation Coefficient	.152	.182
	Sig. (2-tailed)	.605	.533
Zeta potential	Correlation Coefficient	-.903**	-.516
	Sig. (2-tailed)	.000	.059

4. CONCLUSION

This study investigated the effects of polyether-modified silicone, amino-modified silicone, and fatty acid ester softeners on the sewability properties of denim fabrics. The softening-finishing procedures were applied via the impregnation method. Following this treatment, Needle Penetration Force (NPF) values were measured using the L&M sewability tester, thereby providing data regarding the sewability attributes of the fabrics.

Fabric construction, comprising variables such as fiber type, yarn count, yarn density, fabric weight, and loop length, in conjunction with the diverse finishing processes applied to the fabrics, the type of sewing needle utilized, and machine parameters collectively exert an influence on the sewability and Needle Penetration Force (NPF) values of fabrics [5-8, 21]. In the L&M sewability test procedure, the sewing needle penetrates the fabric from bottom to top.

When encountering minimal resistance and smoothly passing through the threads during insertion, it results in a decrease in NPF values. The softeners employed in this study contributed to enhancing the fabric's softness, thereby facilitating the passage of the needle through the threads and subsequently reducing the NPF values.

Fabrics finished with a softener generally showed lower NPF values compared to the reference fabric. The lowest NPF values were obtained in the warp direction of fabrics treated with polyether-modified silicone. NPF values of fabrics treated with softeners having smaller particle sizes were found to be higher than those of fabrics treated with amino-modified silicone. The highest NPF values in both the weft and warp directions were observed in fabrics treated with fatty acid ester softeners. In the warp direction, a significant relationship was observed between Needle Penetration Force (NPF) values and zeta potential, indicating a strong negative correlation. Conversely, in the

weft direction, the correlation between NPF values and zeta potential is insignificant. Subsequent research studies aim to estimate needle penetration force values by maintaining


uniform fabric properties while varying parameters in the softening process.

REFERENCES

1. Bajaj P. 2002. Finishing of textile materials. *Journal of Applied Polymer Science* 83(3), 631-659.
2. Fahmy HM, Okda HMY, Hassabo AG, El-Rafie MH, Youssef MA. 2021. Synthesis of new silicone-based adducts to functionalize cotton fabric. *Silicon* 14, 7613-7621.
3. Mohamed AL, Hassabo AG. 2019. Review of silicon-based materials for cellulosic fabrics with functional applications. *Journal of Textiles Coloration and Polymer Science* 16(2), 139-157.
4. Ala DM, Gülşen Bakıcı G. 2019. Sewability (based on NPF) of 1×1 rib knitted fabrics produced with separate ends of yarns. *Autex Research Journal* 19(4), 340-346.
5. Bansal P, Sikka M, Choudhary AK. 2021. Effect of yarn count and loop length on NPF and needle cut index in single jersey fabrics. *Indian Journal of Fibre & Textile Research* 45(4), 388-394.
6. Carvalho M, Rocha AM, Carvalho H. 2020. Comparative study of NPFs in sewing hems on toweling terry fabrics: Influence of needle type and size. *Autex Research Journal* 20(2), 194-202.
7. Choudhary AK, Sikka MP, Bansal P. 2018. The study of sewing damage and defects in garments. *Research Journal of Textile and Apparel* 22(2), 109-125.
8. Mansouri S, Chaabouni Y, Cheikhrouhou M. 2022. Influence of finishing products on mechanical seam's behavior of natural fabrics. *Journal of Natural Fibers* 19(15), 11404-11412.
9. Gürarda A, Meriç B. 2010. Slippage and grinning behaviour of lockstitch seams in elastic fabrics under cyclic loading conditions. *Tekstil ve Konfeksiyon* 20(1), 65-69.
10. Ateş M, Gürarda A, Çeven EK. 2019. Investigation of seam performance of chain stitch and lockstitch used in denim trousers. *Tekstil ve Mühendis* 26(115), 263-270.
11. Faizur RM, Alam MA, Hossain KR, Baral LM, Sarkar MH, Sarkar P, Rashid MR. 2023. Impact of modified feed mechanism on seam quality of garments. *Annals of the University of Oradea. Fascicle of Textiles, Leatherwork* 24(1), 89-96.
12. Sülar V, Meşegül C, Kefsiz H, Seki Y. 2015. A comparative study on seam performance of cotton and polyester woven fabrics. *The Journal of the Textile Institute* 106(1), 19-30.
13. Zervent Ünal B. 2012. The prediction of seam strength of denim fabrics with mathematical equations. *Journal of the Textile Institute* 103(7), 744-751.
14. Stylios GK, Zhu R. 1998. The mechanism of sewing damage in knitted fabrics. *The Journal of the Textile Institute* 89(2), 411-421.
15. Malek S, Jaouachi B, Khedher F, Ben Said S, Cheikhrouhou M. 2017. Influence of some sewing parameters upon the sewing efficiency of denim fabrics. *The Journal of the Textile Institute* 108(12), 2073-2085.
16. Malek S, Khedher F, Jaouachi B, Cheikhrouhou M. 2018. Determination of a sewing quality index of denim fabrics. *The Journal of the Textile Institute* 109(7), 920-932.
17. Birkocak DT. 2022. Effects of needle size and sewing thread on seam quality of traditional fabrics. *Tekstil ve Konfeksiyon* 32(3), 277-287.
18. Boz S, Birkocak DT, Necfe ÖK, Kiliç A, Öndoğan Z. 2022. June. Investigation of sewing parameters caused fabric damages. Proceedings of the 21st World Textile Conference-AUTEX 2022 (40-44), Lodz, Poland.
19. Atta RM, El-Sayed I, Mohamed AAH. 2021. Fabric properties measurements using real-time sewing machine motor current signature. *Measurement* 173, 108669.
20. Gülşen Bakıcı G. 2019. Eylül. Polyester esash kumaşların tek banyoda boyanması ve dikilebilirlik özelliğinin iyileştirilmesi. Ulusal Çukurova Tekstil Kongresi-UÇTEK'2019. Adana, Türkiye.
21. Gülşen Bakıcı G, Doba Kadem F. 2018. An experimental study on sewability properties of 100% cotton denim fabrics. *Tekstil ve Konfeksiyon* 28(2), 170-176.

Photocatalytic Activity of Zinc Oxide Nanoparticles and Boric Acid for Bleaching Process on Cotton Fabric

Zeynep Cığeroğlu¹  0000-0001-5625-6222

Zeynep Omerogullari Basyigit²  0000-0002-1526-8662

¹Uşak University, Faculty of Engineering and Natural Sciences, Department of Chemical Engineering, 64300, Uşak, Türkiye

²Bursa Uludağ University, Department of Textile, Clothing, Footwear and Leather, Textile Technology, Vocational School of Higher Education of Inegöl, 16059, Bursa, Türkiye

Corresponding Author: Zeynep Omerogullari Basyigit, zeynepbasyigit@uludag.edu.tr

ABSTRACT

In this study, a photocatalytic process was applied as an alternative to conventional hydrogen peroxide bleaching on 100% cotton fabric. The effects of ZnO nanoparticles and boric acid as catalysts were investigated. Additionally, the synergistic impact of boric acid on the well-known bleaching effect of titanium dioxide nanoparticles was explored. Unlike existing literature, the study uniquely addressed whether the photocatalytic process, without the use of any catalyst, has a specific effect, particularly in whitening, on the color spectrum. All conducted photocatalytic processes on cotton fabrics were compared with conventional hydrogen peroxide bleaching in terms of color spectra (CIE L*, a*, b*, whiteness indexes) besides the SEM, SEM-EDX, and FTIR-ATR characterization tests. Moreover, XRD, SEM, and FTIR-ATR analysis results of ZnO nanoparticles were also shared in this study. After the photocatalytic processes, tearing strength of all cotton fabrics were tested. This research is believed to shed light on future studies by evaluating more environmentally friendly pre-treatment processes in textile industry.

ARTICLE HISTORY

Received: 28.11.2023

Accepted: 08.08.2024

KEYWORDS

Photobleaching, Cotton, Zinc Oxide Nanoparticles, Boric Acid

1. INTRODUCTION

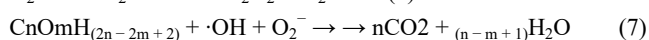
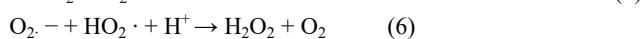
Cotton is one of the most widely used and important natural fibers in the textile industry. It comes from the fibers surrounding the seeds of the cotton plant (*Gossypium*), and it has been used for thousands of years to produce a variety of textiles. Even though cotton's versatility, comfort, and natural properties (breathability, absorbancy, comfort etc.) make it a popular choice for a wide range of textile products, including apparel, home furnishings, and industrial uses; it also comes with certain disadvantages, particularly in its untreated and unprocessed form. Some of the drawbacks associated with raw cotton are being contaminated with impurities such as dust, dirt, plant material, seeds; lack of uniformity which can be varied in terms of fiber length, fineness, color; presence of natural waxes and oils can affect the wettability, dyeing process and the overall quality of the finished product [1,2]. Bleaching is a crucial process in the textile industry that involves treating raw cotton or cotton fabric with chemicals to remove impurities, natural color, and other contaminants. The goal is to achieve a clean, white appearance and

prepare the cotton for dyeing or further processing. Common bleaching agents include hydrogen peroxide, sodium hypochlorite, or chlorine dioxide [3]. Hydrogen peroxide is considered an environmentally friendly bleaching agent compared to chlorine-based alternatives. However, there are some disadvantages of using hydrogen peroxide in the finishing processes such as energy consumption because of high temperatures, pH and temperature sensitivity (higher temperatures generally increase the bleaching rate, but excessive heat may lead to fiber damage) and limited bleaching speed besides post-processing such as stabilization which increases the water consumption overall [4-6]. Researchers are constantly exploring and developing new bleaching agents to improve the efficiency, environmental sustainability, and versatility of the bleaching process in the textile industry. Photocatalysts, such as titanium dioxide, are materials that can accelerate chemical reactions under the influence of light. They are being investigated for their potential to enhance bleaching processes, particularly in the presence of ultraviolet (UV) light. When the photocatalyst absorbs

To cite this article: Cığeroğlu Z, Omerogullari Basyigit Z. 2024. Photocatalytic Activity of Zinc Oxide Nanoparticles and Boric Acid for Bleaching Process on Cotton Fabric. *Tekstil ve Konfeksiyon*, 34(4), 454-466.

light, it creates electron-hole pairs. These charged particles can react with water and oxygen in the surrounding environment to generate reactive oxygen species (ROS), such as hydroxyl radicals ($\cdot\text{OH}$) and superoxide ions ($\text{O}_2^{\cdot-}$). The ROS generated by the photocatalyst can break down organic contaminants, pigments, and other impurities present in the textile fibers. The oxidative reactions lead to the degradation of color molecules and the removal of undesired substances. The photocatalytic process on textiles involves treating textile materials with photocatalysts and exposing them to light to achieve various effects, such as self-cleaning, antibacterial and antifungal properties [7-9].

Zinc oxide nanoparticles (n-ZnO) are commonly used in the textile industry for various purposes due to its unique properties. One of the primary uses of its in textiles is as a UV blocker. Finishing textiles with zinc oxide nanoparticles provides the fabric with enhanced UV-blocking properties. This is especially important in outdoor clothing, swimwear, and other textiles where protection from the sun's harmful ultraviolet (UV) rays is desirable. Zinc oxide has inherent antibacterial and antifungal properties. Treating textiles with zinc oxide nanoparticles can impart these properties to the fabric. This is particularly beneficial in applications where maintaining hygiene and preventing microbial growth are essential, such as in medical textiles or sportswear. In the medical field, zinc oxide nanoparticles have been incorporated into textiles to aid in wound healing. The antimicrobial properties of zinc oxide can help prevent infections in wounds. Zinc oxide nanoparticles can be incorporated into textile fibers or coatings to create nanocomposites. This integration can improve the mechanical, thermal, electroconductive and antimicrobial properties of the textiles [10-14]. The ZnO photocatalysis mechanism for cotton bleaching shown in Eq. (1-7) [15, 16].



Boric acid, a weak acid with antifungal and insecticidal properties, is sometimes used in the textile industry for specific purposes. Boric acid can be used as a flame retardant on textiles. When applied to fabrics, it forms a protective layer that helps reduce the flammability of the material. This is particularly important for textiles used in applications where fire safety is a concern. Due to its antifungal properties, boric acid can be employed as an antimicrobial treatment for textiles. Boric acid is known for its insecticidal properties, and it can be used as an insect repellent on textiles. In textile conservation, boric acid may

be used as a preservative to protect historical textiles from decay and insect damage [17-21]. Boron doping is known to enhance photocatalytic activity under visible light by reducing the bandgap between the photogenerator and the photocatalyst [22-24]. In accordance with the above data, we have used it to whiten cotton material under UV-A light to determine whether boric acid has a direct effect. To the best of our knowledge and based on the literature, this study is the inaugural investigation into the photochemical bleaching process on cotton fiber using ZnO nanoparticles and boric acid under UV-A source. This study diverges from existing literature by exploring an alternative approach to the conventional bleaching process for untreated cotton fabrics. The focus is on investigating the photocatalytic bleaching effects of boric acid and zinc oxide nanoparticles on raw cotton fabrics. Additionally, the study delves into the synergistic impacts on whiteness indexes when boric acid is combined with titanium dioxide nanoparticles (n-TiO₂), renowned for their nano-sized bleaching effects. One distinctive aspect of this article compared to many other photocatalytic textile studies in the literature is the exploration of the impact of the photocatalysis process itself on bleaching, without the use of any catalyst.

2. MATERIAL AND METHOD

2.1 Material

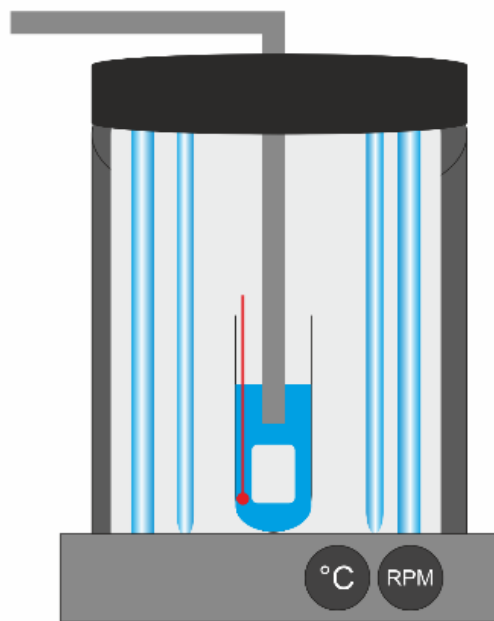
Boric acid (99.8%) was supplied from Alfa Aesar. NaOH and HCl were purchased from Sigma Aldrich. ZnO (99.99%, 18 nm) and TiO₂ (99.99%, 28 nm, anatase) supplied from Nanografi, Turkey. The technical specifications of the ZnO nanoparticles, TiO₂ nanoparticles, H₃BO₃ were detailed in Table 1. In our experimental investigations, 100% woven cotton fabrics (weighing 145 g/m²) consisting of Ne 20/1 fine yarns were sourced from Ege Özteks Tekstil, located in Uşak, Turkey. To conduct the pre-treatment procedures, we acquired alpha-amylase desizing enzyme, NaOH (48 Bé), and a wetting agent from Alfa Kimya, Turkey.

2.2 Method

As part of the pre-treatment phase, following the desizing procedure conducted using a pad-batch machine (Babkok) with an 80% wet-pick-up ratio employing 2g/L of alpha-amylase desizing enzyme and 1 g/L of wetting agent, a solution of 30 g/L NaOH (48 Bé) was applied to the cotton fabrics using the same machine. This step aimed to boost the hydrophilicity of the materials, as per the industrial standards of the supplier company (Ege Özteks Tekstil). The homemade photocatalytic system is shown in Figure 1. There are 15 Watt UV-A lamps (Osram L Blue UVA L 15W/78) each in the system and the system is galvanised. The system was previously homemade and its shape was shown in the previous publication [25].

Table 1. Technical Properties of n-ZnO, n-TiO₂ and Boric acid

Technical data of ZnO				
Purity (%)	99.5			
Average Particle Size (nm)	18			
Morphology	nearly spherical			
Color	white			
Specific Surface Area (m ² /g)	20.0-65.0			
Crystal Phase	single crystal			
True Density (g/cm ³)	5.5			
Elemental Analysis (%)	Mn	Cu	Pb	
	0.0002	0.0004	0.001	
Technical data of n-TiO ₂				
Purity (%)	99.995			
Average Particle Size (nm)	28			
Color	white			
Specific Surface Area (m ² /g)	55.00			
pH	5.5-6.5			
True Density (g/cm ³)	4.1			
Elemental Analysis (%)	K	Na	Fe	Al
	0.0055	0.0053	0.003	0.0022
Technical Data of Boric acid				
Melting point	ca. 185° deg.			
Density	1.435			
Form	+ 8 mesh granular			

**Figure 1.** The illustration of homemade photocatalytic system [25].

The fabrics cut in certain sizes were placed in a 250 mL beaker and the experimental conditions given in Table 2 were applied.

2.3. Performance and characterization tests of the materials

In order to ascertain the crystallographic phase of the specimens, an X-ray diffractometer (Malvern Panalytical, Netherlands) employing Cu K α radiation was utilized. The diffraction patterns were scrutinized within a range spanning from 10 to 90°. Microstructural variations within the materials were examined using a field emission

scanning electron microscope (SEM) equipped with elemental analysis via SEM-EDX, model XL-30 SFEQ, produced by Philips in Eindhoven, Netherlands. Prior to SEM imaging, the specimens were subjected to Au coating to enhance conductivity. Fourier Transform Infrared Spectroscopy (FTIRS) spectra for cotton specimens were acquired using a Spectrum Two FTIR spectrophotometer. Alongside the aforementioned characterization tests, color spectrum analysis and tearing strength evaluations were conducted on the cotton samples. CIELAB color spectrum results, incorporating parameters such as L*, a*, b*, whiteness and yellowness indexes and ΔE were determined using a Konica Minolta CM-3600D Spectrophotometer from Japan. Tearing strength assessments on cotton samples, in both warp and weft directions, were carried out in accordance with Elmendorf ASTM D1424 standards. The tear strengths were measured utilizing a D-type pendulum with a weight of 64 N.

Table 2. Experimental Set-up

Sample Code	Finishing Process
S1	Untreated fabric
S2	n-ZnO 1 g/L pH 10.5 60 C 60 min
S3	n-ZnO 5 g/L pH 10.5 60 C 60 min
S4	n-ZnO 5 g/L pH 4.5 60 C 60 min
S5	n-ZnO 5 g/L pH 7 60 C 60 min
S6	n-ZnO 5 g/L pH 4.5 30 C 60 min
S7	n-ZnO 5 g/L pH 10.5, 95 C 60 min
S8	Boric acid/n-TiO ₂ (2.5+2.5) g/L pH 5.5 60 C 60 min
S9	Boric acid 5g/L pH 5.5 60 C 60 min
S10	Without catalyst 30 C 60 min pH 7
S11	Without catalyst 60 C 60 min pH 7
S12	Without catalyst 95 C 60 min pH 7
S13	Conventional bleaching process

3. RESULTS AND DISCUSSION

3.1 Characterization Results of ZnO nanoparticles, H₃BO₃ and TiO₂ nanoparticles

3.1.1. FTIR of ZnO nanoparticles, H₃BO₃ and TiO₂ nanoparticles

Zinc oxide nanoparticles (ZnO-n) exhibited vibrations in the 420-600 cm⁻¹ range, which correspond to Zn-O stretching vibrations in the 434 cm⁻¹ range [26], as mentioned in our previous publication [27] (Figure 2). The distinctive peak of the B-O bond is 1430 cm⁻¹, whereas the stretching vibration of the intermolecular hydrogen bond (O-H) is 3200 cm⁻¹, whereas the O-H surface curvature at 699 cm⁻¹ [28]. The transmittance peaks, spanning from 600 to 850 cm⁻¹, are associated with the Ti-O-Ti links seen in TiO₂ nanoparticles (n-TiO₂) [29]. The unique band corresponding to anatase titania was observed at 745 cm⁻¹ in the FTIR spectra of pure n-TiO₂ [30]. In the FTIR spectra of the pure n-TiO₂, a noticeable stretching peak at 1640 cm⁻¹ indicates the stretching of Ti-OH [30]. It was determined that the big peak at 3305 cm⁻¹ was caused by the stretching vibration of the -OH group.

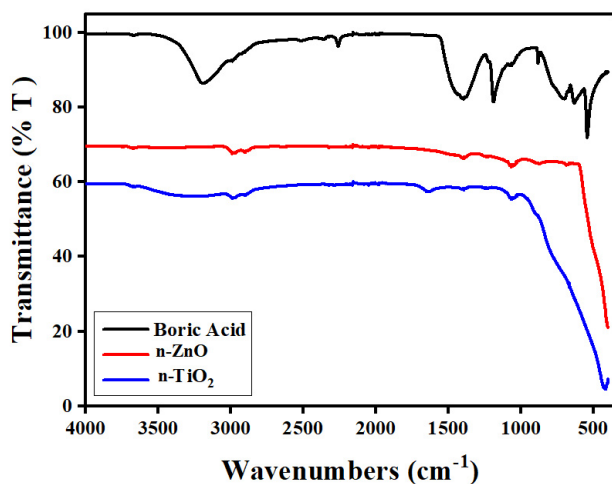


Figure 2. FTIR graph of n-ZnO, H₃BO₃ and n-TiO₂

3.1.2. XRD analysis of ZnO nanoparticles, H₃BO₃ and TiO₂ nanoparticles

Zinc oxide nanoparticles with 2θ values of 31.71, 34.58, 36.20, 47.53, 56.65, 62.88, 66.47, 67.96, and 69.34 degrees are evident, as previously mentioned in our published paper [31]. XRD pattern of ZnO obtained from Nanografi agrees with JCPDS Data Card No. 36-1451 (Figure 3). The main signal was seen in XRD pattern of boric acid at 28.00° [32]. The primary peaks are seen in the XRD patterns of the boric acid (H₃BO₃) card number, ICDD-00-030-0620 [33]. The anatase peaks (JCPDS Card no. 21-1272) at 2θ values of 25.31, 37.81, 48.05, 53.91, 55.06, and 62.68 are displayed in Figure 3 [25, 34]. The anatase structure is clearly indicated by these peaks.

3.1.3. SEM analysis of ZnO nanoparticles, H₃BO₃ and TiO₂ nanoparticles

Based on the SEM image (Figure 4), the majority of the ZnO nanopowder displayed a spherical morphology with a minor rod shape [35]. Boric acid has a surface that is essentially flat and roughened by fibrils, according to SEM observation [36]. Upon closer examination, the 500 nm SEM picture in Figure 4 clearly resembles a cauliflower [37]. This study shows that the anatase form of n-TiO₂ adopts a structure with several anatase nanoparticle microspheres, like a hierarchical cauliflower.

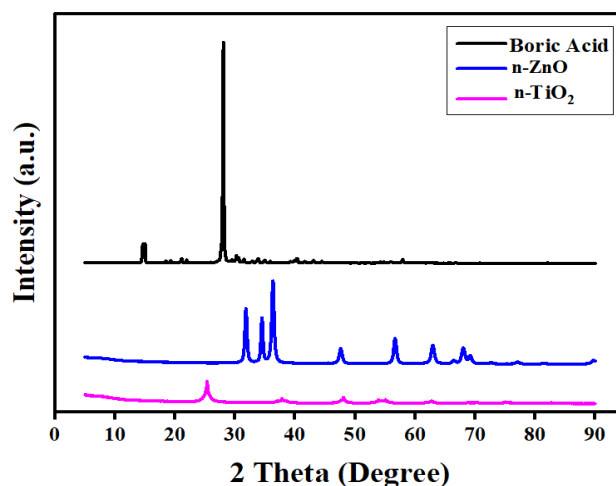
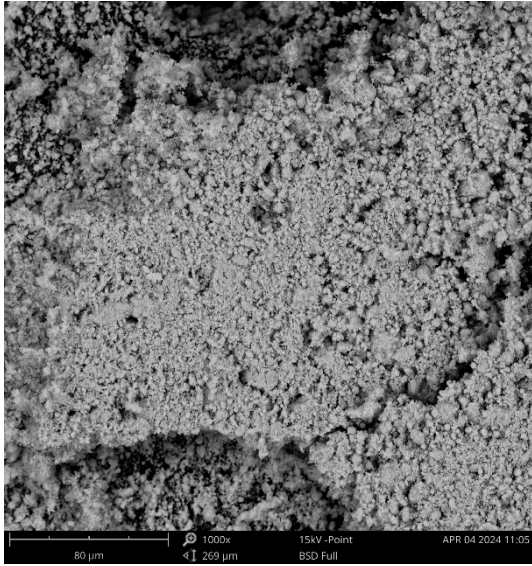
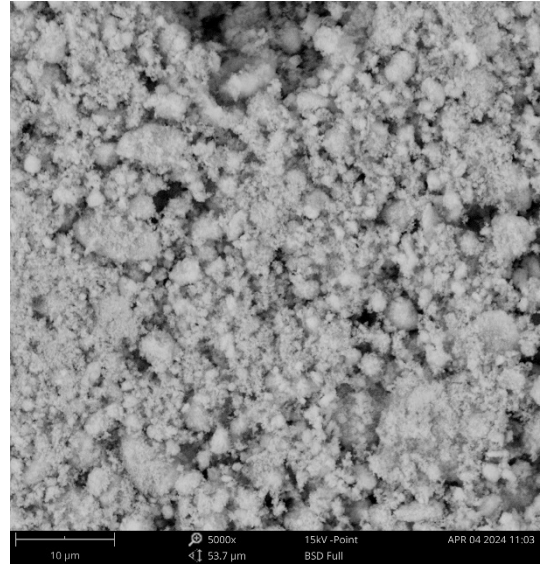


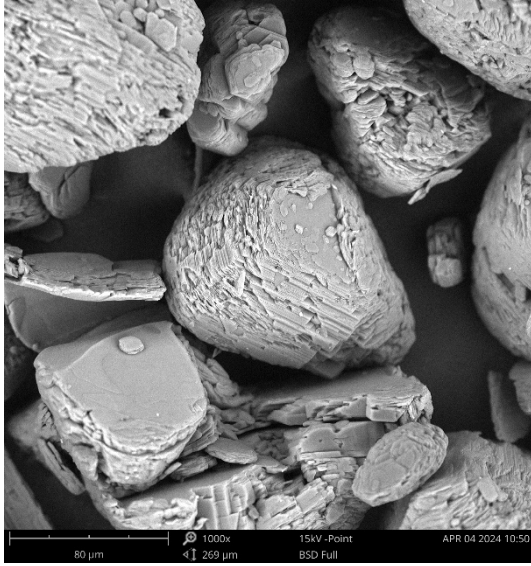
Figure 3. XRD patterns of n-ZnO, H₃BO₃ and n-TiO₂



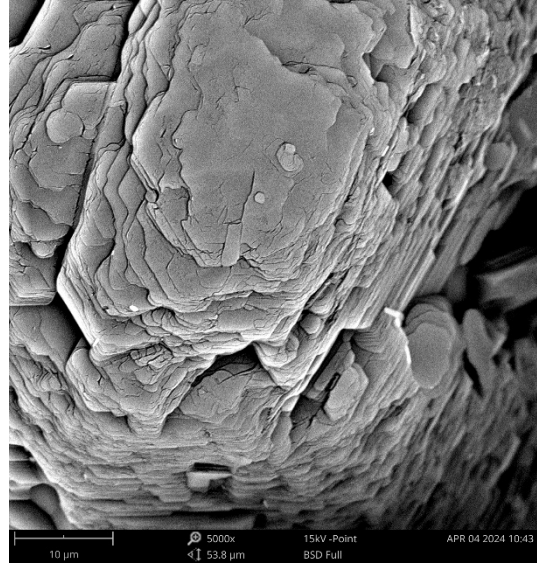
a) n-ZnO X1000



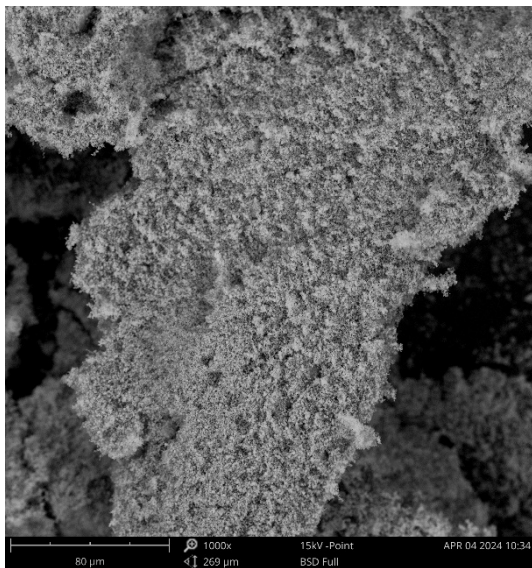
b) n-ZnO X5000



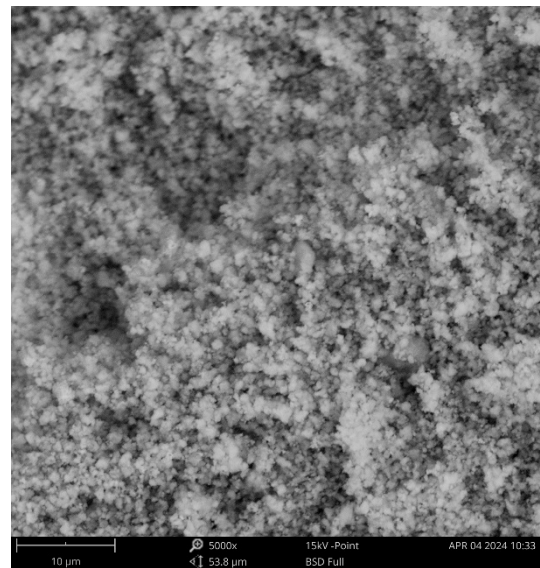
c) Boric acid X1000



d) Boric acid X5000



e) n-TiO₂ X1000



f) n-TiO₂ X5000

Figure 4. SEM image of n-ZnO powder, n-TiO₂ powder and boric acid.

3.2. Characterization Results of Fabric Samples

3.2.1. SEM Results of Cotton Fabric

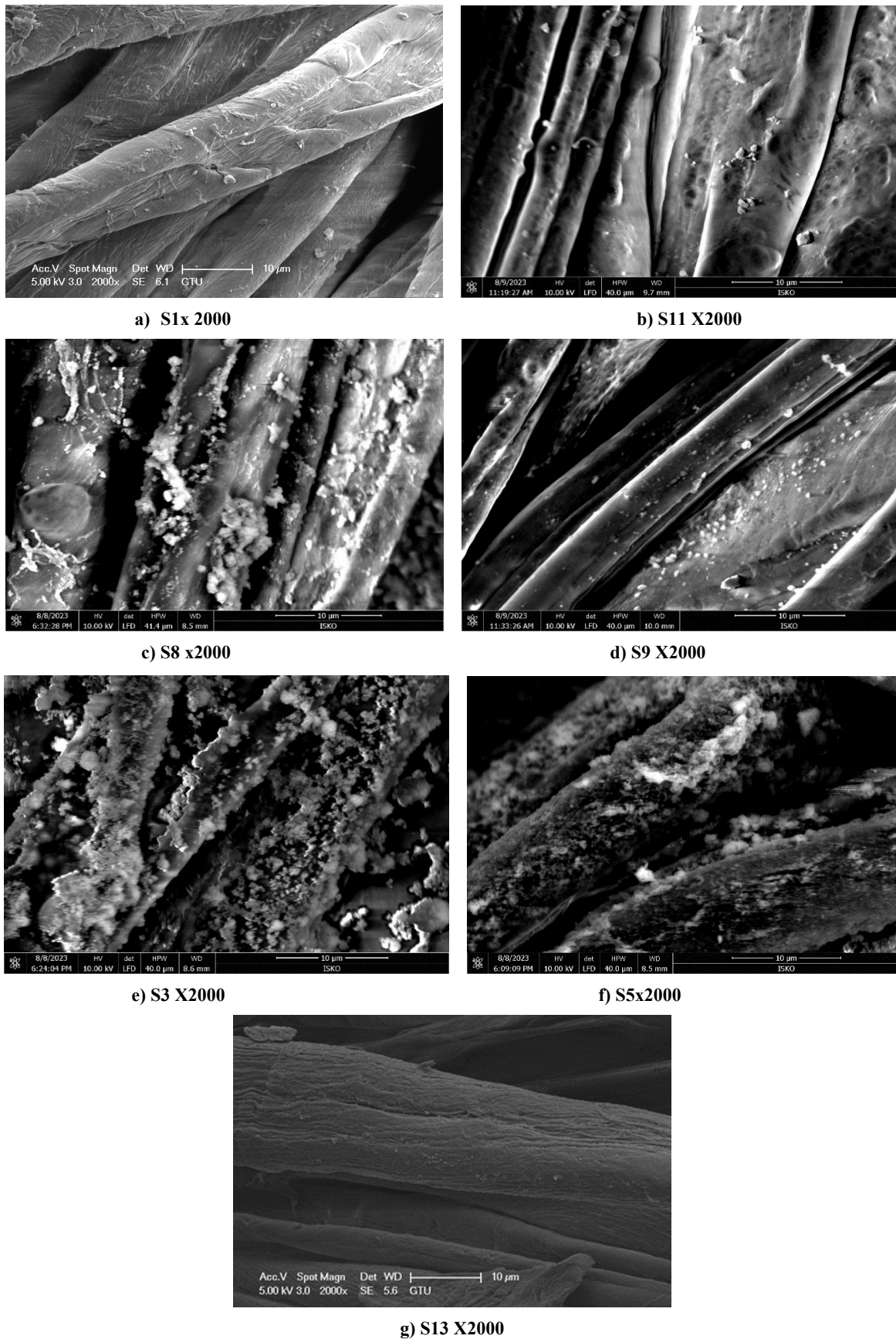
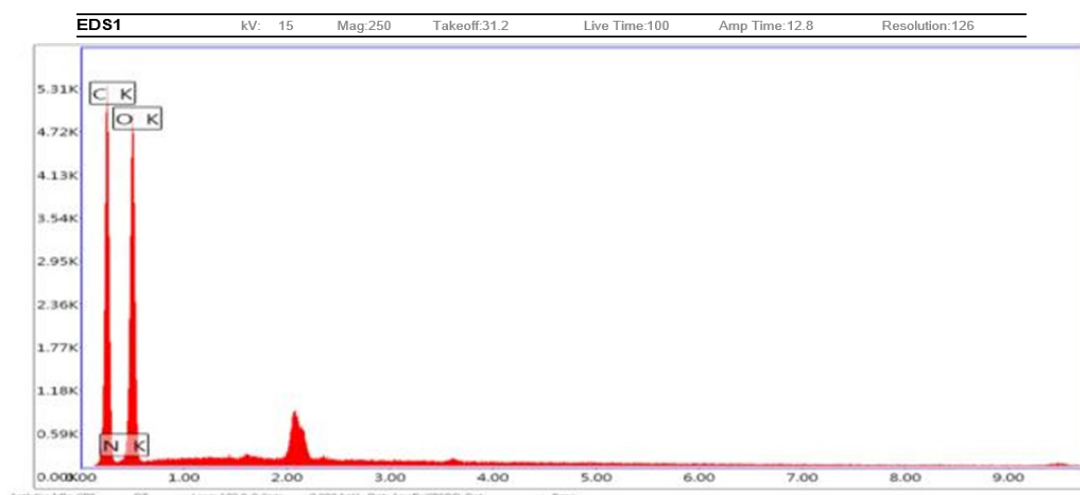


Figure 5. SEM pictures of untreated and treated cotton fabrics

Figure 5 displays SEM images of both untreated and treated cotton fabrics. In Figure 5.a, the surface of the untreated cotton fabric appears clear and smooth. In Figure 5.b, on the other hand, fluctuations and pits are evident on the surface of cotton fabric subjected to photocatalytic treatment without any catalyst used, as indicated. It is presumed that this effect is a result of the impact of UV rays used in the photocatalytic process on the surface. The SEM micrograph in Figure 5.d depicts a cleaner surface compared to Figure 5.c. This can be attributed to the fact that in S9, only the cotton surface treated with boric acid is

present, while the sample in S8 undergoes treatment with TiO₂ nanoparticles and boric acid. The particles observed in S8 belong to n-TiO₂. Figs.5.e and 5.f showcase the fiber surfaces of cotton fabrics treated with ZnO nanoparticles at pH 10.5 and pH 7, respectively. ZnO nanoparticles are distinctly visible in both micrographs. In the final figure, Fig.5g, the micrograph illustrates a conventionally hydrogen peroxide-bleached raw cotton fabric. Unlike all other figures, it is apparent that this treatment causes abrasions on the fiber surface and damages the fibers.

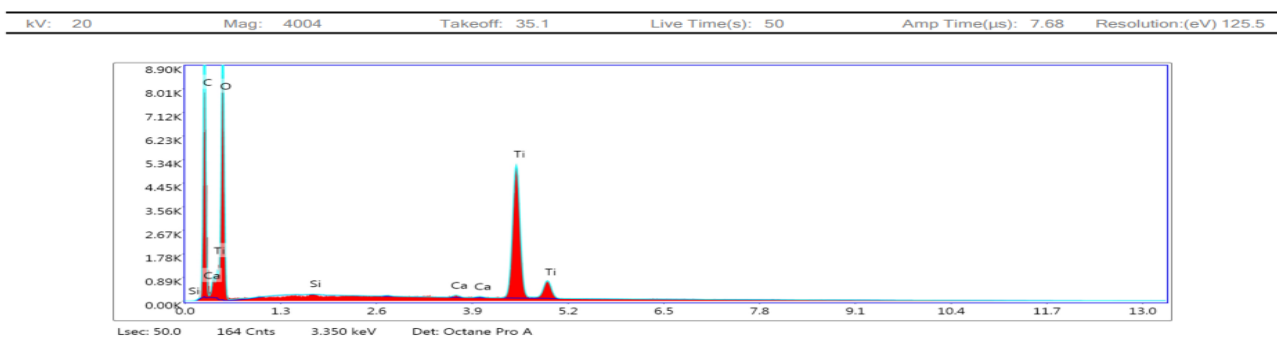
3.2.2. SEM-EDX Results of Cotton Fabric



a) SEM-EDX analysis of S1

Element	W %	Atomic	Net Int.	Net Int. Error
C K	45.2	52.17	288.41	0.01
N K	2.74	2.71	3.93	0.11
O K	52.06	45.12	289.84	0.01

b) SEM-EDX analysis of S1 table 2

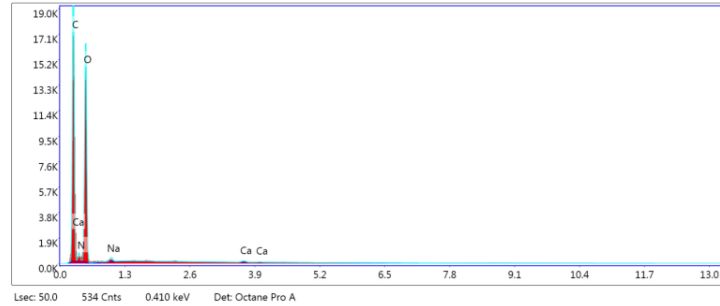


eZAF Smart Quant Results

Element	Weight %	Atomic %	Net Int.	Error %	Kratio	Z	A	F
C K	32.91	44.49	884.52	6.57	0.1757	1.0664	0.5008	1.0000
O K	48.43	49.16	974.13	9.86	0.0784	1.0209	0.1586	1.0000
Si K	0.02	0.01	1.91	76.01	0.0001	0.9285	0.7533	1.0058
Ca K	0.26	0.10	21.07	15.43	0.0025	0.8768	1.0181	1.0730
Ti K	18.39	6.23	1224.81	2.05	0.1517	0.7948	1.0247	1.0133

c) SEM-EDX analysis of S8

kV: 20 Mag: 4004 Takeoff: 35.2 Live Time(s): 50 Amp Time(µs): 7.68 Resolution:(eV) 125.5

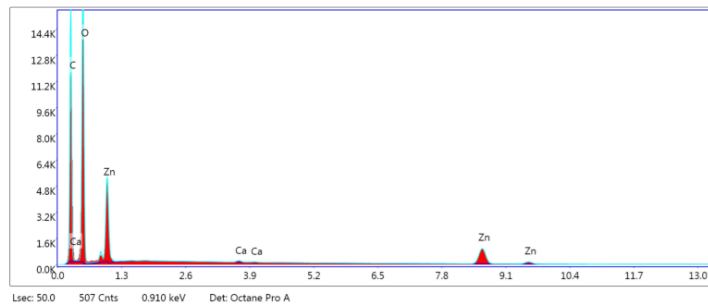


eZAF Smart Quant Results

Element	Weight %	Atomic %	Net Int.	Error %	Kratio	Z	A	F
C K	45.86	52.89	1945.57	5.59	0.2714	1.0239	0.5777	1.0000
N K	3.92	3.88	50.04	34.03	0.0047	0.9995	0.1188	1.0000
O K	49.47	42.83	1692.83	9.37	0.0958	0.9784	0.1978	1.0000
NaK	0.55	0.33	35.23	15.87	0.0017	0.8873	0.3575	1.0009
CaK	0.20	0.07	21.77	18.00	0.0018	0.8362	1.0306	1.0477

d) SEM-EDX analysis of S9

kV: 20 Mag: 4004 Takeoff: 35.2 Live Time(s): 50 Amp Time(µs): 7.68 Resolution:(eV) 125.5

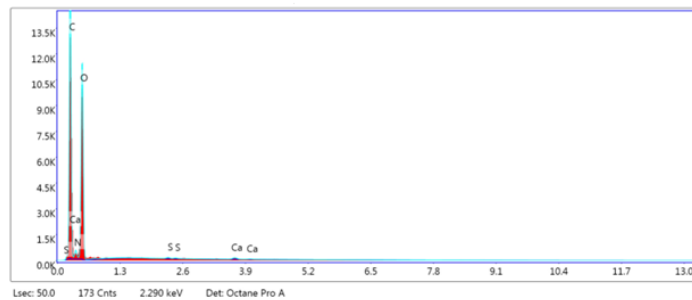


eZAF Smart Quant Results

Element	Weight %	Atomic %	Net Int.	Error %	Kratio	Z	A	F
C K	43.12	53.93	1319.68	7.30	0.1874	1.0468	0.4153	1.0000
O K	46.49	43.65	1757.71	9.13	0.1012	1.0016	0.2174	1.0000
CaK	0.22	0.08	23.73	21.14	0.0020	0.8595	1.0105	1.0373
ZnK	10.17	2.34	313.65	3.63	0.0810	0.7307	1.0159	1.0732

e) SEM-EDX analysis of S3

kV: 20 Mag: 4004 Takeoff: 35 Live Time(s): 50 Amp Time(µs): 7.68 Resolution:(eV) 125.5



eZAF Smart Quant Results

Element	Weight %	Atomic %	Net Int.	Error %	Kratio	Z	A	F
C K	47.21	54.21	1462.88	5.60	0.2824	1.0231	0.5845	1.0000
N K	3.63	3.58	32.50	47.88	0.0042	0.9986	0.1153	1.0000
O K	48.81	42.08	1181.77	9.52	0.0923	0.9775	0.1935	1.0000
S K	0.09	0.04	10.92	24.89	0.0008	0.8675	0.9605	1.0121
CaK	0.25	0.09	20.25	20.72	0.0023	0.8355	1.0313	1.0476

f) SEM-EDX analysis of S13

Figure 6. SEM-EDX analysis of untreated and treated cotton fabrics

Figure 6 showcases the SEM-EDX analysis results for both treated and untreated cotton fabrics. In Figure 6a, the untreated cotton fabric and Fig. 6b, where no catalyst was used, prominently exhibit the presence of C and O elements. Moving to Fig. 6c, the photocatalytic process with the introduction of titanium dioxide nano particles in the process reveals a 18.39% presence of Ti element. Fig. 6d, on the other hand, depicts a photocatalytic process applied solely with boric acid. Since boric acid, unlike nano materials, does not increase surface roughness (refer to SEM micrographs) and spreads on the surface, it could not be captured elementally in SEM-EDX analysis. In addition, the inconspicuous appearance of the boron element in SEM-EDX analysis is attributed to boron's low atomic number, which results in its inability to generate X-ray fluorescence signals. Furthermore, the detection is complicated by the fact that boron's characteristic X-ray spectral lines are weaker compared to other elements.

However, in Fig. 6e, the SEM-EDX analysis of cotton fabric exposed to photocatalytic treatment with 5 g/L ZnO nanoparticles at pH 10.5 for 60 minutes at 60 C reveals the presence of 10.17% Zn element in addition to the dominant C and O elements. The last figure illustrates the SEM-EDX analysis of conventionally hydrogen peroxide-treated cotton fabric. The hydrogen molecule, because of being very small, could not be captured in the elemental analysis, but the presence of the other basic elements that make up the cotton fibers (carbon and oxygen) has been demonstrated.

3.2.3. FTIR-ATR Analysis of Cotton Fabric

In Figure 7, FTIR-ATR spectra of untreated cotton fabric, conventionally hydrogen peroxide-bleached fabric, fabric subjected to photocatalytic treatment without any catalyst, fabric treated with a combination of boric acid and TiO₂ nanoparticles in a photocatalytic process, fabric treated solely with boric acid in a photocatalytic process, and fabric subjected to photocatalytic treatment with 5 g/L ZnO nano particles under the same conditions are sequentially presented. The characteristic peaks of cotton are discernible in the graph. When the FTIR-ATR analysis of the untreated fabric was examined, distinctive peaks associated with cotton fibers were observed at the following wavenumbers: 3300 cm⁻¹ (OH stretching), 1030 cm⁻¹ (CO stretching), 2900 cm⁻¹ (CH stretching), and 1310 cm⁻¹ (CH vibration). However, the FTIR spectras for both untreated and treated cotton fabrics are overlapped. This is attributed to the inorganic nature of the catalysts and chemical agents, such as n-ZnO, n-TiO₂, boric acid, and hydrogen peroxide, and their usage in relatively low proportions.

3.3. Color Spectrum Results

Table 3 provides the whiteness indexes (Berger) and yellowness indexes (ASTMD1925) along with CIE L*, a*, b* and ΔE values for untreated and treated cotton fabrics. According to this table, it is observed that photocatalytic

processes with zinc oxide nano particles at different pH levels and temperatures slightly increased the whiteness index values. Among the processes conducted with nano zinc oxide, the best result was achieved with the treatment at pH 10.5 and 60C for 60 minutes. Although these values are lower compared to bleaching results obtained using different catalysts or conventional bleaching process with hydrogen peroxide, the results of zinc oxide nano particles are in line with the literature [38] In their study, Arık and Atmaca [38] utilized various zinc-based nano particles, including nano zinc oxide with sizes ranging from 10 to 30 nm, and found that Stensby whiteness ratings were consistently at similar levels (with a 3-unit increase). The 18 nm zinc oxide used in this study marginally increased whiteness values but did not result in effective bleaching. Additionally, examining the color spectrum results of photocatalytic processes with boric acid showed a slight increase in whiteness and decrease in yellowness indexes. The combination with n-TiO₂ significantly enhanced the whiteness index result whereas the yellowness indexes decreased; however, it is believed to be attributed to the high photocatalytic effect of n-TiO₂. No significant differences in ΔE values were observed for any samples processed, except for those involving the use of titanium dioxide. Unlike other photocatalytic textile applications, this study explored the impact of photocatalytic processes on bleaching without using a catalyst, revealing that the treatment conducted at pH 7 and 60 C for 60 minutes, excluding n-TiO₂, had the highest bleaching effect. In catalyst-free photocatalytic processes, the formation of whiteness is generally associated with the oxidative properties of the mechanism and the nature of the reaction. Photocatalytic processes involve catalysts that trigger and accelerate chemical reactions using light energy. However, catalyst-free photocatalytic processes typically encompass conditions where various components are directly exposed to light, leading to oxidation-reduction reactions. Whiteness often arises from the breakdown or reaction of colored pigments or organic substances. Catalyst-free photocatalytic processes, especially those involving the breakdown or degradation of organic materials and the increased solubility of color pigments, can result in the appearance of whiteness. This occurs as the impact of colored substances diminishes, allowing lighter to be reflected. These processes are commonly utilized in applications such as the removal of organic pollutants or the bleaching of materials. For example, catalyst-free photocatalytic reactions under sunlight can lead to the breakdown of colored stains or pigments, resulting in the material becoming whiter [39].

3.4. Tearing Strength Results

In Figure 8, the results of the tear strength for untreated cotton fabric, fabric subjected to conventional bleaching, fabric treated with zinc oxide nanoparticles under various conditions of photocatalytic treatment, fabric treated with boric acid and boric acid with n-TiO₂ photocatalytic

treatment, and finally, cotton fabric subjected to photocatalytic treatment without any catalyst are presented. According to Figure 8, it can be observed that the tear strength of all fabrics decreased to some extent. While the decrease caused by conventional bleaching in cotton fabric was 7.62%, this value increased to 12.7% as a result of the photocatalytic treatment with zinc oxide nanoparticles. When the amount of zinc oxide nanoparticles increased to 5 g/L, this value was observed to reach the range of 13-14%. The further increase in the decrease is thought to be due to

the accumulation of nanoparticles at the intersections and surfaces of fibers, leading to an increase in the coefficient of friction between the fibers. Moreover, while a 9.6% decrease in tear strength was observed as a result of photocatalytic treatment with boric acid alone, this decrease reached 13% when nano TiO₂ was used as a catalyst together with boric acid. It was observed that photocatalytic treatments conducted without catalysts resulted in less tear strength loss (7.99%) compared to those conducted with catalysts.

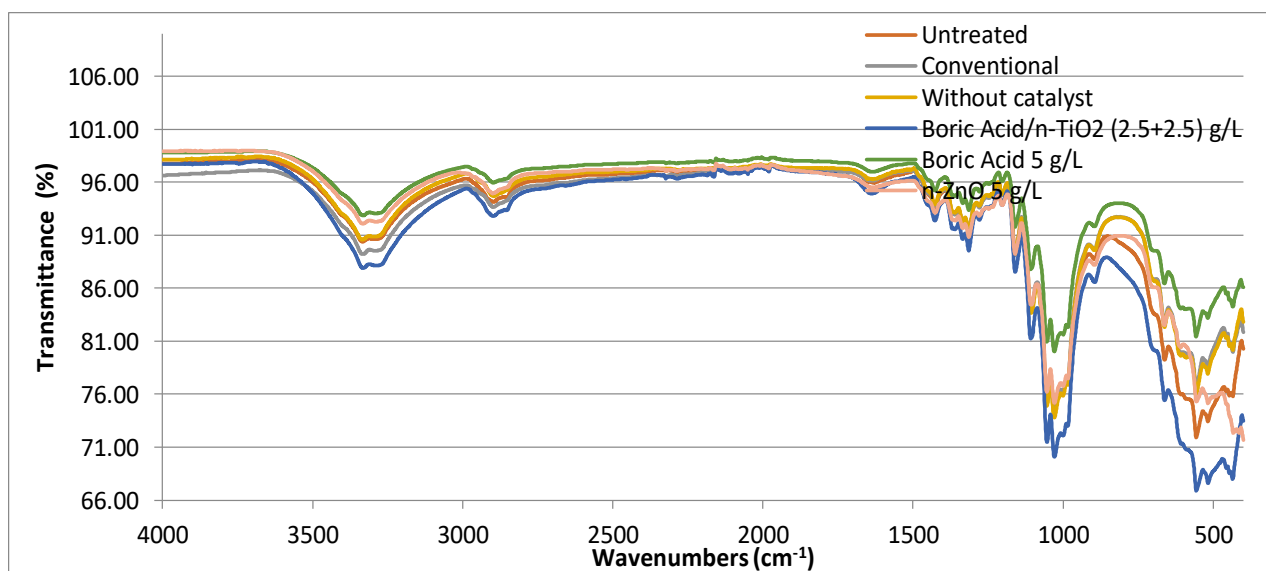


Figure 7. FTIR-ATR analysis of untreated and treated cotton fabrics

Table 3. Color spectrum values

SAMPLES		Whiteness Index-BERGER	Yellowness Index ASTMD 1925	L*	a*	b*	ΔE
S1	Untreated fabric	63.15	7.42	92.54	-0.18	4.01	-
S2	n-ZnO 1 g/L pH 10.5 60 C 60 min	64.36	7.17	92.98	-0.28	3.98	0.45
S3	n-ZnO 5 g/L pH 10.5 60 C 60 min	64.38	7.14	93.54	-0.94	4.48	1.34
S4	n-ZnO 5 g/L pH 4.5 60 C 60 min	64.12	7.29	93.73	-0.71	4.52	1.40
S5	n-ZnO 5 g/L pH 7 60 C 60 min	63.77	7.39	93.61	-1.06	4.69	1.54
S6	n-ZnO 5 g/L pH 4.5 30 C 60 min	63.12	7.38	93.36	-0.61	4.01	1.07
S7	n-ZnO 5 g/L pH 10.5 95 C 60 min	61.65	9.14	93.73	-0.94	5.14	1.81
S8	Boric acid/n-TiO ₂ (2.5+2.5)g/L pH 5.5 60C 60min	73.98	3.36	94.88	-0.18	4.01	2.64
S9	Boric acid 5g/L pH 5.5 60 C 60 min	64.84	7.20	93.00	-0.23	3.86	0.49
S10	Without catalyst 30 C 60 min pH 7	66.50	6.60	93.08	-0.21	3.52	0.328
S11	Without catalyst 60 C 60 min pH 7	66.67	6.15	93.55	-0.27	3.70	0.253
S12	Without catalyst 95 C 60 min pH 7	65.98	6.02	93.07	-0.20	3.62	0.250
S13	Conventional bleaching process	70.50	4.87	93.98	-0.36	3.12	0.832

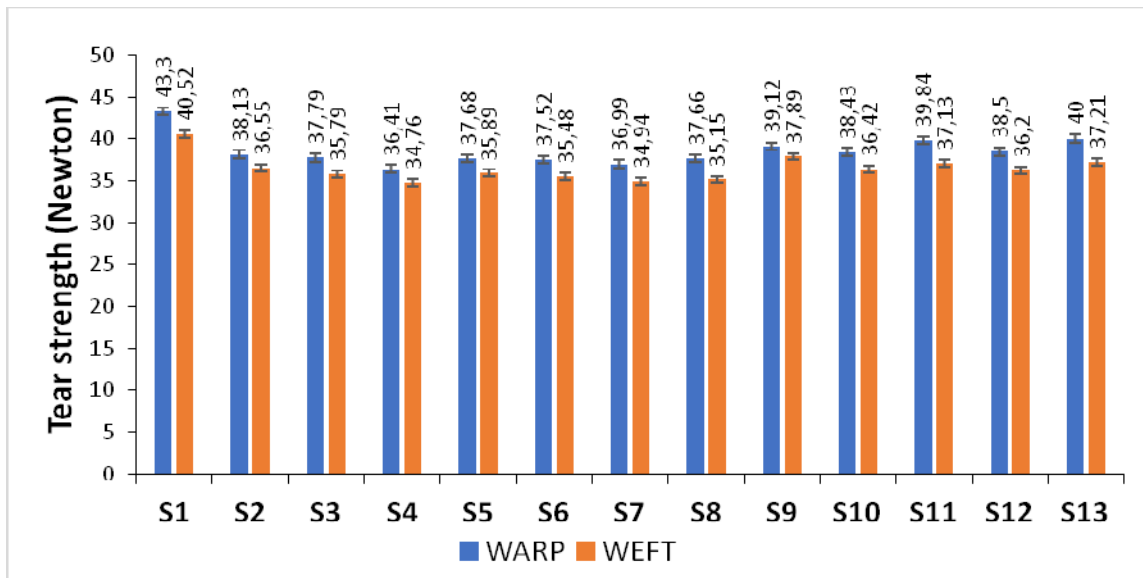


Figure 8. Tearing strenght results of cotton samples

3.5. UV intensity results

The characteristics of the lamp used are given in Table 4.

Table 4. Electrical and photometrical fata for Osram L Blue UVA L 15W/78

Electrical Data		Photometrical Data	
Nominal Voltage	55 V	Luminous Intensity	7800 cd
Lamp Voltage	55 V	Radiated Power 315...400 nm (UVA)	4 W
Construction Voltage	230 V		
Lamp Current	0.33 A		
Nominal Wattage	15 W		

Consider it endless and visualize the source as a cable. From then on, it is acknowledged that it only radiates in the form of $2\pi rL$ from the lateral field. by considering the source as an infinitely long cylinder with r near to zero and using in Eq (8) as follows;

$$I = \frac{P}{2\pi rL} \quad (8)$$

Where P is radiated power, r is radius and L is cyclinder of length.

$$I = \frac{4 \times 4}{2 \times \pi \times 0.15 \times 0.39}$$

Thus, UV intensity of our lamps are calculated as; 43.53 W/m^2 .

4. CONCLUSION

In this study, due to the disadvantages of conventional hydrogen peroxide bleaching for cotton fabrics, a quest for a more environmentally friendly method for bleaching was

initiated. Various catalysts were examined individually or in combination, and their effects on whiteness indexes were investigated. Characterization studies were also conducted. Unlike other textile photocatalytic studies, this research addressed the question of whether catalyst-free photocatalytic processes would induce any changes in cotton fiber surface and color performance. According to the results, zinc oxide nano particles did not provide a significant bleaching effect; however, they slightly increased whiteness indexes, with the best values observed under the parameters of a photocatalytic process conducted at 60 C, pH 10.5, and for 60 minutes. Additionally, the photocatalytic process with boric acid, although marginally, increased whiteness indexes. Catalyst-free photocatalytic processes, excluding $n-TiO_2$ and conventional methods, yielded the highest whiteness index. Characterization tests and elemental analyses were conducted to elucidate the impact of catalysts. In conclusion, the increase in whiteness index without the use of any chemical or catalyst suggests that it could be an alternative method to hydrogen peroxide bleaching, which involves high water and energy consumption and poses a significant environmental burden.

Acknowledgement

This study was not funded by any organisation. The authors thank Ege Özteks Tekstil for providing the cotton fabrics.

REFERENCES

1. Wang H., Siddiqui M. Q., & Memon H. (2020). Processing Physical Structure, properties and quality of cotton. Wang, H, Memon, H. Cotton science and processing technology: Gene, ginning, garment and green recycling. *Springer* 79–97.
2. Gordon S., Rodgers J., & Abidi N. (2017). Cotton fibre cross-section properties. Cotton fibres, characteristics, uses and performance, *Nova* 65–86.
3. Pereira L., Bastos C., Tzanov T., Cavaco-Paulo A., & Gübitz G. M. (2005). Environmentally friendly bleaching of cotton using laccases. *Environmental Chemistry Letters* 3, 66–69.
4. Wang N., Tang P., Zhao C., Zhang Z., & Sun G. (2020). An environmentally friendly bleaching process for cotton fabrics: mechanism and application of UV/H₂O₂ system. *Cellulose* 27(2), 1071–1083.
5. Fei X., Yao J., Du J., Sun C., Xiang Z., & Xu C. (2015). Analysis of factors affecting the performance of activated peroxide systems on bleaching of cotton fabric. *Cellulose* 22, 1379–1388.
6. Farooq A., Ali S., Abbas N., Fatima G A., & Ashraf, M A. (2013). Comparative performance evaluation of conventional bleaching and enzymatic bleaching with glucose oxidase on knitted cotton fabric. *Journal of Cleaner Production* 42, 167–171.
7. Zeghioud H., Assadi AA., Khellaf N., Djelal H., Amrane A., & Rtimi,S. (2018). Reactive species monitoring and their contribution for removal of textile effluent with photocatalysis under UV and visible lights: dynamics and mechanism. *Journal of Photochemistry and Photobiology A: Chemistry* 365, 94–102.
8. Rahal R., Pigot T., Foix D., & Lacombe S. (2011). Photocatalytic efficiency and self-cleaning properties under visible light of cotton fabrics coated with sensitized TiO₂. *Applied Catalysis B: Environmental* 104(3–4), 361–372.
9. Ashar A., Bhutta Z A., Shoaib M., Alharbi NK., Fakhar-e-Alam M., Atif M., et al. (2023). Cotton fabric loaded with ZnO nanoflowers as a photocatalytic reactor with promising antibacterial activity against pathogenic E. coli. *Arabian Journal of Chemistry* 105084.
10. Xia C., Liu S., Cui B., Li M., Wang H., Liang C. (2022). In situ synthesis of zinc oxide/selenium composite for UV blocker application. *International Journal of Applied Ceramic Technology* 19(5), 2437–2449.
11. Sirelkhatim A., Mahmud S., Seeni A., Kaus NHM., Ann LC., Bakhori SKM.(2015). Review on zinc oxide nanoparticles: antibacterial activity and toxicity mechanism. *Nano-micro letters* 7, 219–242.
12. Raghupathi KR., Koodali RT., & Manna, AC. (2011). Size-dependent bacterial growth inhibition and mechanism of antibacterial activity of zinc oxide nanoparticles. *Langmuir* 27(7), 4020–4028.
13. Miri A., Mahdinejad N., Ebrahimi O., Khatami M., & Sarani M. (2019). Zinc oxide nanoparticles: Biosynthesis, characterization, antifungal and cytotoxic activity. *Materials Science and Engineering: C* 104, 109981.
14. Singh P., & Nanda A. (2013). Antimicrobial and antifungal potential of zinc oxide nanoparticles in comparison to conventional zinc oxide particles. *J. Chem. Pharm. Res* 5(11), 457–463.
15. Montazer M., & Morshedi S. (2012). Nano photo scouring and nano photo bleaching of raw cellulosic fabric using nano TiO₂. *International Journal of Biological Macromolecules* 50(4), 1018–1025.
16. Behnajady MA., Modirshahla N., & Hamzavi R. (2006). Kinetic study on photocatalytic degradation of C.I. Acid Yellow 23 by ZnO photocatalyst. *Journal of Hazardous Materials*, 133(1), 226–232. <https://doi.org/https://doi.org/10.1016/j.jhazmat.2005.10.022>
17. Selvakumar N., Azhagurajan A.,Natarajan TS., & Mohideen Abdul KhadirM. (2012). Flame-retardant fabric systems based on electrospun polyamide/boric acid nanocomposite fibers. *Journal of applied polymer science* 126(2), 614–619.
18. Arvanitis C., Rook T., & Macreadie I. (2020). Mechanism of action of potent boron-containing antifungals. *Current Bioactive Compounds* 16(5), 552–556.
19. Estevez-Fregoso E., Farfán-García E D., García-Coronel I H., Martínez-Herrera E., Alatorre A., Scorei R. I., Soriano-Ursúa M. A. (2021). Effects of boron-containing compounds in the fungal kingdom. *Journal of Trace Elements in Medicine and Biology* 65, 126714.
- 20.Mehedintu C., Bratila E., Cirstoiu M., Petca A., Brinduse L. A., Berceanu C. (2019). Evaluation of effectiveness and tolerability of boric acid in the treatment of vaginal infection with Candida Species. *Rev Chim* 70, 2375–2378.
21. Istriana N., & Priadi T. (2021, November). The resistance of modified manii wood with boric acid and chitosan/glycerol and heating against fungi and termites. In IOP Conference Series: Earth and Environmental Science (Vol. 891, No. 1, p. 012010). IOP Publishing.
- 22.Huang Y., Ho W., Ai Z., Song X., Zhang L., & Lee, S. (2009). Aerosol-assisted flow synthesis of B-doped, Ni-doped and B–Ni-codoped TiO₂ solid and hollow microspheres for photocatalytic removal of NO. *Applied Catalysis B: Environmental* 89(3), 398–405.
23. Zheng, J., Liu, Z., Liu, X., Yan, X., Li, D., & Chu, W. (2011). Facile hydrothermal synthesis and characteristics of B-doped TiO₂ hybrid hollow microspheres with higher photo-catalytic activity. *Journal of Alloys and Compounds* 509(9), 3771–3776.
24. Bilgin Simsek E. (2017). Solvothermal synthesized boron doped TiO₂ catalysts: Photocatalytic degradation of endocrine disrupting compounds and pharmaceuticals under visible light irradiation. *Applied Catalysis B: Environmental* 200, 309–322.
25. Erim B., Çiğeroğlu Z., & Bayramoğlu M. (2021). Green synthesis of TiO₂/GO/chitosan by using leaf extract of *Olea europaea* as a highly efficient photocatalyst for the degradation of cefixime trihydrate under UV-A radiation exposure: An optimization study with d-optimal design. *Journal of Molecular Structure* 1234, 130194.
26. Steffy K., Shanthi G., Maroky A. S., & Selvakumar S. (2018). Synthesis and characterization of ZnO phytonanocomposite using *Strychnos nux-vomica* L. (Loganiaceae) and antimicrobial activity against multidrug-resistant bacterial strains from diabetic foot ulcer. *Journal of Advanced Research* 9, 69–77.
27. Çiğeroğlu Z., ŞahinS., Kazan E. S. (2022). One-pot green preparation of deep eutectic solvent-assisted ZnO/GO nanocomposite for cefixime trihydrate photocatalytic degradation under UV-A irradiation. *Biomass Conversion and Biorefinery* 12, 73–86.
28. Zhang W., Liu T., & Xu, J. (2016). Preparation and characterization of 10 B boric acid with high purity for nuclear industry. *SpringerPlus* 5, 1-10.
29. Mallakpour S., Dinari M., (2012). Fabrication of polyimide/titania nanocomposites containing benzimidazole side groups via sol–gel process. *Prog. Org. coatings* 75, 373–378.
30. Ahmad A.A., Alakhras L.A., Al-Bataineh Q.M., Telfah A., 2023. Impact of metal doping on the physical characteristics of anatase titanium dioxide (TiO₂) films. *J. Mater. Sci. Mater. Electron* 34, 1552. <https://doi.org/10.1007/s10854-023-10948-z>
31. Erim B., Çiğeroğlu Z., Şahin S., & Vasseghian Y. (2022). Photocatalytic degradation of cefixime in aqueous solutions using functionalized SWCNT/ZnO/Fe₃O₄ under UV-A irradiation. *Chemosphere* 291, 132929.

-
32. Harabor A., Rotaru P., Score, R. I., & Harabor N. A. (2014). Non-conventional hexagonal structure for boric acid. *Journal of Thermal Analysis and Calorimetry* 118, 1375-1384.
33. Elbeyli İY. (2015). Production of crystalline boric acid and sodium citrate from borax decahydrate. *Hydrometallurgy* 158, 19-26.
34. Li W., Liang R., Hu A., Huang Z., & Zhou YN. (2014). Generation of oxygen vacancies in visible light activated one-dimensional iodine TiO₂ photocatalysts. *RSC advances* 4(70), 36959-36966.
35. Bai, W., Zhang, Z., Tian, W., He, X., Ma, Y., Zhao, Y., & Chai, Z. (2010). Toxicity of zinc oxide nanoparticles to zebrafish embryo: a physicochemical study of toxicity mechanism. *Journal of Nanoparticle Research* 12, 1645-1654.
36. Deniz F., & Akarsu C. (2018). Operating cost and treatment of boron from aqueous solutions by electrocoagulation in low concentration. *Global Challenges* 2(5-6), 1800011.
37. Perales-Martínez I A., & Rodríguez-González V. (2017). Towards the hydrothermal growth of hierarchical cauliflower-like TiO₂ anatase structures. *Journal of Sol-Gel Science and Technology* 81, 741-749.
38. Arik B., & Karaman Atmaca OD. (2020). The effects of sol-gel coatings doped with zinc salts and zinc oxide nanopowders on multifunctional performance of linen fabric. *Cellulose*, 27, 8385-8403.
39. Gao Y., Li Y., Yao L., Li S., Liu J., & Zhang H. (2017). Catalyst-free activation of peroxides under visible LED light irradiation through photoexcitation pathway. *Journal of hazardous materials*, 329, 272-279.

